2010

Manganese superoxide dismutase (MnSOD) 3'-untranslated region: a novel molecular sensor for environmental stress

Leena Chaudhuri
University of Iowa

MANGANESE SUPEROXIDE DISMUTASE (MnSOD) 3'-UNTRANSLATED REGION:

A NOVEL MOLECULAR SENSOR FOR ENVIRONMENTAL STRESS

by

Leena Chaudhuri

An Abstract

Of a thesis submitted in partial fulfillment
of the requirements for the Doctor of
Philosophy degree in Free Radical and Radiation Biology
in the Graduate College of
The University of Iowa

December 2010

Thesis Supervisor: Associate Professor Prabhat C. Goswami

ABSTRACT

Eukaryotic gene expression is a complex process that can be controlled at the level of transcription, post-transcription or translation and post-translation. In recent years, there has been a growing interest in understanding the role of 3'-untranslated region (UTR) in regulating mRNA turnover and translation. The 3'-UTR harbors the poly(A) signal and post-transcriptional regulatory sequences, like miRNA and AU-rich elements (AREs). The presence of multiple poly(A) sites often results in multiple transcripts; shorter transcripts correlating with more protein abundance. Manganese superoxide dismutase (MnSOD) is a nuclear encoded and mitochondrial matrix localized antioxidant enzyme that catalyzes the dismutation of superoxide to hydrogen peroxide. Human MnSOD has two poly(A) sites resulting in two transcripts: 1.5 and 4.2 kb. We hypothesize that the 3'-UTR of MnSOD regulates its mRNA and protein levels as well as activity in response to growth states and environmental stress. Results from a Q-RT-PCR assay showed a preferential accumulation of the shorter MnSOD transcript during quiescence, which correlated with an increase in MnSOD activity. The accumulation of the longer MnSOD transcript during proliferation was associated with a decrease in MnSOD activity. Log transformed expression ratio of the longer to shorter transcript was also higher in proliferating epithelial non-cancerous (mammary: MCF-10A) and cancer cells (mammary: MB-231, SUM 159; oral squamous: SQ20B, FaDu, Cal27; and lung: A549, H292), suggesting that the abundance of the longer transcript is independent of cellular transformation status, instead it is dependent on cellular growth state. Interestingly, the abundance of the longer transcript directly correlated with percent S-phase (R^2=0.86). The shorter transcript was enriched in irradiated MB-231 cells. MCF-10A cells exposed to 2-(4-chlorophenyl)benzo-1,4-quinone (4-Cl-BQ), a metabolite of the environmental pollutant polychlorinated biphenyl 3, showed a significant decrease in the abundance of the 4.2 kb transcript due to a faster mRNA turnover, 14 h compared to

20 h in untreated control cells. The decrease in the 4.2 kb transcript levels was associated with a corresponding decrease in MnSOD protein levels and activity, which resulted in a significant inhibition of quiescent cells entry into the proliferative cycle. Deletion and reporter assays showed: (a) a significant decrease in reporter activity in constructs carrying multiple AREs that are present in the 3'-UTR of the longer MnSOD transcript; (b) irradiation increased the reporter activity of the constructs carrying the 3'-UTR sequence of the shorter MnSOD transcript and (c) N-acetyl-cysteine increased the reporter activity of constructs carrying multiple AREs. Because the longer transcript carries AREs, our results identified redox sensitive AREs as novel regulators of MnSOD transcript levels. We conclude that the MnSOD 3'-UTR is a novel molecular sensor regulating MnSOD mRNA levels in response to different growth states and environmental stress. A better understanding of the 3'-UTR regulating gene expression could lead to the development of new molecular biology-based redox therapy designed to treat proliferative disorders.

Abstract Approved: _____
Thesis Supervisor

_____
Title and Department

_____
Date

MANGANESE SUPEROXIDE DISMUTASE (MnSOD) 3'-UNTRANSLATED REGION:

A NOVEL MOLECULAR SENSOR FOR ENVIRONMENTAL STRESS

by

Leena Chaudhuri

A thesis submitted in partial fulfillment
of the requirements for the Doctor of
Philosophy degree in Free Radical and Radiation Biology
in the Graduate College of
The University of Iowa

December 2010

Thesis Supervisor: Associate Professor Prabhat C. Goswami

Graduate College
The University of Iowa
Iowa City, Iowa

CERTIFICATE OF APPROVAL

_____

PH.D. THESIS

_____

This is to certify that the Ph.D. thesis of

Leena Chaudhuri

has been approved by the Examining Committee
for the thesis requirement for the Doctor of Philosophy
degree in Free Radical and Radiation Biology at the December 2010
graduation.

Thesis Committee: _____
Prabhat C. Goswami, Thesis Supervisor

_____
Douglas R. Spitz

_____
Garry R. Buettner

_____
Joseph J. Cullen

_____
Larry W. Robertson

To my mother, father, brother, sister-in-law and my husband.
For your immense faith, love and belief.

Man is made by his belief. As he believes, so he is.

Bhagwad Gita

ACKNOWLEDGMENTS

In the first place, I would like to express my gratitude to my mentor, Dr. Goswami for his guidance and advice from the very beginning. He has been a constant source of inspiration and a wonderful teacher in every sense of the word. His unflinching support and constant encouragement during difficult times has made this journey memorable. His passion for work and persistence taught me to believe in myself, stand up for myself in order to achieve my goals. He has taught me how to think scientifically, how to approach a problem and ask the right questions. His methodical teaching have helped me develop not only my approach towards science but also equipped me with orating and writing skills. With his commitment and encouragement, I have grown as a person both professionally and personally.

A special thanks to all my committee members. Dr. Spitz who has always contributed valuable opinions to improve my project. Dr. Buettner and Dr. Cullen for their insightful comments and judicious review of my work. Dr. Robertson, who has been extremely helpful during the course of my work by providing the polychlorinated biphenyls and introducing me to the PCB literature.

I also extend my heartfelt gratitude to my lab members, Ehab, Amanda, Venkat, Gao, Carolyn, Maneesh, Jennifer and Jaimee for their help and support. I have some wonderful memories of the jokes and banter while trying to run PCR reactions. All the support and useful suggestions before every presentation to make it perfect, the entire computer related ‘tech’ support, all the lunches together; I will cherish all of these. A very special thanks to Adam and Monali, you both have been more than undergrads in our lab. Our projects would never run as smoothly if it were not for you both. You have not only ensured the lab is always fully stocked, run our experiments, but also made the lab a fun place to come to every morning.

I would also like to thank all faculty in the department for being so inspirational and making seminars and journal clubs a fun place to be. Thanks to Nukhet for helping me with DHE, DCFH oxidation and antioxidant measurements. Thanks to Laura Hefley, for handling all the student paper work and concerns and always reminding us when deadlines are approaching. Special thanks to Peter Scarbrough, Yueming Zhu, Jordan Witmer, Gaowei Mao for all their help, friendship and for being wonderful office-mates.

I am also greatful to my friends in Iowa city; Lalita, Puja, Pradeep, Samrat, Mary, Disha who have been here with me and without their support, and friendship these four years would have been a very difficult time. Special thanks to my roommate, Madhuparna for making our apartment a true home in this last year. We encouraged each other as budding scientists, shared excitement over the first experiment which worked, first paper published, first rejection and I am sure first of many more things to come. Not to forget celebrating with lunches and dinners whenever experiments worked!

This would not have been possible without the support of my family. My mother and father and their enquiring about my work, always encouraged me to produce the best. I did not have to look far for my source of inspiration, which my brother and sister-in-law fits so well into. The inspiring speeches over the telephone from far far away India, encouraged me to try harder each time to make this effort of staying away from loved ones even more meaningful. Last but not the least, this work would have been impossible without the support of my husband. I cannot imagine how I could have finished these four years without his support in every step of it. Special thanks for formatting all my presentation slides, word documents, and helping me understand that the computer is a friendly machine. Encouraging me every time I would wonder why things are not working, I could not have made this journey without you. I would like to also thank my in-laws for being a constant source of joy and blessing.

TABLE OF CONTENTS

LIST OF TABLES

LIST OF FIGURES

LIST OF ABBREVIATIONS

4-Cl-BQ: 2-(4-chlorobiphenyl)benzo-1, 4-quinone

AhR: Aryl hydrocarbon receptor

APA: Alternate polyadenylation

ARE: AU-rich elements

AUF1: Heterogenous ribonucleoprotein D

BrdU: Bromodeoxyuridine

CAR: Constitutive androstane receptor

CDCFH2: 5, -6-chloromethyl- 2', 7'-dichlorodihydro fluorescein

CDK: Cyclin dependent kinase

CKI: Cyclin dependent kinase inhibitor

CPSF: Cleavage and polyadenylation specificity factor

CF: Cleavage factors

CstF: Cleavage stimulation factor

CuZnSOD: Copper Zinc superoxide dismutase

CYP450: Cytochrome P450

DHE: Dihydroethidium

FITC: Fluorescein isothiocyanate

GSH: Glutathione

GPx: Glutathione peroxidase

Hip: Huntington interaction protein

HuR: Hu-antigen R

IR: Irradiation

miR: microRNA

MnSOD: Manganese superoxide dismutase

mRNA: Messenger ribonucleic acid

NAC: N-acetyl-L-cysteine

ORF: Open reading frame

PAS: Polyadenylation signal

PCB: Polychlorinated biphenyl

PCB 153: 2, 2', 4, 4', 5, 5' –hexachlorobiphenyl

PGST: Placenta glutathione S- transferase

PEG: Polyethylene glycol

PEG-SOD: Polyethylene glycol superoxide dismutase

PEG-CAT: Polyethylene glycol catalase

PI: Propidium iodide

Q-RT-PCR: Quantitative reverse transcriptase polymerase chain reaction

REMSA: RNA electrophoretic mobility shift assay.

ROS: Reactive oxygen specie

UTR: Untranslated region

UV: Ultraviolet

CHAPTER I

INTRODUCTION

3' Untranslated Region (UTR)

Eukaryotic gene expression is a complex process and can be controlled at the level of transcription, post-transcription or translation and post-translation. Single strand precursor RNA is transcribed from double stranded DNA. The precursor RNAs made in the nuclei of eukaryotic cells by RNA polymerase II undergoes a series of post-transcriptional processing to form the mature messenger RNA (mRNA). The mature mRNA is then exported to the cytoplasm. Post-transcriptional modifications include methylation of the 2'-hydroxyl group of the ribose sugar near the 5' end cap, splicing to remove introns and polyadenylation at the 3' end. Apart from this, most eukaryotic mRNAs also have these common structural identities, untranslated regions (UTRs) at the 5' and 3' end and conserved sequences within the mRNA signaling for translational start, stop, transcriptional stop and regulatory elements (Edwalds-Gilbert *et al.,*1997).

Recent reports suggest the relative utilization of the 5' and 3' end in controlling gene expression. Computational analysis suggests that the average 3' UTR length in humans is four times longer (~500 nucleotides) than the average 5' UTR length (~150 nucleotides). The same database suggests that the length of the 3' UTR increases over evolution and species complexity. In contrast, the 5' UTR length remains constant from fungi to plants, from invertebrates to vertebrates including humans. This ‘evolutionary expansion’ of the 3' UTR preferentially, suggests that there is a scope for 3' UTR based translation regulation in humans. Thus, the extended 3' UTR length could provide significant potential for transcript specific regulation (Mazumder *et al.,*2003).

The precursor RNA (pre-mRNA) are not processed efficiently for a large number of genes and these are mostly degraded in the nucleus before they can reach the cytoplasm. Functional polyadenylation signal (PAS) is required for terminating transcription by RNA polymerase II. Almost all eukaryotic mRNAs have an uncoded poly(A) tail at the 3' end *via* polyadenylation. A consensus sequence AAUAAA (or variant) within 10-35 nucleotides upstream of cleavage and PAS is present (Mayr and Bartel,2009). The more efficient a PAS is at processing, the more efficient RNA polymerase II elongation complexes and hence mature mRNA will be formed. Thus, PAS strength can directly influence the amount of cytoplasmic RNA and eventually protein from a transcript. Apart from harboring the PAS, the 3' UTR also has cis elements responsible for regulating RNA stability (Goswami *et al.,*2000). In the cytoplasm, the poly(A) tail along with the 3' UTR plays a role in mRNA stability and translation ability by stabilizing the RNA from degradation or destabilizing the RNA thereby decreasing its half life. How long the mature RNA persists in the cytoplasm can directly impact the amount of protein encoded by the RNA. Thus, cleavage and polyadenylation at the 3' end is important for not only terminating transcription but also stability and translation of mRNA and its export from the nucleus to the cytoplasm (Edwalds-Gilbert *et al.,*1997; Martincic *et al.,*1998). Changes in RNA processing efficiency or effective strength of splicing or polyadenylation signal (PAS) can serve as a very important control for gene expression.

3' UTR Mediated Gene Regulation

Previous studies report that alterations in the 3' UTR of genes can lead to increased stability leading to overexpression of proteins and thereby being responsible for oncogenesis (Mayr and Bartel,2009). The 3' UTR harbors several cis-acting elements to which proteins bind to regulate mRNA stability. A major class of the regulatory cis-elements comprises adenosine-uridine pentamers (AUUUA) which are known as AU-rich

elements (AREs). Ten percent of human mRNAs are reported to contain AREs in their 3' UTR. In 1986, Shawn and Kamen showed that insertion of a conserved region of 51 nucleotides containing AUUUA sequence from 3' UTR of human granulocyte macrophage colony stimulating factor (GM-CSF) into the 3' UTR of β-globin mRNA considerably reduced its mRNA stability (Shaw and Kamen,1986). Typically the AREs contains the AU-pentamer repeated several times within the 3' UTR. Variations of the traditional pentamer, such as extended pentamers AUUUUA and AUUUUUA have also been identified. Recent work has also suggested that a nonamer UUAUUUA could cause rapid destabilization of the mRNA (Balmer *et al.,*2001).

One of the most commonly studied mechanisms of ARE mediated mRNA degradation or stabilization involves ARE binding proteins. These proteins have been identified by RNA electrophoretic mobility shift assay (REMSA). They can bind to mRNA containing AREs with high affinity resulting in either stabilization or destabilization of the target mRNA (Balmer *et al.,*2001; Goswami *et al.,*2000). AREs can thereby act as positive or negative regulators of mRNA stability depending on the sequence on the mRNA and the proteins binding to these sequence. The most well studied ARE binding proteins are HuR (Hu-antigen R) and AUF1 (heterogenous ribonucleoprotein D). HuR, a 36 kDa protein is mainly located in the nucleus, but shuttles between the cytoplasm and nucleus and functions to stabilize the mRNA (Nabors *et al.,*2001). AUF1 protein binding to AREs is known to destabilize mRNAs (Pende *et al.,*1996). Activity of the ARE binding proteins is also known to be dependent on external stimuli (Chen and Shyu,1995), thereby rendering 3' UTR regulation of gene expression responsive to the environment.

AREs play a role in 3' UTR mediated post-transcriptional regulation. Deletion of AREs or overexpression of 3' UTR containing AREs could contribute to pathogenesis of various disorders like cancer. MCF-7 cells stably transduced with retroviral vector containing 3' UTR of cyclin D2 increased the fraction of cells in S-phase and lowered the

fraction of cells in G_1 phase. NIH3T3 cells stably transduced with retroviral vector expressing the 3' UTR of insulin-like growth factor mRNA binding protein, IMP-1showed colony formation on soft agar plates 28 days post transduction. Over-expressing the truncated 3' UTR of growth promoting genes increased the number of colonies and fraction of cells in S-phase. These reports confirm the role of 3' UTRs in regulating gene expression and subsequently affecting cell phenotypes (Mayr and Bartel,2009). Microinjection of full length 3' UTR of a growth inhibitory gene like prohibitin into human diploid fibroblasts (CF-3) could inhibit cell cycle progression between G_1 and S-phase which was not observed for the truncated transcript (Jupe *et al.,*1996a; Jupe *et al.,*1996b). This previously published study highlights the role of the full length 3' UTR of prohibitin having tumor suppressor functions.

Alternate Polyadenylation

Pre-mRNA is cleaved 10-30 nucleotides post polyadenylation signal (AAUAAA). Although a polyadenylation signal (PAS) is present in the 3' UTR of all genes, many genes have additional PAS sequences in their 3' UTR, *e.g*. AUUAAA, AAGAAA, UAUAAA and AGUAAA. The variants of the traditional signal are used mostly as the PAS for the shorter isoform (Edwalds-Gilbert *et al.,*1997). GU- or U rich sequences often found within 50 nucleotide downstream of the functional poly(A) signal are the binding sites for the multi-subunit cleavage stimulation factor (CstF) (Dickson and Wilusz*;* Ji *et al.,*2009; Sandberg *et al.,*2008). Besides these 'core' elements, auxiliary elements are identified both upstream and downstream of the core elements that can influence the efficiency of polyadenylation (Edwalds-Gilbert *et al.,*1997; Lutz*,*2008). In addition to cis-elements, multi-subunit protein factors of the mammalian polyadenylation and cleavage machinery, polyadenylation specificity factor (CPSF), CstF, cleavage factors I_m, II_m (CFI_m, $CFII_m$) and poly(A) polymerase also play an important role in PAS mediated transcript selection (Edwalds-Gilbert *et al.,*1997; Lutz*,*2008). These factors interact to

form a complex on the precursor RNA prior to cleavage and polyadenylation reactions (Figure I-1).

Alternate polyadenylation (APA) can be of three types. In Type I, one polyadenylation signal is present on the mRNA and is splicing independent. In Type II APA, tandem PAS are present in the last exon at the 3' end. Both Type I and II APAs result in mRNA transcripts encoding the same protein. Type III APA has two different terminal exons using two different C-terminal ends. With alternate splicing, they are processed into different mRNAs by using the PAS on one exon or skipping/splicing the entire exon to use the second PAS (Figure I-2). In most cases APA coupled splicing results in different proteins (Edwalds-Gilbert *et al.,*1997; Lutz*,*2008; Tian *et al.,*2005).

Effective strength of a PAS site can be an important balance for controlling gene expression. Changing the efficiency of PAS can impact the amount of gene expression. Both cis-elements like upstream elements of the canonical PAS and trans-factors like the cleavage and polyadenylation stimulation factor dictate the 'strength' of one polyadenylation factor over the others (DeZazzo and Imperiale*,*1989; Edwalds-Gilbert *et al.,*1997; Lutz*,*2008). Polyadenylation enzyme activity has been shown to increase when cells proceed from G_0 to S-phase of the cell cycle. An increase in polyadenylation of mRNA was observed as a response to entry into S phase in 3T6 fibroblasts and primary human splenic B cells (Coleman *et al.,*1974; Colgan and Manley*,*1997; Edwalds-Gilbert *et al.,*1997; Martincic *et al.,*1998). The 64 kDa subunit of the CstF complex has been shown to increase during progression through the cell cycle. (Edwalds-Gilbert *et al.,*1997; Martincic *et al.,*1998). Increase in polyadenylation activity has been shown to favor the use of the first PAS in the eIF-2α primary transcript leading to an increase in protein synthesis (Edwalds-Gilbert *et al.,*1997; Martincic *et al.,*1998). Mutations to the cis elements of the canonical PAS or the downstream GU-rich sequences have also been shown to affect polyadenylation efficiency. In addition, increased availability and activity of trans-factors like the multi-subunit protein factors of the mammalian polyadenylation

and cleavage machinery-cleavage and polyadenylation polymerase could also influence utilization of PAS. Therefore, both cis elements and trans-factors are important regulators for selecting one PAS over the other in alternate polyadenylated genes.

Transcript Selection

Selection of one PAS over the other can result in the formation of multiple transcripts for the same gene. These transcripts may code for the same protein (Type I and II APA) or code for different proteins (Type III APA). More than half of human genes have been reported to have multiple polyadenylation sites (Tian *et al.,*2005). Alternate processing or recognition of the polyadenylation signal defined as alternate polyadenylation (APA), is being recognized as an important mechanism regulating gene expression. APA could dictate transcript stability, localization and transport (Sandberg *et al.,*2008). Multiple transcripts have been found to be present in different stages of the cell cycle, tissues and developmental stages (Ji *et al.,*2009; Wang *et al.,*2008a). Multiple transcripts have often been suggested as a possible mechanism of evolution for phenotypic complexity in mammals (Edwalds-Gilbert *et al.,*1997; Johnson *et al.,*2003). However, the extent to which a differential abundance of these transcripts is used to regulate mRNA and protein expression in cellular proliferation and in response to environmental stress is poorly understood.

Recent studies have identified selection of transcripts as being one of the key factors responsible for transformation. Mayr *et al.* has shown that cancer cells express higher levels of oncogenes carrying the shorter 3' UTR compared to non-transformed cells, suggesting that the selection of the shorter transcripts could facilitate carcinogenesis. The full length 3' UTR is believed to maintain the normal functions of proto-oncogenes in normal cells. Expression of the truncated 3' UTR was also associated with an increase in their corresponding protein levels. Truncation of the 3' UTR could thereby be a mechanism to activate proto-oncogenes by escaping the regulatory

mechanisms that are effective for the full length 3' UTR (Mayr and Bartel,2009). Additional studies also report the abundance of shorter 3' UTRs of a variety of genes correlating with proliferation in primary murine CD4+ T lymphocytes that is independent of transformation status. The authors identified several miRNA regulatory elements on the full length 3' UTR of the Huntington interacting protein (Hip2) gene. Deletion of the predicted target sites of the miRNAs could reverse the reduced protein expression conferred by the 3' UTR (Sandberg *et al.,*2008).

The above literature supports our hypothesis that changes in cellular redox environment during quiescent and proliferative growth states could be regulated by a preferential selection of antioxidant enzyme transcripts: shorter transcripts leading to more protein levels thereby protecting quiescence, and longer transcripts leading to lower protein levels facilitating proliferation.

Cellular Antioxidant Enzymes

Antioxidant enzymes, *e.g*. MnSOD, CuZnSOD, GPx-1 are known to have multiple transcripts. These genes are well known to regulate cellular redox environment. Enzymatic reactions of superoxide dismutase (SOD) convert superoxide to hydrogen peroxide; catalase and glutathione peroxidases (GPx) neutralize hydrogen peroxide and organic hydroperoxides. Mammalian cells have three SODs; MnSOD located in the mitochondrial matrix, EcSOD in the plasma membrane and extracellular space, and CuZnSOD in the cytosol, nucleus, peroxisome, and intermembrane space of mitochondria (Folz and Crapo,1994; McCord and Fridovich,1969; Valko *et al.,*2006; Zelko *et al.,*2002). Different isozymes of GPx and peroxiredoxin (Prx) are found in most subcellular compartments (Huang and Philbert,1995), while catalase is localized primarily in peroxisomes (Yamamoto *et al.,*1988). The primary function of antioxidant enzymes is protection against elevated levels of ROS (McCord and Fridovich,1969). In addition, antioxidant enzymes also regulate physiologic process involving ROS. In 1995,

reports confirmed that MnSOD activity and protein was decreased during the phase of DNA synthesis (S-phase) compared to quiescence (G_0), whereas CuZnSOD activity was higher during S-phase as compared to G_0 phase (Oberley *et al.,*1995). This strongly suggests the possibility that increased MnSOD may correlate with decreased cell proliferation and suggests alterations in SOD activities during the cell cycle. MnSOD activity was also found to be elevated in confluent WI38, human embryonic lung fibroblasts compared with cells in exponential phase (Oberley *et al.,*1989). Interestingly, inhibition of enzymes activity by microinjection of anti-CuZnSOD and anti-GPx antibodies into human fibroblasts and bovine chondrocytes, resulted in accelerated cell proliferation in case of anti-CuZnSOD antibody, while anti-GPx antibody inhibited cell proliferation (Michiels *et al.,*1988). Earlier reports have also shown that transfection of cDNA for MnSOD into cultured melanoma cells protected cells from the transformed phenotype and suppressed the expression of proliferating cell nuclear antigen, a marker of cellular proliferation (Church *et al.,*1993). In 1998, Li demonstrated that NIH 3T3 cells overexpressing MnSOD showed decreased cell growth corresponding to increased steady state levels of ROS and decreased glutathione levels during mitosis (Li and Oberley*,*1998; Li *et al.,*1998). Consistent with earlier reports, we have also shown previously that overexpression of MnSOD inhibits age-associated increase in cyclin dependent kinase inhibitor (p16) protein levels, and protects the proliferative capacity of normal human skin fibroblasts. In contrast, overexpression of a dominant negative mutant form of MnSOD inhibits quiescent fibroblasts' entry into the proliferative cycle (Sarsour *et al.,*2008). Taken together, these reports suggest that antioxidant enzyme expression is critical during proliferation by controlling the intracellular redox balance. Our results suggest that this delicate balance could be maintained by preferential selection of transcripts encoded by antioxidant genes.

MnSOD: Structure and Regulation

MnSOD is a homotetramer, with individual subunit weight of about 23,000 Da (Zelko *et al.,*2002). The locus for mitochondrial SOD has been assigned to chromosome 6. Human MnSOD gene consists of 5 exons, interrupted by 4 introns (Wan *et al.,*1994). A distinctive transcription initiation site was identified 74 bp upstream from the translation start site. This transcription initiation site is preceded by a GC-rich promoter region (78%) containing a cluster of transcription factor binding sites like seven specificity protein (SP-1) and three activating protein (AP-2) consensus sequences with no TATA box or CAAT box.

Although MnSOD is present at basal levels in normal tissues; its expression is also highly inducible, indicating that MnSOD is a stress responsive gene. Binding of transcription factor SP-1 is essential to the constitutive expression of the gene, whereas binding of transcription factor AP-2 is antagonistic (Xu *et al.,*1999a; Xu *et al.,*1999b; Zhu *et al.,*2001). Colon cancer cells have mutations in the promoter region increasing AP2 binding sites, resulting in reduced MnSOD transcription (Xu *et al.,*1999a; Xu *et al.,*1999b).

MnSOD has also been shown to be post transcriptionally regulated by alteration in mRNA stability and/or mRNA translational rate. Destabilization of the MnSOD mRNA is mediated by a ~280 base sequence element within the coding region of the rat MnSOD mRNA that is functional during both basal and stimulus-dependent gene expression (Davis *et al.,*2001). A 41-base region located 111 bases downstream of the stop codon in rat MnSOD has been identified as the 3' UTR cis element involved in protein binding. Translation of MnSOD RNA from which the 3' UTR element was deleted decreased 60% compared with translation of MnSOD RNA containing the 3' UTR cis element as seen in rat reticulocyte lysate system (Chung *et al.,*1998). These results indicated that the 3' UTR of MnSOD may function as an important control for regulating translational efficiency. The results from *in vitro* experiments in rat lung

fibroblast RFL-6 cells indicate that MnSOD RNA binding protein (MnSOD-BP) is post-translationally modified by tyrosine phosphorylation and that the dephosphorylated protein is more active in binding to the MnSOD 3' UTR cis element. In the cell culture studies, data show that inhibition of tyrosine kinase increases MnSOD-BP activity and also elevates level of MnSOD protein without changes in MnSOD RNA concentration (Chung *et al.,*1998). Caloric restriction has been shown to alter lysine acetylation in mitochondrial proteins including MnSOD.

While there are reports of multiple MnSOD mRNAs in different species, humans have two transcripts of length1.5 and 4.2 kb respectively due to the presence of tandem PAS on the 3' UTR (Figure I-3). The MnSOD mRNAs share the identical coding region and differ only in the length of their 3' UTR, 0.24 kb and 3.4 kb, respectively. The longer mRNA transcript (4.2 kb) contains several regulatory elements like the AU-rich elements and miRNA seed matches (Figure I-4). mRNA binding proteins and miRNAs can bind to sequences in the 3' UTR of the longer transcript and result in either stabilization or destabilization of the mRNA (Gorospe,2003; Goswami *et al.,*2000; Wang *et al.,*2008b). The longer mRNA transcript (4.2 kb) contains regulatory elements like ~8 AU-rich elements ($A(U)_{3-7}A$) and several miRNA seed matches (miRNA 377, 222, 21) (Church,1990; Liu *et al.,*2009; St Clair and Oberley,1991; Wang *et al.,*2008b). AU-binding proteins and miRNAs can bind to sequences on the 3' UTR of the longer transcript and result in either stabilization or destabilization of the mRNA (Gorospe,2003; Goswami *et al.,*2000). Variability in the relative level of the two MnSOD mRNAs have been previously reported (Melendez and Baglioni,1993; Yan *et al.,*1996), but functional significance of the relative abundance of the two transcripts is largely unknown. Level of MnSOD expression may be optimally regulated by producing at high rate an unstable mRNA (4.2 kb) and at low rate a stable mRNA (1.5kb) coding for the same enzyme. The benefit of this type of regulation is proposed to be response of cells to an increase of

oxidative stress by rapidly increasing the levels of the unstable 4.2 kb mRNA followed by a gradual accumulation of the stable 1.5 kb mRNA (Melendez and Baglioni, 1993).

MnSOD regulation is a highly complex process. Apart from transcriptional and post-transcriptional regulation, MnSOD levels inside the cell can also be tightly controlled by post-translational modifications. In quiescent cells, MnSOD has been found to be up-regulated due to FOXO dephosphorylation/activation which protects it from oxidative stress (van der Horst and Burgering, 2007). Decreased MnSOD enzyme activity in acutely rejecting cardiac allografts has been attributed to a post-translational modification related to nitration arising via an iNOS-dependent pathway (Nilakantan *et al.,* 2005).

MnSOD as a Molecular Player in Cell Cycle Progression

MnSOD is a nuclear encoded mitochondrial matrix localized antioxidant enzyme. It is a 88 kDa metalloprotein which catalyzes the dismutation of superoxide radicals to oxygen and hydrogen peroxide. Alterations in intracellular redox environment have been long believed to play a regulatory role in modulating gene expression. MnSOD is a key player in maintaining the intracellular redox balance and has been shown to regulate transition between quiescence and proliferation. Decreased MnSOD activity has been found during S-phase of the cell cycle (Seegal *et al.,* 1997) and increased MnSOD activity has been correlated with inhibition in cell proliferation (Sarsour *et al.,* 2005; Sarsour *et al.,* 2008; Seegal *et al.,* 1997). MnSOD protein levels and mRNA has been showed to be reduced in human cancer cells and transformed cell lines (Oberley, 2001; St Clair and Oberley, 1991; Yan *et al.,* 1996). SV40 transformed W138, human embryonic lung fibroblasts have been shown to have lower MnSOD activity and protein than the non-transformed counterpart (Oberley *et al.,* 1989). Transfection of MnSOD cDNA into cultured melanoma cells inhibited the transformed phenotype and also suppressed the

expression of proliferating cell nuclear antigen, which is a marker of cellular proliferation (Church *et al.,*1993).

These observations led to the hypothesis that an antioxidant gene MnSOD could be an effective tumor suppressor (Church *et al.,*1993; Oberley,2001; Oberley,2005; Oberley and Buettner,1979). Nude mice when injected with adenoviral constructs of MnSOD showed inhibited tumor cell growth and extended survival compared to the parental cell line (Weydert *et al.,*2003). Ectopic expression of MnSOD has been shown to significantly inhibit tumor growth *in vivo*. Thus, in malignant cells when oncogenes express higher abundance of truncated 3' UTR to express more of the growth-promoting proteins, one would expect tumor suppressor genes to express higher abundance of the full length 3' UTR to maintain a lower level of the growth-inhibitory proteins.

Cell Cycle and Intracellular Redox State

Cell growth is a tightly regulated sequence of events from G_0 (quiescence) /G_1 to S (DNA synthesis) to G_2/M (mitosis) phases. Progression through the proliferative cycle is orchestrated by a sequential and periodic activation of the positive regulators, cyclins and cyclin dependent kinases (CDKs). Progression from G_0/G_1 to S is largely regulated by the D-type cyclins in association with CDK4/6, and cyclin E/CDK2 kinase complexes (Grana and Reddy,1995; Sherr,1993; Sherr,1995). The cyclins associated with G_1/S progression in mammalian cells are D (with three isoforms, D1, D2 and D3), and E. The cyclin D1/CDK4/6 kinase complex functions in early G_1 while cyclin E/CDK2 is activated during late G_1 and S phases (Ohtsubo and Roberts,1993). The cyclin D1/CDK4/6 kinase complex partially phosphorylates the retinoblastoma (Rb) protein causing a conformational change that releases the E2F family of transcription factors. E2F activates the expression of multiple S-phase specific genes that are required for DNA replication and progression through S-phase (Sherr,1995). The cyclin A/CDK2 kinase complex regulates progression through S and G_2 phases, while cyclin B1/CDK1

kinase complex along with Cdc25C phosphatase, regulates progression from G_2 to M phase. While cyclins are the positive regulators of cell cycle progression, cyclin dependent kinase inhibitors (CKIs) are the negative regulators of progression. The INK family of CKIs (p15, INK4B; p16, INK4A; p18, INK4C; p19, INK4D) specifically inhibits cyclin D/CDK4-6 kinase complexes. The KIP family of CKIs (p27 and p57) inhibits mainly cyclin E/CDK2 kinase complexes (Figure I-5). The inhibitory effect of p21 is ubiquitous and it can inhibit all cyclin/CDK kinase activities. Because cyclins are the positive regulators of cellular proliferation, cyclin D1 and cyclin B1 protein levels are often used as indicators of cells entering into and exiting from the proliferative cycle. Although, the exact mechanistic role of intracellular redox state on regulation of cell cycle protein expression is not clearly understood, cell cycle regulators like Cdc25, p21 and Rb, cyclin D1/Cdk (Esposito *et al.,*1997; Savitsky and Finkel*,*2002; Sekharam *et al.,*1998; Yamauchi and Bloom*,*1997) have been shown to be redox regulated. Consistent with the theory of redox regulation of the cell cycle, we have recently shown that overexpression of MnSOD inhibits age-associated increase in cyclin dependent kinase inhibitor (p16) protein levels, and protects the proliferative capacity of normal human skin fibroblasts cultured in vitro (Sarsour *et al.,*2005; Sarsour *et al.,*2008). Overexpression of a dominant negative mutant form of MnSOD inhibits quiescent fibroblasts' entry into the proliferative cycle (Sarsour *et al.,*2005). MnSOD activity-dependent regulation of quiescent fibroblasts' entry into the proliferative cycle was associated with the activation of G_1- and mitotic-cyclins (Sarsour *et al.,*2005). Cyclin D1 in association with cyclin dependent kinases (CDK4/6) has been shown to regulate transition from quiescence to the proliferative cycle (Grana and Reddy*,*1995; Muller *et al.,*1993; Sherr*,*1993; Sherr*,*1995).

Quiescence

The mammalian cell cycle can also be divided into the quiescent (G_0) and proliferative (G_1, S, G_2, and M) growth states. In response to mitogenic stimuli, quiescent cells enter the proliferative cycle, eventually transiting back to quiescence. This return to G_0 state is essential to prevent aberrant proliferation as well as protecting cellular lifespan. Unlike differentiation, which is an irreversible growth arrest, quiescence is a reversible process that protects the proliferative capacity of cells and is essential for cell and tissue renewal. Mammalian cells are responsive to the presence or absence of mitogens in this period of the cell cycle only. The absence of mitogens at other times, does not affect cell cycle progression and the cells will proceed through S, G_2 and M phases (Coller,2007; Pardee,1974). As early as 1974, Pardee reported of a quiescent state that cells enter in response to suboptimal conditions, and named it the "restriction point"; a point in the cell cycle at which cells can leave and re-enter the cell cycle (Coller,2007; Pardee,1974).

MnSOD and Cellular Response to Environmental Stress

Irradiation

Irradiation induces superoxide radicals and MnSOD is known to scavenge superoxide. Metal ions (Cu+, Fe 2+) may undergo Fenton and Haber-Weiss reaction to generate hydroxyl radical, which can damage DNA bases, and act as pathological mediators of disorders like cancer (Guo *et al.,*2003). In response to these stresses, cells induce the synthesis or activate proteins with antioxidant protective capacity. Previous studies have shown induction in MnSOD activity, immunoreactive protein and mRNA postirradiation (Guo *et al.,*2003; Macmillan-Crow and Cruthirds,2001). MnSOD expression has been shown to be induced by single or multiple doses of ionizing radiation (Guo *et al.,*2003). Pre-treatment with antioxidant enzymes have also been reported to reverse ionizing radiation induced cytotoxicity (Robbins and Zhao,2004). Therefore

induction of MnSOD by environmental stress like ionizing radiation could be an adaptive response. Recent work from our lab has also shown that late ROS accumulation in CuZnSOD overexpressing human glioma cells confers radioresistance (Gao *et al.,*2008). Significant increase in cellular ROS levels in MnSOD (-/-) mouse embryonic fibroblasts (MEF) has been shown at 72 h post irradiation as compared to wild type MnSOD (+/+) MEFs (Du *et al.,*2009). This is also consistent with previous observation in our lab that showed late accumulation of ROS by an increase in DHE fluorescence in 2-8 days postirradiation of glioma cells (Gao *et al.,*2008). It is currently unknown whether a preferential transcript selection could regulate MnSOD mRNA levels (and subsequently its protein and activity) in irradiated cells.

Polychlorinated Biphenyls

Polychlorinated biphenyls (PCBs) are a group of widely dispersed environmental pollutants. PCBs were used as coolants and lubricants in transformers and as a dielectric in capacitors [5]. These compounds are ubiquitous environmental contaminants resulting from intensive industrial uses, improper disposal practices, and unintentional releases. PCBs are strongly lipophilic and highly stable compounds. These characteristics cause them to bioaccumulate in the food chain and concentrate in the fatty tissue, including breast tissues (Falck *et al.,*1992; Johansen *et al.,*1994; Oakley *et al.,*1996; Quinsey *et al.,*1995). Over a period of more than 50 years of their use in the United States, it has been observed that PCBs can have adverse biological effect and can cause carcinogenicity, apoptosis, neurotoxicity, estrogenicity, insulin release, neutrophil function, and aberrant calcium regulation (Fischer *et al.,*1999; Ganey *et al.,*1993; Korach *et al.,*1988; Seegal *et al.,*1997; Wong and Pessah*,*1996; Wong and Pessah*,*1997). The persistence and ubiquitous distribution of these compounds cause them to remain potentially serious hazards to human and animal health and hence their use was banned by the United States in 1977. In spite of the official ban on their use, it has been observed

that serum levels of PCBs in Americans average about 10 ppb (~30 nM); and occupationally exposed individuals may have PCB blood levels in the hundreds of ppb (Warshaw *et al.,*1979). Recently in 2003, PCB blood levels in individuals living in Anniston, Alabama have been found to vary widely, 0.003 – 6.5 μM (Hansen *et al.,*2003). PCB levels in adipose tissue are much higher than those in blood, with levels in low ppm range (Johnson-Restrepo *et al.,*2005). While the mechanisms regulating the biological effects of PCBs are not completely understood, recently reported literature suggests that the PCB-induced perturbation in cellular redox environment could regulate many of the biological effects of PCB exposures (Oakley *et al.,*1996; Song *et al.,*2008a; Song *et al.,*2008b; Venkatesha *et al.,*2008).

The biological effects of individual PCBs are determined by the number and position of chlorines in the biphenyl rings, which also determine their chemical and physical properties. PCBs in general and lower halogenated PCBs in particular are metabolized by microsomal enzymes to mono- and di-hydroxy metabolites. Metabolism of the di-hydroxy metabolites, catechols and hydroquinones, may result in semiquinones and quinones that are highly reactive electrophiles (Srinivasan *et al.,*2001). There are at least two mechanisms by which PCB metabolites can produce ROS: (a) autoxidation of di-hydroxy PCBs, and (b) reduction of quinones via Michael addition of GSH with autoxidation. There is considerable evidence that semiquinone radical can be a primary source for formation of hydrogen peroxide from the hydroquinone/quinone redox system (Eyer*,*1991; Guo *et al.,*2002; Hall *et al.,*1994; Song *et al.,*2008a; Song *et al.,*2008b; Song *et al.,*2009). Lower chlorinated biphenyls are capable of getting metabolized by cytochrome P450 CYP 1A1, 1A2, 2B1/B2 to mono and dihydroxylated intermediates which finally forms quinines (Song *et al.,*2009). Quinones are reactive electrophiles which can undergo Michael addition with intracellular nucleophiles like GSH, amino acids, proteins and nucleic acids. Quinones can also be reduced to semiquinone radical which will further lead to formation of superoxide (Song *et al.,*2009). Superoxide will

dismutate to hydrogen peroxide and eventually form hydroxyl radical. These reactive oxygen species will not only exhaust antioxidants, but also oxidize lipids, proteins and DNA resulting in oxidative imbalance (Song *et al.,*2008b). Greater the number of chlorine atoms on the quinone ring, higher is the steady-state level of semiquinone radicals at neutral pH (Song *et al.,*2008a). Consistent with these earlier reports, we have previously shown that 4-Cl-BQ undergoes redox-cycling resulting in increased production of superoxide and hydrogen peroxide (Venkatesha *et al.,*2008). We used electron paramagnetic spectroscopy to demonstrate that a semiquinone radical was formed in 4-Cl-BQ-treated MCF-10A human non-malignant breast epithelial cells, suggesting that this species could be the source of the apparent higher flux of ROS levels (Venkatesha *et al.,*2008).

In 2003, a report showed that 30 years after accidental contamination of rice oil with PCBs in Japan, high concentrations of PCBs and low concentrations of CuZnSOD persisted in serum of the victims (Shimizu *et al.,*2003).The enzyme activity for SOD, catalase and GPx was shown to be down-regulated in Aroclor 1254 exposed Leydig cells (Murugesan *et al.,*2008). Simultaneous administration of Vitamin E and C could reduce oxidative stress in Aroclor 1254 treated rat sertolli cells. Vitamin E could also protect PCB 77 mediated endothelial cell activation (Senthil kumar *et al.,*2004; Slim *et al.,*1999). We are presenting data demonstrating that PCB 3 metabolite downregulates MnSOD expression in MCF 10A quiescent human mammary epithelial cells and inhibits quiescent cells re-entry to the proliferative cycle. PCB 3 metabolite induced inhibition during transition from quiescent to proliferative growth state is associated with a significant suppression in cyclin D1 accumulation.

Select PCB congeners including Arcolor 1254 have been shown to rapidly increase levels of intracellular free calcium in rat insulinoma cells, RINm5F. Increase in extracellular free calcium induced the release of insulin (Fischer *et al.,*1999). Offspring of Sprague-Dawley rats exposed to PCBs from gestational day 6 showed significant

decreases in dopamine and its metabolite concentrations when sacrificed on postnatal days 35-90 (Seegal *et al.,*1997).

Epidemiological studies indicate that exposure to PCBs might be causally linked to an increased incidence of hepatocarcinoma, breast cancer and prostate cancer (Espandiari *et al.,*2003a; Oakley *et al.,*1996; Ritchie *et al.,*2003). Epidemiological studies also indicated increased mortality of capacitor and electric utility workers from various cancers (Bertazzi *et al.,*1987; Brown,1987; Gustavsson *et al.,*1986; Loomis *et al.,*1997; Sinks *et al.,*1992). Recent evidence suggests that exposure to PCBs might be causally linked to an increased incidence of breast and prostate cancer (Demers *et al.,*2002; Falck *et al.,*1992; Laden *et al.,*2002; Moysich *et al.,*2002; Ritchie *et al.,*2003). Metabolites of PCB3 are known to possess tumor initiating activities in rat liver (Espandiari *et al.,*2003a; Espandiari *et al.,*2004). Commercial PCB mixtures have been shown to act as tumor promoters in two stage hepatocarcinogenesis (Glauert, 2001, Safe, 1989). The mechanism of their tumor promoting activity is not clearly known, but oxidative stress has been suggested as a possible mechanism. Rats receiving biweekly injections of PCB 77 and PCB 153 formed higher numbers of placenta glutathione S-transferase (PGST) positive foci, with higher number seen with PCB 77 treatment. The same rats also showed significant increase in NFκβ and AP-1 binding activities in their hepatic nuclear extracts. NFκβ and AP-1 are well known oxidative stress-response transcription factors. Cell proliferation as shown by increase in 5-bromo-2'-deoxyuridine (BrdU) uptake was also higher in the focal hepatocytes by PCB 77 treatment (Tharappel *et al.,*2002).

PCB3 and its dihydroxylated metabolites have also been shown to upregulate prostaglandin H synthase (PGHS) in 'hormonally sensitive' tissues like prostate, breast, and ovary. PGHS has both cycloxygenase and peroxidase activity (Wangpradit *et al.,*2009). Increased levels of cycloxygenase-2 and peroxidase activity have been correlated with higher incidence of prostate cancer (Yoshimura *et al.,*2000). Non-coplanar PCBs are constitutive androstane receptor (CAR)-activators (*e.g*. PCB153) and

have been suggested to increase the risk of prostate cancer presumably via the Cytochrome P450 mediated metabolism by activating CYP2 gene family of Phase I enzymes (Ritchie *et al.,*2003). PCBs that are coplanar bind to aryl hydrocarbon receptor (AhR) and exhibit Ah receptor agonist activity (Safe*,*1993). They are known to activate CYP1 gene family of Phase I enzymes. Higher levels of PCBs have also been identified in breast adipose tissue of breast cancer patients than in benign patients in an epidemiology study, associating breast cancer to PCB exposure (Aronson *et al.,*2000; Bake *et al.,*2007; Demers *et al.,*2002; Falck *et al.;* Furst*,*2006). PCBs irrespective of their planarity have been linked to be responsible for developmental and reproductive toxicity, skin lesions, endocrine effects, hepatotoxicity, carcinomas by the induction of Phase I and Phase II drug metabolizing enzymes (Espandiari *et al.,*2003a; Falck *et al.,*1992; Safe*,*1993; Seegal *et al.,*1997; Zheng *et al.,*2000).

We used PCB 153, 2-(4 chlorophenyl)benzo-1,4-quinone (4-Cl-BQ) and Aroclor 1254 in our study. The structures of these compounds are illustrated in Figure I-6. PCB 153 is a constitutive androstane receptor (CAR) agonist and is known to be highly stable. Also, elevated levels of PCB 153 have been isolated in human milk from PCB exposed individuals (Johansen *et al.,*1994; Quinsey *et al.,*1995). 4-Cl-BQ is a metabolite of PCB 3 and because of its quinone like structure, it undergoes redox cycling. There is considerable evidence that semiquinone radicals generated from the hydroquinone/quinone redox system can be a primary source for formation of ROS (Eyer*,*1991; Guo *et al.,*2002; Hall *et al.,*1994; Song *et al.,*2008a; Song *et al.,*2008b; Song *et al.,*2009). Aroclor 1254 was a commercially available mixture (Ballschmiter and Zell*,*1980). The first two digit of the numbers following Aroclor signifies the number of carbon atoms in the biphenyl ring, and the last two digits represents the percent of chlorine by mass.

Overall, compelling evidence from previous literature reports support our hypothesis of preferential selection of MnSOD transcripts in response to environmental

stress. Our data indicate that MnSOD gene expression is regulated in human cells such that proliferation is associated with abundance of full length 3' UTR, 4.2 kb MnSOD transcript and its regulatory capacity. Alternate 3' end processing and preferential abundance of MnSOD transcripts may be means of balancing the redox flux of intracellular MnSOD activity in response to its environment.

Rationale and Hypothesis

MnSOD is an antioxidant gene which plays an important role in transition between quiescence and proliferative growth. Antiproliferative function of MnSOD has also been observed in various cancer cells where ectopic expression of MnSOD has been shown to inhibit tumor growth both *in vitro* and *in vivo*. We have also reported that pre-treatment of cells with a metabolite of environmental pollutant PCB, 4-Cl-BQ resulted in increased degradation of the 4.2 kb MnSOD transcript selectively. This resulted in lowered MnSOD expression in 4-Cl-BQ treated cells thereby inhibiting the entry of quiescent cells into S phase (Chaudhuri *et al.*). The goal of the current work was to investigate the novel hypothesis that the 3' UTR of MnSOD is responsible for regulating the mRNA, protein and activity of MnSOD *via* preferential abundance of its transcripts, in response to growth states and environmental stress. This hypothesis was based on observations that (a) preferential abundance of the longer 4.2 kb transcript during proliferation, (b) abundance of the 4.2 kb transcript during proliferation correlated with decrease in MnSOD protein levels and activity, and (c) the shorter 1.5 kb transcript is enriched in quiescent cells, irradiated cells and cells exposed to 4-Cl-BQ. Based on these observations, the proposed hypothesis will be investigated by accomplishing the following aims:

Specific Aim 1: Determine if the 3' UTR of MnSOD regulates its mRNA and protein levels as well as activity in quiescent and exponential growth, and in response to environmental stress: ionizing radiation and polychlorinated biphenyls.

Specific Aim 2: Determine if polychlorinated biphenyl induced down-regulation of MnSOD expression inhibits quiescent human non-malignant epithelial mammary and prostate cells entry into the proliferative cycle.

Significance

The significance of this research is to establish MnSOD 3' UTR as a novel target that is amenable for molecular manipulations to regulate its protein levels as well as activity. This study also aims to establish transcript selection as a novel mode of MnSOD gene regulation. The regulation of MnSOD gene expression is complex and can occur at many levels, transcriptional, post-transcriptional, translational or post-translational. In addition to the existing knowledge, two human MnSOD mRNA transcripts of 4.2 kb and 1.5 kb in length, have been identified. The presence of multiple PAS in the 3' UTR gives rise to these multiple transcripts. The use of the proximal PAS results in a shorter transcript (1.5 kb) that correlates with more protein, while the use of the distal PAS generates a longer transcript (4.2 kb) that correlates with less protein. The 3' UTR of the 4.2 kb transcript harbors cis-acting elements (*e.g.* AU-rich (AREs) and microRNAs) responsible for regulating the stability and translation of MnSOD.

The proposed research is of highest significance because it addresses a novel mode of gene expression of MnSOD under normal growth conditions and in response to environmental stress. Our results could explain the functions of MnSOD as an inducible gene. Preferential abundance of transcripts in response to intracellular environment could help select to turn on the 'switch' for additional regulation offered by the full length 3' UTR. This fascinating aspect of RNA-biology may have evolved to fine-tune protein levels and functions for key cellular processes. An in-depth understanding of differential abundance of MnSOD transcripts to regulate mRNA and protein expression in cellular proliferation, carcinogenesis and in response to its environment is indispensable to the

development of molecular biology based approaches to mitigate polychlorinated biphenyl and other environmental induced cytotoxicity.

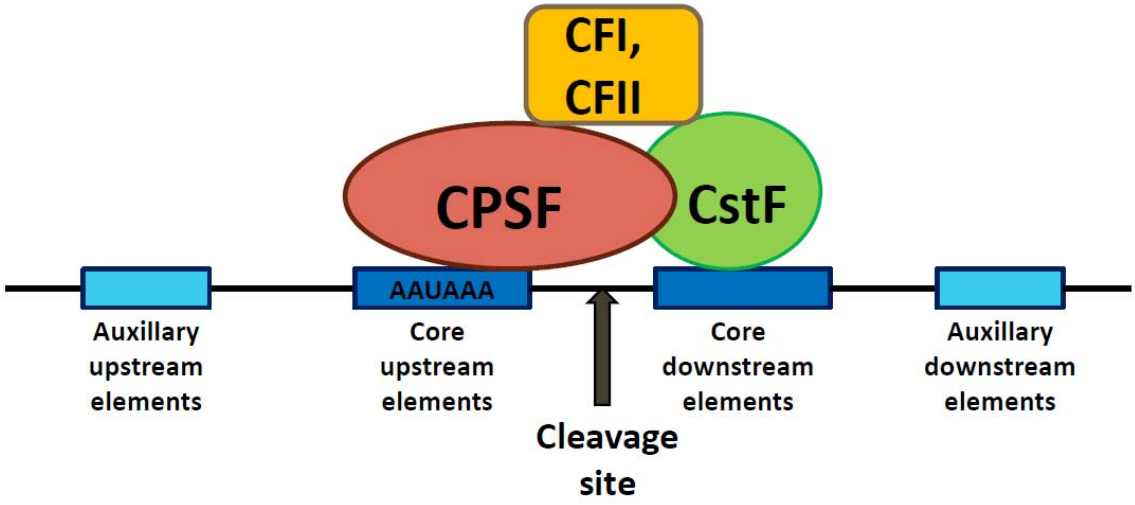

Figure I-1 Schematic illustration of RNA sequences and protein factors involved in polyadenylation. CPSF: cleavage and polyadenylation specificity factor, CstF: cleavage specificity factor, CF: cleavage factors. Adapted from ACS Chem Biol. 2008: 3(10):609-17.

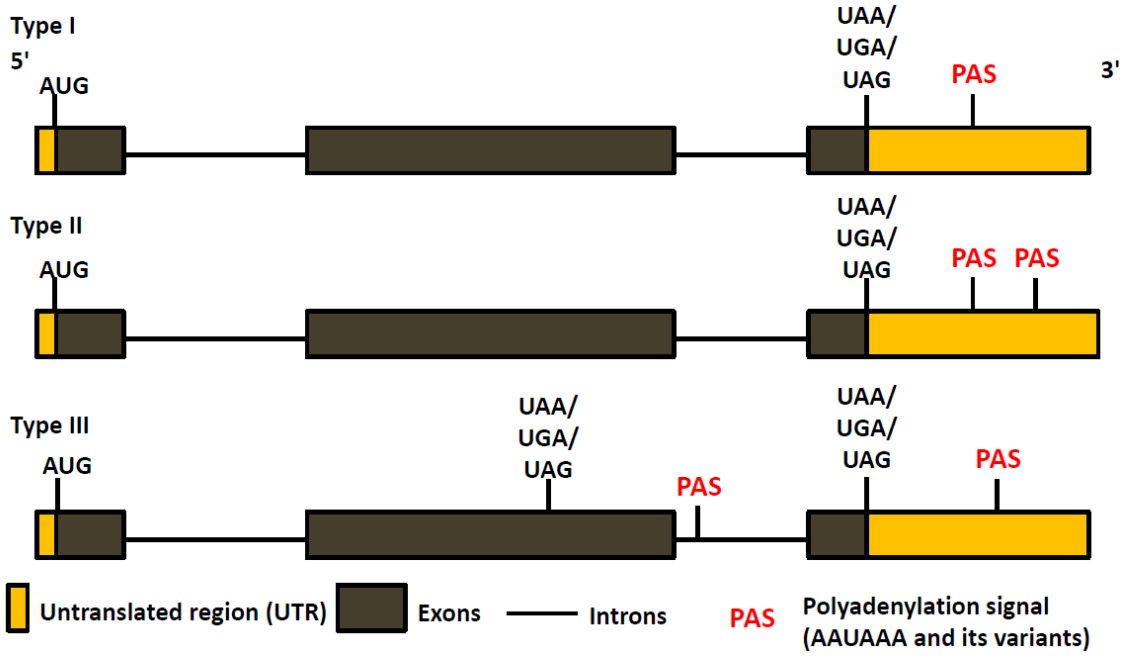

Figure I-2 Types of alternate polyadenylation. Adapted from ACS Chem Biol. 2008: 3(10):609-17.

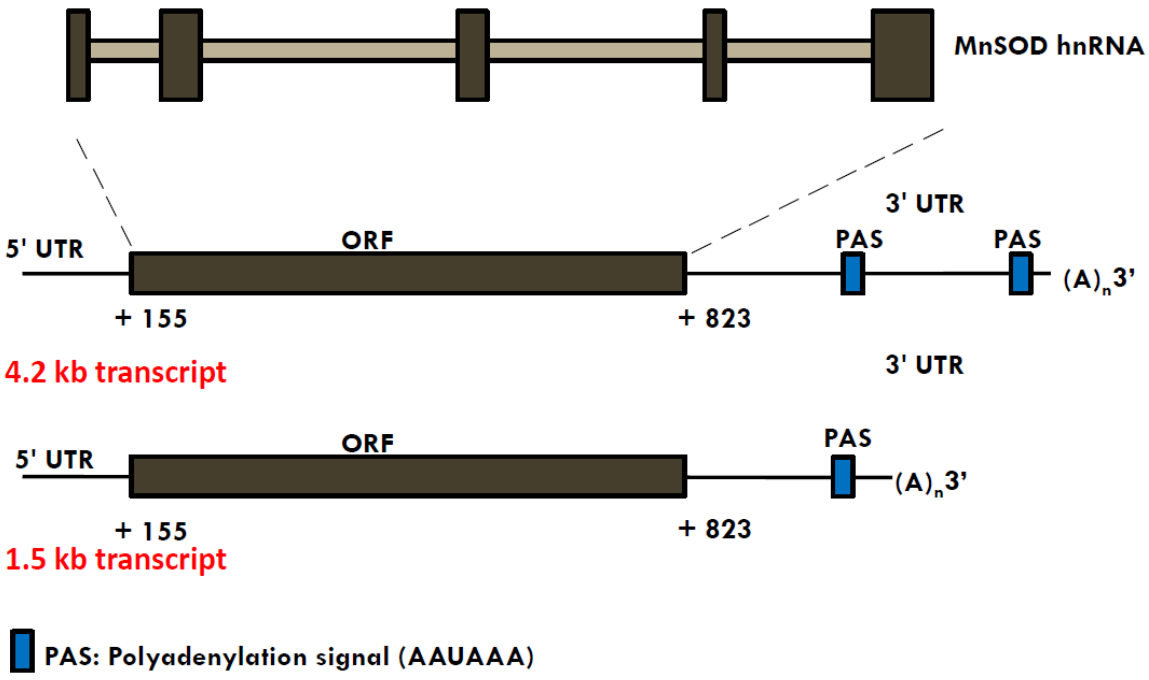

Figure I-3 Schematic illustration of MnSOD gene structure. hnRNA: heterogenous nuclear ribonucleic acid, ORF: open reading frame, MnSOD: manganese superoxide dismutase, UTR: untranslated region.

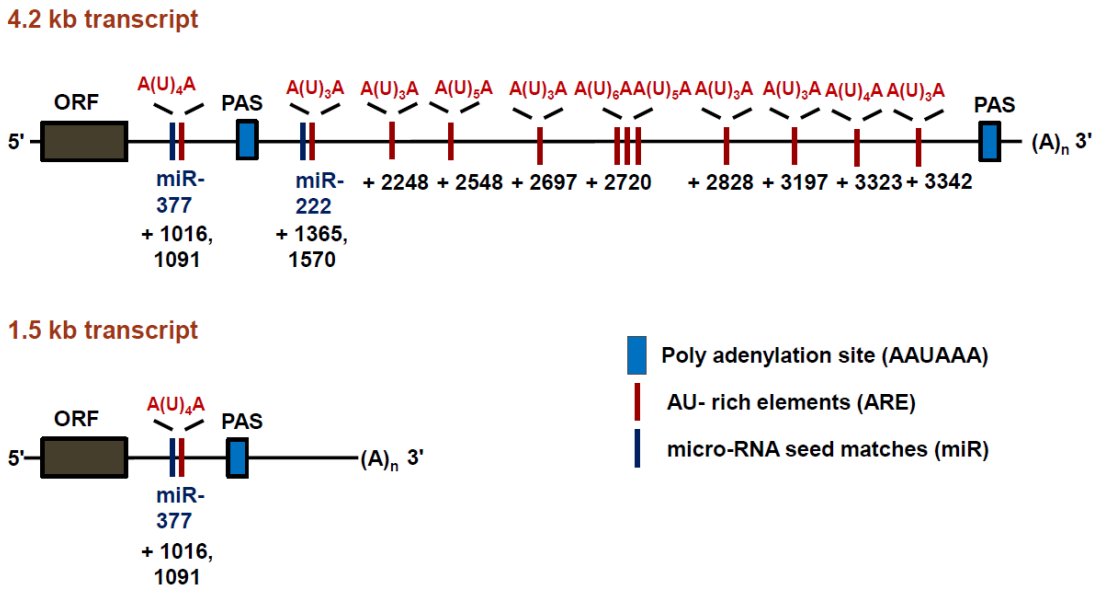

Figure I-4 Schematic illustration of MnSOD 3'UTR: miRNAs and mRNA stability and translational control sequence (Adapted from Biochim Biophys Acta. 1087:250-252; 1990)

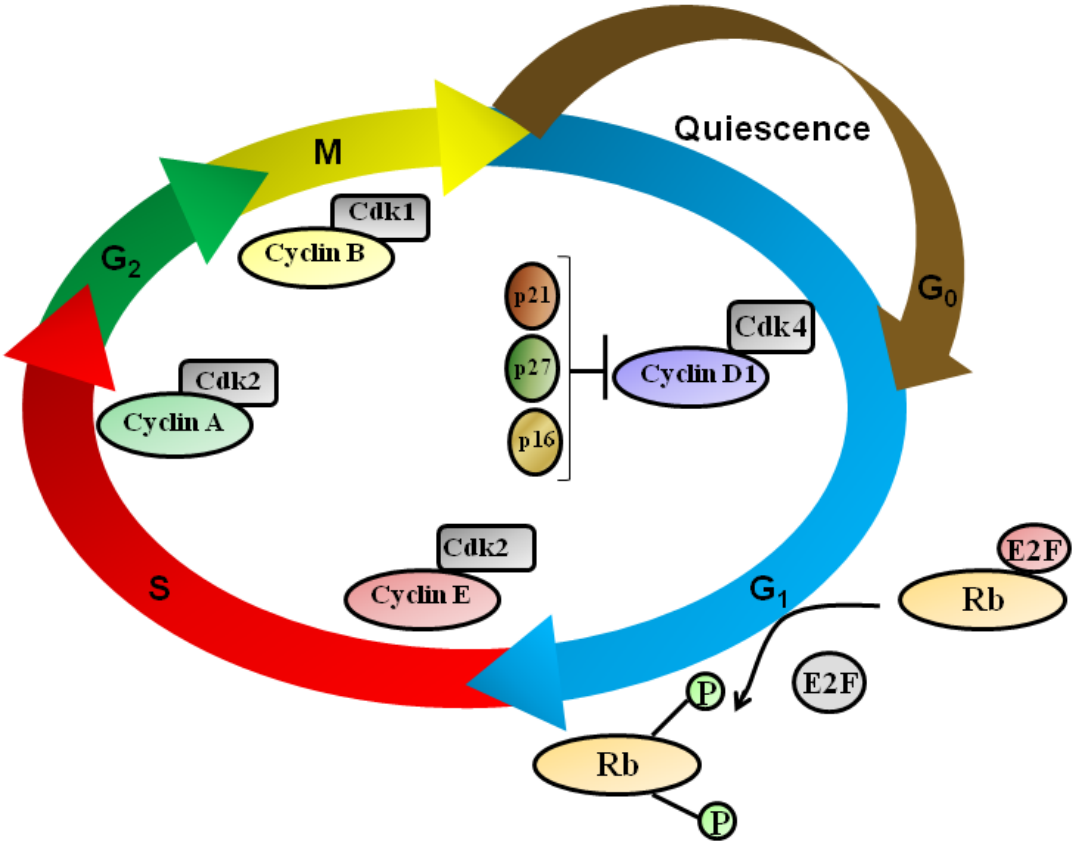

Figure I-5 Schematic illustration of the cell cycle

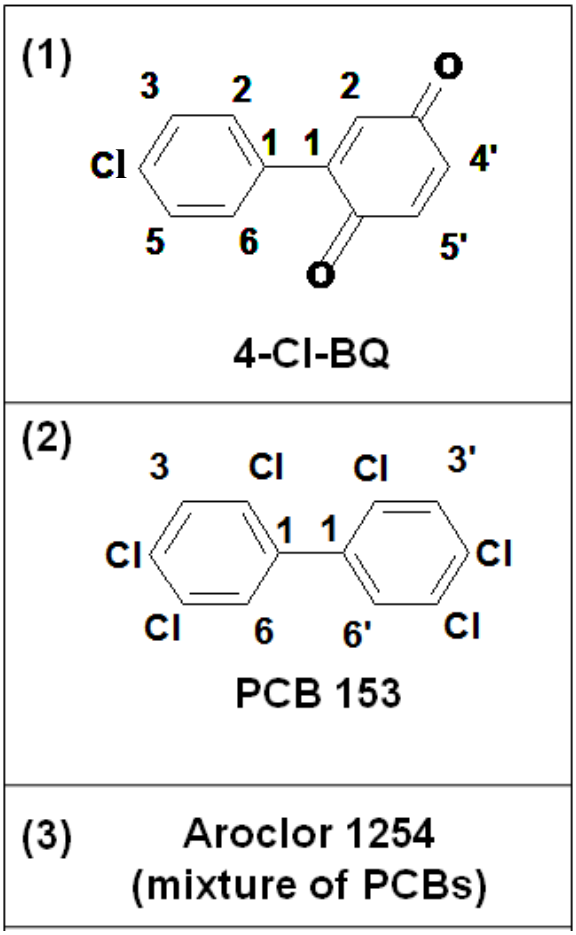

Figure I-6 Structure of PCBs used in our study. Characterization of PCBs in Crit Rev Toxicol. 1990: 20(6):440-96.

CHAPTER II

MATERIALS AND METHODS

Cell Culture and Reagents

MCF-10A human mammary epithelial cells were purchased from the American Tissue Culture Collection (ATCC). MCF-10A cells are spontaneously immortalized cells that possess the characteristics of human normal mammary epithelial cells. Cells were grown in mammalian epithelial growth medium (MEGM, Cell Applications Inc., San Diego, California) supplemented with growth factors and antibiotics following our previously published cell culture protocol (Venkatesha *et al.,*2008). Cells were grown at 37^{o}C, 5% CO_2 and 95% humidity. Cells were sub-cultured upon confluence with 0.25% trypsin and 1% EDTA. Contact inhibited quiescent growth state was achieved by plating cells at a higher density and culturing for an additional 2 days prior to experiments. RWPE-1 human non-malignant prostate epithelial cells were obtained from the American Tissue Culture Collection (ATCC). RWPE-1 cells are spontaneously immortalized and these cells possess characteristics of normal epithelial cells. Monolayer cultures were grown in keratinocyte growth medium (Gibco) supplemented with 10% FBS, growth factors and antibiotics. Cells were grown at 37^{o}C, 5% CO_2 and 95% humidity (Chaudhuri *et al.*). Normal human fibroblasts (NHF) were obtained from Coriell cell repository. Cal 27, SQ20B and FaDu are oral squamous cell carcinoma obtained from ATCC. NHF, Cal27, SQ20B, FaDu cells were grown in Dulbeco minimal eagle media (DMEM) with 10% FBS, 2 ml Fungizone and 6 ml PenStrep. MDA-MB-231 (ER-/PR-/HER2-) cells are adenocarcinoma cells from human mammary gland obtained from ATCC and grown in RPMI media supplemented with 10% FBS, 2 ml Fungizone and 6 ml PenStrep. Sum159 cells (ER-/PR-) were purchased from Asterand plc. Sum159 cells were grown in Ham's

F-12 media with 5% FBS, Insulin and hydrocortisone. H292 is a pulmonary carcinoma cell line and were grown in F-12 media with 10% FBS, 2ml Fungizone and 6 ml PenStrep. All the cancer cell lines used carry p53 mutation. Cell line information is summarized in Table II-1. All cells were grown at 37^{o}C, 5% CO_2 and 95% humidity. Cells were sub-cultured upon confluence with 0.25% trypsin and 1% EDTA.

Chemicals

2-(4-Chlorophenyl)benzo-1,4-quinone (4-Cl-BQ), 2, 2', 4, 4', 5, 5'-hexachlorobiphenyl (PCB 153), and Aroclor 1254 (commercial mixture of various PCB congeners) (Ballschmiter and Zell,1980; Kania-Korwel *et al.,*2005) were provided by Dr. Hans-Joachim Lehmler, Occupational & Environmental Health, University of Iowa. The synthesis and purity of these PCBs were performed following the previously published methods (Amaro *et al.,*1996; Espandiari *et al.,*2003b; Lehmler and Robertson,2001; Schramm *et al.,*1985). PCB stock solutions were made in dimethyl sulfoxide, and appropriate dilutions of the stock solution were added to cell culture medium where the final concentrations of dimethyl sulfoxide were adjusted to less than 0.5%. Control cultures were adjusted to the same concentrations of dimethyl sulfoxide as the PCB treated cells. 4-Cl-BQ dose selection was based on a recent study where it was reported that the blood levels of PCBs in individuals living in Anniston, Alabama varied from 0 - 6.5 μM (Hansen *et al.,*2003). Actinomycin D, polyethylene glycol conjugated (PEG)-superoxide dismutase and catalase were purchased from Sigma Chemical Co. DHE (dihydroxyethidium) and $CDCFH_2$ (5, 6-chloromethyl-2', 7'-dichlorodihydro fluorescein diacetate) were purchased from Molecular Probes (Eugene, Oregon). N-acetyl-L-cysteine (NAC) was purchased from Sigma Aldrich (St. Louis, Missouri). Anti-cyclin D1mouse monoclonal antibody, and anti-MnSOD were purchased from Pharmingen (San Diego, California). Anti-mouse antibody was purchased from Santa Cruz biotechnology, Santa Cruz, California.

Irradiation

Exponentially growing MDA-MB-231 cells (~ 50% confluency) were irradiated with a single dose γ rays by the ^{137}Cs irradiator (JL Shephard, San Fernando, California) in the Radiation Core Laboratory of the University of Iowa. The dose rate was 0.83 Gy/min.

PCB Treatment

Contact inhibited quiescent growth state was achieved by plating cells at a higher density and culturing for an additional 2 days prior to the PCB treatments. The percentage of S phase, less than 2%, was considered a quiescent growth state. Cells were sub-cultured upon confluence with 0.25% trypsin and 1% EDTA. Control and 0-6 μM PCB treated quiescent cells were replated at a lower cell density and cultured for the indicated times in regular growth medium without any PCBs (Chaudhuri *et al.*).

Cell Number Counting and Doubling Time Calculations

Cells were plated in 100 mm or 60 mm dishes. Cells were counted using a Beckman Z1 particle counter (Beckman Coulter, Fullerton, California) at indicated days. Cell population doubling time (Td) was determined by counting cells at the time of replating, and 2, 4, and 6 days post-replating. Td was calculated from the exponential portion of the growth curve using the following equation: $Td=0.693t/\ln(N_t/N_0)$ where t is time in days, and N_t and N_0 represent cell numbers at time t and initial time, respectively.

Propidium Iodide (PI) Staining for DNA Content Measurement

Cells were trypsinized and fixed in 70% ethanol at the time of collection. Cell pellet was washed with phosphate buffered saline (PBS) and treated with RNaseA (0.1 mg/ml) for 30 min followed by staining with PI (35 μg/ ml). DNA content was measured

using flow cytometry. 10,000 events were collected and percent of cells in each phase of the cell cycle was analyzed using MODFIT software.

Bromodeoxyuridine (BrdU) Labeling

Control and PCB treated quiescent cells were replated and incubated with growth medium containing 10 μM BrdU (Sigma Aldrich, St Louis, Missouri). BrdU is a thymidine analog which is preferentially incorporated into cells that synthesize DNA (S-phase). Cells were harvested at indicated times by trypsinization and fixed in 70% ethanol and stored at 4ºC. Ethanol fixed cells were washed with PBS containing 0.1% Tween 20, and treated with Pepsin-HCl (0.3 mg pepsin/ ml 2 N HCl). 0.1 M Borax (pH 8.5) was added to neutralize the HCl and cells were pelleted by centrifugation at 1200 rpm for 5 min. Isolated nuclei were incubated with anti-BrdU antibody (dilution 1:20, Becton Dickinson, San Jose, California) for 1 h at room temperature followed by incubation with fluorescein isothiocyanate (FITC) conjugated goat anti-mouse IgG secondary antibody. Nuclei were then washed with PBS and incubated with 1 mg/ ml RNase A, PI (35 μg/ ml) and cell cycle distribution was analyzed by FACSCalibur (Becton Dickinson, San Jose, California). Red fluorescence from PI was detected through a 640 nm long pass filter and green fluorescence from FITC was detected through a 535 nm band pass filter. Data were collected from 20,000 events and analyzed by using the FlowJo software (Tree star, Inc., Ashland, Oregon). The acquired data were analyzed as dual parameter PI vs. log FITC histograms, and three compartments (BrdU positive S phase, and BrdU negative G_1 and G_2 phases) were identified. The number of nuclei in each compartment was calculated and expressed as percentage of the total gated population.

DHE Fluorescence Measurement

Control and quiescent cells incubated with PCBs were harvested by trypsinizing the monolayer cultures. Cell suspensions were washed with PBS containing pyruvate (5

mM) and incubated with 10 μM DHE for 40 min at 37°C. DHE fluorescence was analyzed by flow cytometry using the excitation wavelength 488 nm, and emission 585 nm (Zielonka *et al.,*2008). The mean fluorescence intensity (MFI) of 10,000 cells was recorded. MFI of cells incubated with buffer alone was used to correct for autofluorescence. The fold change in MFI was calculated relative to the MFI of untreated control cells. The specificity of the DHE fluorescence for the measurement of superoxide was determined by incubating the cells with 100 U/ml PEG-SOD or 18 μM PEG 2 h prior to and during the assay. The fluorescence of cells treated with PCBs and PEG-SOD was subtracted from the fluorescence measured in cells treated with PCBs and PEG, and MFI calculated relative to the difference in untreated control cells that were incubated with PEG and PEG-SOD.

$CDCFH_2$ Fluorescence Measurement

Cellular hydrogen peroxide levels were measured by incubating cells with 5, 6-chloromethyl-2', 7'-dichlorodihydro fluorescein diacetate (CDCFH2, Molecular Probes, Eugene, Oregon). Monolayer cultures of control and cells incubated with PCBs were washed once with PBS, and incubated with 10 μg/mL CDCFH2 for 10 min at 37°C. Cells were harvested on ice, resuspended in PBS, and fluorescence measured by flow cytometry using an excitation wavelength 488 nm and emission 530 nm band-pass filter. An oxidation insensitive chemical, CDCF, was included to account for differences in dye uptake and ester-cleavage. The specificity of the CDCFH2 fluorescence for the measurements of cellular hydrogen peroxide was determined by incubating cells with 100 U/mL PEG-CAT prior to and during the assay. Fluorescence of cells incubated with 18 μM PEG alone was included in the calculation of MFI as described above. These probes do not always detect specific ROS like H_2O_2, but rather detect a broad range of ROS. Furthermore, presence of adventitious Fe^{2+} could also oxidize these probes. It is therefore important to take into account these factors in interpreting the data (Hempel *et al.,*1999).

Protein Isolation and Western Blot Analysis

Cells were collected by scrape harvesting in phosphate buffered saline (PBS) and pelleted by centrifugation. Total proteins extracts were prepared by sonification on ice for 5 pulses of 5 sec each at 32% amplitude using a Vibra Cell cup horn sonicator (Sonics and Materials Inc.). Protein concentrations were determined using Bradford Assay. Equal amounts of total cellular proteins were separated by SDS-PAGE and transferred to 0.45 μm nitrocellulose membrane (BIORAD Labs, Hercules, California) at 100 V for 1 h at room temperature. Blots were incubated with antibodies to cyclin D1 (PharMingen, San diego, California), and MnSOD (PharMingen, San diego, California). Immunoreactive polypeptide was visualized using horseradish peroxidase-conjugated secondary antibodies and enhanced chemiluminescence detection reagents (GE Healthcare, Waukesha, Wisconsin) following manufacturer supplied protocols. Blots were re-probed with antibodies to actin (Santa Cruz Biotechnology, Santa Cruz, California) for comparison of results. The dilutions of antibodies used were as follows: MnSOD, primary: 1:1000, secondary: 1:10,000; cyclin D1, primary: 1:1000, secondary: 1:3000; actin, primary: 1:1000, secondary: 1:3000. Results were quantitated using AlphaImager 2000 (Alpha Innotech, San Leandro, California) and ImageJ software. The images were first corrected for background and then the integrated density value was obtained by selecting the region of interest for each band with fixed area size for all bands. The integrated density values were calculated by using the sum of the gray values in the selection. Actin levels were used to correct for loading in each sample and fold change calculated relative to control.

SOD Biochemical Activity Assay

MnSOD activity was determined by the indirect competitive inhibition assay originally developed by Spitz and Oberley (Spitz and Oberley,1989). A constant flux of superoxide is generated by the conversion of xanthine by xanthine oxidase to uric acid

and superoxide. The superoxide reduces the indicator substrate nitroblue tetrazolium (NBT) and turning it blue. When increasing concentrations of SOD from crude cell extracts present in the reaction, SOD converts the superoxide rapidly to hydrogen peroxide and the rate of NBT reduction is thereby inhibited. This reaction is spectrophotometrically monitored at 560 nm. The activities between CuZnSOD and MnSOD can be distinguished by using sodium cyanide to specifically inhibit CuZnSOD activity. The difference between the total SOD activity and cyanide insensitive MnSOD activity will determine CuZnSOD activity. The protein levels in each sample were measured using the Lowry protein assay (Lowry *et al.,*1951).

Quantitative Real Time PCR Analysis

Total cellular RNA was isolated from control and PCB treated quiescent cells using the Trizol reagent (Invitrogen, Eugene,Oregon). The isolated RNA was quantified using a ND1000 nanodrop spectrophotometer (Nanodrop, Wilmington, Delaware) and one microgram of RNA from each sample was reverse transcribed using the High Capacity cDNA Archive Kit (Applied Biosystems, Foster city, California) for 2 hr at 37^{o}C. Two microlitres of cDNA was subjected to Real Time PCR assay using primers specific to MnSOD (ORF, 4.2 and 1.5 kb transcripts), and 18S; MnSOD ORF, forward primer: 5'-GGCCTACGTGAACAACCTGAA-3', reverse primer: 5'-CTGTAACATCTCCCTTGGCCA-3', amplicon size, 70 bp; MnSOD 4.2 kb transcript, forward primer: 5'-GCTTTGGTGGTGGATTGAAAC-3', reverse primer: 5'-CATCCCTACAAGTCCCCAAAGT-3', amplicon size, 187 bp; MnSOD 1.5 kb transcript, forward primer: 5'-TAATGATCCCAGCAAGATAA-3', reverse primer: 5'-TTTTTTTTTTTTTTTGATGGTTG-3', amplicon size, 184 bp; 18S, forward primer: 5'-CCTTGGATGTGGTAGCCGTTT-3', reverse primer: 5'-AACTTTCGATGGTAGTCGCCG-3', amplicon size, 104 bp. Figure II-1 shows the primer design for selective amplification of the 4.2 kb and 1.5 kb transcripts. The real

time PCR assay was carried out with the 2x Power SYBR Green real time master mix (Applied Biosystems); reverse transcriptase inactivation at 95^{o}C for 10 min, followed by 40 cycles of 95^{o}C for 15 sec and 60^{o}C for 1 min (ABI 7000 Sequence Detection System, Applied Biosystems). A threshold of amplification in the linear range of each sample was selected to calculate the cycle threshold (C_T) for each sample. The relative mRNA levels were calculated as follows: ΔC_T (sample) = C_T (mRNA of interest) - C_T (18S); $\Delta\Delta C_T$ = ΔC_T (post-treatment time point) - ΔC_T (control); Relative expression = $2^{-\Delta\Delta C}{}_T$.

Plasmids

The 3'UTR of MnSOD was amplified by RT-PCR from total cellular RNA isolated from MDA-MB-231 cells and cloned into the NotI and XhoI sites of the psiCHECK-2 reporter vector (Promega). In this way, psiCHECK-2/Δ3'UTR plasmids were generated. The inserts were cloned in the multiple cloning site downstream of the stop codon of SV40 promoter driven Renilla luciferase gene. The primers used for PCR amplification were: 1.5 kb MnSOD transcript, FP: 5' TTTTCTCGAGGCACTGAAGTTCAATGGTGGTGGT-3'; RP: 5'-AAAAGCGGCCGCCCAGGACCTTATAGGGTTTTCAGTATGTACC-3'; Δ2ARE4.2kb, FP: 5'- TTTTCTCGAGGCTCATGCTTGAGACCCAAT-3'; RP: 5'-AAAAGCGGCCGCGCTGAGGTGGGACAATCACT-3'; Δ5ARE4.2kb, FP: 5'-TTTTCTCGAGTCTAGGTGACTCTAACTTCCCTGGC-3'. All plasmids were verified by (a) separating on agarose gel electrophoresis and determining the appropriate size band and (b) sequencing the purified plasmid for correct insertion of DNA in the vector.

Cloning of MnSOD 3'UTR

Total cellular RNA was isolated from exponential and quiescent cells using the Trizol reagent. RNA was quantified using a ND1000 nanodrop spectrophotometer and one microgram of RNA from each sample was reverse transcribed using the High Capacity cDNA Archive Kit for 2 hr at 37^{o}C. Semi quantitative PCR assay was

performed using primers specific to MnSOD (1.5 kb transcript, Δ4.2 kb transcripts), and 18S, FP: 5'-CCTTGGATGTGGTAGCCGTTT-3', RP: 5'-AACTTTCGATGGTAGTCGCCG-3'.We used Expand High Fidelity Taq DNA polymerase (Roche) for generating the 1.5 kb MnSOD transcript insert and the Δ2ARE4.2kb plasmid. The PCR reaction comprised initial denaturation at 94^{o}C for 2 min followed by10 cycles of denaturation at 94^{o}C for 30 s, annealing at 54^{o}C for 30 s followed by extension at 72^{o}C for 2 min. This was followed by 25 cycles of denaturation at 94^{o}C for 30 s, annealing at 54^{o}C for 30 s, extension at 72^{o}C for 2 min + 5 s/cycle, final extension at 72^{o}C for 7 min and 4^{o}C indefinitely. We used Phire Taq DNA polymerase (Finnzymes) for generating the Δ5ARE4.2kb plasmid. The PCR reaction comprised 35 cycles of initial denaturation at 98 ^{o}C for 30 s followed by denaturation at 98^{o}C for 5 s, annealing at 63^{o}C for 5 s, extension at 72^{o}C for 20 s and final extension at 72^{o}C for 1 min followed by 4^{o}C indefinitely. PCR generated inserts were verified by separating on an agarose gel and checking for the matching molecular size of the band. PCR products are purified using a PCR purification kit from Qiagen. Both the psiCHECK 2 vector and the inserts are linearized by using 1 µl each of Not I and Xho I restriction enzymes (New England Biosystems) in a 50 µl total reaction volume. Half a µl of BSA and 5 µl of 10X Buffer R (New England Biosystems) were also added to the reaction. Restriction digestion reaction was carried overnight at 37ºC. Digested products are analyzed by separation on 1 % agarose gel electrophoresis. The appropriate band is cut out and purified using a Gel purification kit (Qiagen). The entire volume of purified digested vector and inserts are ligated using 1.5 µl of T4 DNA Ligase (New England Biosystems). Ligation reaction is carried out at 16ºC overnight. Ten microlitres of the ligated psiCHECK 2-PCR product is used to transform in 50 µL DH5α competent cells. Cells are heat shocked at 42ºC for 45 s in a water bath and immediately transferred to ice for 2 min. Two hundred microlitres of room temperature SOC media is added to the tube containing the cells and incubated for 1.5 h at 37ºC at 200 rpm. The whole transformation

reaction is then plated on LB agar plates containing ampicillin for selection. The plates are incubated overnight at 37ºC and distinct single colonies are picked up the following day. A control plate with only the vector and no insert is included which has very few colonies. The selected clone is cultured overnight at 37ºC in 3 ml LB broth containing ampicillin. The following day, the plasmid is purified from the bacteria using a miniprep kit (Qiagen). The product is tested two fold (a) by separating on a 1% agarose gel electrophoresis and determining the appropriate vector-insert size and (b) sequencing the purified product for presence of insert in the vector. Once the insert was confirmed in the vector, we did large scale amplification and purification of the plasmid DNA using maxiprep kit (Qiagen). This process was repeated for at least three different clones for each plasmid.

Dual Luciferase Reporter Assay

MDA-MB-231 cells were seeded at a density of 1 X 10^5 cells per 24 well dish. Twenty four h later, 100 ng of empty psiCHECK 2 or psiCHECK-2/Δ3'UTR plasmids were transfected. Two microlitres of Lipofectamine 2000 was used as a transfectant per well in a 24 well plate. Forty eight h post-transfection, luciferase activity was measured using Dual luciferase reporter assay system (Promega). Cells were washed with 1X PBS once before adding 100 µl of 1X PBS to 24 well plates. Cells were incubated for 15 min with occasional shaking of the plate to ensure cells do not clump. Twenty microlitres of the lysed cells were collected in BD luminometer tubes and 100 µl of the Luciferase assay reagent (LAR II) was added. Firefly luciferase activity was measured on a moon light luminometer (Pharmingen). Hundred microlitres of the Stop and Glo reagent was added to the same tube and Renilla luciferase was measured using the luminometer.

Since the 3'UTR inserts were cloned downstream of the stop codon of the Renilla luciferase gene, this allows for expression of the Renilla transcript with the specific 3'UTR sequence inserted. Renilla luciferase activity is used to assess the effect of the

specific 3'UTR sequence on transcript stability and translation efficiency. psiCHECK 2 vector also contains constitutively expressed firefly luciferase gene. Firefly luciferase is used as an internal control to normalize transfection efficiency. After normalizing for transfection efficiency, all plasmid luciferase activities were normalized to the empty vector.

Statistics

Statistical significance was determined by one and two-way ANOVA with Tukey's post hoc test and Student t-tests using GraphPad Prism, version 4 and SPSS. Results are presented as mean ± standard deviation. Results from at least $n \geq 3$ with $p < 0.05$ are considered significant. All western blots were performed at least twice to show reproducibility.

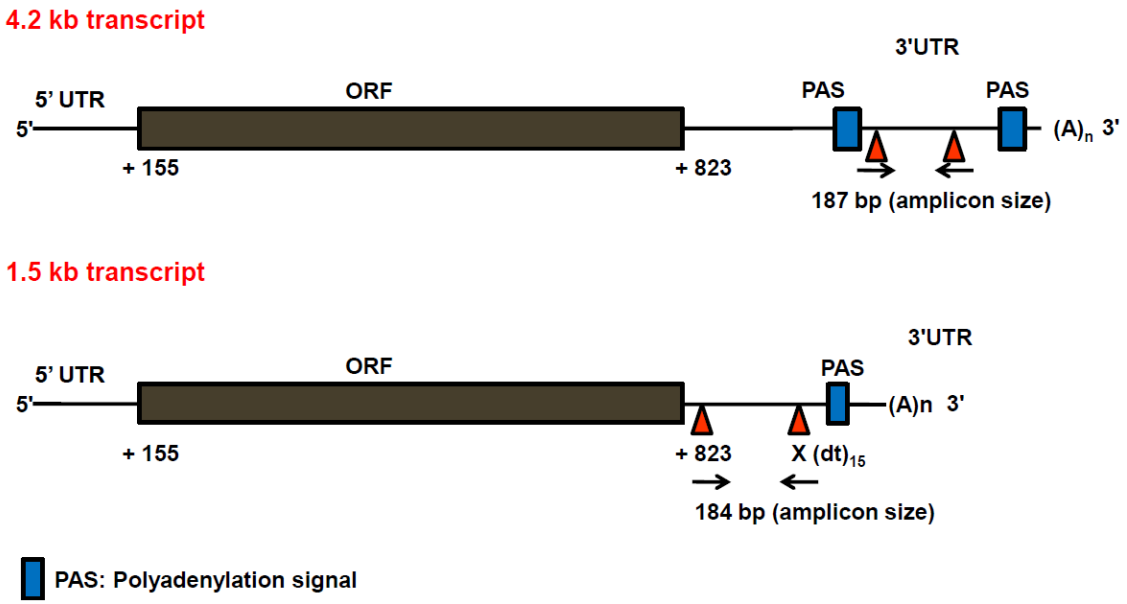

Figure II-1 Schematic illustration of primer design used to selectively amplify the 4.2 kb and 1.5 kb MnSOD transcripts.

Cell line	Source	Tissue	Cell	Oncogene status
MCF-10A	ATCC	Mammary	Epithelial	Non-malignant
RWPE-1	ATCC	Prostate	Epithelial	Non-malignant
NHF	Coriell	Foreskin	Fibroblast	Non- malignant
Cal 27	ATCC	Oral	Epithelial	Malignant
SQ20B	ATCC	Oral	Epithelial	Malignant
FaDu	ATCC	Oral	Epithelial	Malignant
MDA-MB-231	ATCC	Mammary	Epithelial	Malignant
Sum 159	Asterand	Mammary	Epithelial	Malignant
H292	ATCC	Lung	Epithelial	Malignant

Table II-1. Summary of cell lines used

CHAPTER III

MANGANESE SUPEROXIDE DISMUTASE 3' UNTRANSLATED REGION: SENSOR FOR CELLULAR RESPONSES TO ENVIRONMENTAL STRESS

Overview

Manganese superoxide dismutase (MnSOD) is a nuclear encoded and mitochondrial matrix localized antioxidant enzyme that converts mitochondrial generated superoxide to hydrogen peroxide. Human MnSOD has two poly(A) sites resulting in two transcripts: 1.5 and 4.2 kb. We hypothesize that the 3'-untranslated region (UTR) of MnSOD regulates its mRNA levels during quiescent and proliferative growth, and in response to environmental stress. Results from a Q-RT-PCR assay showed a preferential accumulation of the shorter MnSOD transcript during quiescence, which correlated with an increase in MnSOD activity. The accumulation of the longer MnSOD transcript during proliferation was associated with a decrease in MnSOD activity. Log transformed expression ratio of the longer to shorter transcript was also higher in proliferating epithelial non-cancerous (mammary: MCF-10A) and cancer cells (mammary: MB-231, SUM 159; oral squamous: SQ20B, FaDu, Cal27; and lung: A549, H292), suggesting that the abundance of the longer transcript is independent of cellular transformation status. Interestingly, the abundance of the longer transcript directly correlated with percent S-phase (R^2=0.86). The shorter transcript was more abundant in irradiated MB-231 cells, and MCF-10A cells that were exposed to environmental pollutant, polychlorinated biphenyl. Deletion and reporter assays showed: (a) a significant decrease in reporter activity in constructs carrying multiple AREs that are present in the 3'UTR of the longer MnSOD transcript; and (b) N-acetyl-L-cysteine, irradiation, and a combination of the two

treatments increased the reporter activity of the constructs carrying the 3'UTR sequence of the shorter MnSOD transcript. Because the shorter transcript has miR-377 target sequence and the longer transcript carries AREs, our results identified miRs and AREs as potential regulators of MnSOD transcript selection. We conclude that MnSOD 3'UTR is a novel molecular sensor regulating MnSOD mRNA levels in response to different growth states and environmental stress. (NIEHS P42 ES 013661, NIH RO1 CA 111365, Superfund training core grant). L.C, E.H.S, P.C.G designed research, L.C, E.H.S, A.L.K, N.A.B performed research, D.R.S supported the radiation and free radical research core, L.C, E.H.S, A.L.K, N.A.B, P.C.G analyzed data, L.C and P.C.G wrote the paper.

Results

Preferential Abundance of the 4.2 kb MnSOD Transcript During Proliferation

To determine whether there are changes in MnSOD expression during cell cycle progression, exponentially growing asynchronous population of NHF cells were plated at low density. Cells were collected every alternate day for cell number and fixed in 70% ethanol for flow cytometry measurement of cell cycle distribution. Replicate plates were used to harvest cells for total cellular RNA at similar time points. Results from cell number in Figure III-1A and cell cycle distribution show low density NHF cells begin with a lag phase 48 h post plating and proliferate exponentially thereafter (28% S-phase on day 6) and reach stationary phase within 8 days of post-plating (7 % S-phase on day 10). In order to determine abundance of MnSOD transcripts correlating with the proliferative capacity of the NHF cells, quantitative RT-PCR assays were performed using primer pairs designed to specifically amplify the 3'UTRs of the 4.2 and 1.5 kb MnSOD transcripts (Figure III-1B) as described in Chapter II. Our results show that the longer transcript (4.2 kb) was more abundant in the proliferative growth state (Figure III-1C). We observe a direct correlation between the abundance of the 4.2 kb transcript and

percent S-phase (R^2=0.84). Interestingly, when cells had low S-phase distribution, the shorter transcript (1.5 kb) was more abundant. Total MnSOD mRNA was also observed to be lower in cells with higher percentage of S-phase compared to cells with lower percent S-phase.

To determine if a preferential accumulation of the longer MnSOD transcript (4.2 kb) in proliferating cells is unique to normal cells, we further extended transcript selection measurements to transformed human mammary cells. Asynchronous proliferating MDA-MB-231 cells were plated in high and low cell density. Since cancer cells do not contact inhibit, low S-phase percentage was achieved by plating cells at a higher density and culturing for an additional 7 days prior to harvesting cells. MDA-MB-231 cell density was controlled to achieve cell population with higher and lower percent S-phase (45%, 25% and 15%); measured by propidium iodide staining of DNA content. Cells with different S-phase distributions were harvested and MnSOD transcript levels were measured by Q-RT-PCR assay using primers specific to MnSOD ; 4.2 and 1.5 kb transcripts. Fold change was calculated by first normalizing to 18S mRNA levels in individual samples and then calculated relative to MnSOD transcript levels in cells with the highest S-phase (~45% S-phase). Similar to our results in Figure III-1C, the longer transcript (4.2 kb) correlated with proliferation (R^2=0.95) and the shorter transcript (1.5 kb) was more abundant in MDA-MB-231 cells with lower percentage of S-phase cells (Figure III-1D).

To further determine if a preferential accumulation of the 4.2 kb MnSOD transcript also occurs in other cancers Q-RT-PCR assay was performed to measure the abundance of the 4.2 kb and 1.5 kb MnSOD transcript levels in cancer cells representative of human mammary, head & neck and lung cancers (Table III-1). Expression ratio of the longer to shorter transcript was calculated by normalizing to 18S and transformed to $\log_2$ values. The $\log_2$values for all cell types were higher than 1, suggesting that the abundance of the 4.2 kb MnSOD transcript was higher in proliferating

cells. Because this ratio was also higher in non-malignant cells (NHF and MCF-10A), these results also suggest that a preferential selection of the 4.2 kb transcript is closely related to the proliferation *vs* transformation status of the cells.

Preferential Abundance of the 1.5 kb MnSOD Transcript in Response to Environmental Stress.

Our results in Figure III-1 suggest that normal (NHF) and malignant (MDA-MB-231) cells with a low percentage of S-phase enriched the abundance of the shorter 1.5 kb MnSOD transcript. Radiation has long been used as an agent to induce growth delay by accumulating cells at G2/M phase and increasing cyclin B protein levels (Smeets *et al.,*1994). To determine if irradiation can influence MnSOD transcript distributions in proliferating MDA-MB-231 cells, we measured the abundance of the 4.2 and 1.5 kb transcripts in control and irradiated cells. Exponentially growing MDA-MB-231 cells were irradiated with 0-8 Gy and cells were harvested at 0-72 h post-irradiation for analysis of MnSOD transcript levels. Cells irradiated with 2 and 4 Gy of ionizing radiation exhibited minimal change in MnSOD transcript levels, while 6 and 8 Gy of irradiation increased MnSOD transcript levels by approximately 3-fold at 48 h post-irradiation (Figure III-2A). MnSOD transcript levels showed approximately 2- and 8-fold increase at 24 and 72 h post 8 Gy irradiation, respectively (Figure III-2B). Irradiation induced increase in total MnSOD transcript levels correlated with a corresponding increase in the abundance of the shorter transcript, while there were no significant changes in the abundance of the longer transcript (Figure III-2C).

To further confirm if the 4.2 kb transcript had any role in suppressing MnSOD expression, immunoblot and biochemical activity assays were performed on cells with different S-phase percentages. In Figure III-3B, we observed that MnSOD activity inversely correlates to proliferation ($R^2 = 0.97$). Concomitant with changes in the MnSOD activity, MnSOD protein levels were 8-fold lower in cells with the highest S-

phase compared to cells with a lower S-phase percentage (Figure III-3C). These results suggest that the selection of the shorter transcript during slow growth correlates with a higher level of MnSOD protein while the abundance of the longer transcript during proliferation was associated with a lower level of MnSOD protein. Growth-state dependent abundance of MnSOD protein levels correlated with changes in its activity. Similar results were observed in normal human fibroblasts. Our results showed that irradiation initiated a preferential selection of the 1.5 kb transcript that contributed to an overall increase in the abundance of MnSOD transcript levels.

Decrease in Luciferase Activity in Reporter Constructs Carrying the Full Length 3'UTR *vs* Shorter MnSOD 3'UTR

To investigate if a preferential selection of MnSOD transcript regulates translation we used a luciferase reporter assay. The short 3'UTR and deletion constructs of the full length 3'UTR of the longer transcript were cloned downstream of a renilla luciferase gene. A complete sequence analysis of the full length 3'UTR of the 4.2 kb transcript revealed several AU-rich elements (A (U) $_{3\text{-}6}$ A) which were not present in the shorter 3'UTR transcript. This suggested that the presence of AREs in the 4.2 kb transcript could be an important regulator for controlling MnSOD mRNA levels during cell cycle progression. MnSOD 3'UTR cis-acting elements with and without AREs were amplified by PCR and cloned into the 3' end of the renilla luciferase reporter gene in psiCHECK2 plasmid. These results showed ARE-dependent expression of reporter activity: constructs carrying 2 and 5 AREs showed approximately 40 and 60% decrease in reporter activity compared to reporter construct carrying no AREs (Figure III-3A).

This indicated that the presence of multiple AREs on the longer transcript could direct translational repression of MnSOD. We had earlier observed in Figure III-1 and Table III-1, that the 4.2 kb transcript was abundant in the proliferative growth state.

We conclude that a preferential selection of the MnSOD transcripts can serve as an important control point for regulating gene expression during cell cycle progression. Such a regulation is probably necessary to maintain redox flux during progression from one cell cycle phase to the next.

Irradiation Increases Luciferase Activity in Construct Carrying 3'UTR of the Shorter Transcript

Irradiation is well known to delay cell cycle progression by activating cell cycle checkpoints. To determine if the radiation induced growth arrest is due to a preferential enrichment of the shorter 1.5 kb MnSOD transcript, MDA-MB-231 cells carrying the reporter constructs of MnSOD 3'UTR were irradiated with 8 Gy and reporter activity assayed 48 h post-irradiation. Relative luciferase expression of the plasmids carrying the 3'UTR of the longer MnSOD transcript showed approximately 20-40% decrease in irradiated *vs* control cells (Figure III-4A). Interestingly, reporter activity of the plasmids carrying the 3'UTR of the shorter MnSOD transcript showed a significant increase in irradiated *vs* control cells. Irradiation induced increase in luciferase activity correlated with a significant increase in MnSOD protein levels and MnSOD activity (Figure III-4B-C). This correlation is also consistent with our earlier observations in Figure III-1-3 where we found that the abundance of the 1.5 kb transcript in cells with a lower percentage of S-phase correlated to a higher level of MnSOD protein and activity. We conclude that the shorter 3'UTR containing MnSOD transcript confers higher protein expression as well as higher activity in irradiated cells.

Redox Sensitivity of MnSOD 3'UTR

The full length 3'UTR of the 4.2 kb MnSOD transcript contains a higher number of AREs than the shorter transcript. In Figure III-3A reduced luciferase activity was observed when multiple AREs were present in the reporter plasmids compared to reporter plasmid without any AREs. Proteins that bind to AREs have been previously

demonstrated to alter its binding based on the redox state of the protein complexes (Goswami *et al.,*2000). To investigate if manipulating the intracellular redox status could influence the MnSOD mRNA levels, asynchronously growingMDA-MB-231 cells were pre-treated with 5 mM N-acetyl-L-cysteine (NAC) and assayed for luciferase activity of the reporter constructs 48 h post NAC addition. Results presented in Figure III-5A showed approximately 60% and 40% decrease in luciferase activity in reporter constructs carrying 5 and 2 AREs respectively compared to the reporter construct carrying no AREs from the 3'UTR of the shorter transcript. This suggested that multiple AREs present on the 3'UTR is redox sensitive. This redox sensitivity could come from proteins known to bind AREs on the 3'UTR. Simultaneous treatment of both NAC and irradiation resulted in approximately 2 fold increase in luciferase activity of the short transcript compared to the long transcript (Figure III-5B). Our results suggest that altering the redox environment of the cell with NAC could further enhance MnSOD expression by enriching the short transcript.

In summary, human MnSOD has two mRNAs due to the presence of tandem alternate polyadenylation sites in its 3'UTR (Figure III-12C). These two mRNAs are 1.5 kb and 4.2 kb in length; they differ only in the length of their 3'UTR. The full length 3'UTR of the 4.2 kb transcript is rich in AREs and hence subjected to regulation. The truncated 3'UTR of the 1.5 kb transcript contains only one identified ARE, which makes it more stable. The selective abundance of the 4.2 kb transcript during proliferation is responsible for lower MnSOD protein and activity levels. The enrichment of the 1.5 kb transcript during slow growth is responsible for higher MnSOD protein expression as well as activity. This novel mechanism of transcript selection may be used to fine-tune MnSOD expression in response to cellular growth state and environmental stress.

Discussion

Alterations in intracellular redox environment have been long believed to play a regulatory role in modulating gene expression. MnSOD is a key player in maintaining the intracellular redox balance and has been shown to regulate transition between quiescence and proliferation. High levels of MnSOD activity are associated with quiescent growth while lower levels support proliferative growth (Sarsour *et al.,*2008). MnSOD protein as well as mRNA levels are reduced in human cancer cells (St Clair and Oberley,1991). How MnSOD expression is coordinately regulated to respond to intracellular environment is a very complex process and largely unknown. The present study investigates whether MnSOD 3'UTR can act as a sensor controlling MnSOD expression in response to differences in growth states as well as environmental stress. A sequence analysis showed that human MnSOD is encoded by two mRNAs, 1.5 kb and 4.2 kb in length. Both mRNAs are transcribed from the same gene and have an identical coding sequence, but differ in the length of their 3'UTR due to alternate polyadenylation. The length of their 3'UTR is 240 bp and 3.4 kb respectively. Recent studies suggest that changes in the length of the 3'UTR due to alternate polyadenylation and cleavage are important mechanism for balancing gene expression.

In the present study, cellular growth state and cell cycle phases, proliferative (high S-phase) and slow growing cells (low S-phase) were used to determine the abundance of the two MnSOD transcripts. Radiation was used as an environmental stress agent to delay cell growth so as to obtain a population of lower S-phase cells. Under these cell growth conditions, changes in MnSOD expression were investigated by measuring the preferential abundance of its two transcripts. Asynchronous population of normal human fibroblasts and cell density modulated cultures of malignant MDA-MB-231 were used to demonstrate that MnSOD expression varied during quiescence and proliferative growth. Using Q-RT-PCR assay we have demonstrated that there is a preferential abundance of the longer transcript (4.2 kb) during proliferation. We observed abundance of the longer

transcript during proliferation irrespective of cellular transformation status. In Figure III-1C-D and Table III-1 we did not observe any significant difference in the fraction of the 4.2 kb transcript between the transformed and non-transformed cells lines. While the 4.2 kb MnSOD transcript is directly correlated with proliferation, the shorter 3'UTR containing 1.5 kb transcript is enriched in cells with a low S-phase fraction (Figure III-1C-D, 2C-D). Radiation has long been used as a tool to delay cell growth and interestingly, in the irradiated cells we observed preferential enrichment of the 1.5 kb transcript, without any significant changes in the abundance of the 4.2 kb transcript.

The preferential selection of the 4.2 kb MnSOD transcript during proliferation indicated that there could be regulatory function of additional elements present in between the tandem poly(A) sites of the full length 3'UTR. The 3'UTR is known to harbor regulatory elements like the AREs and the miRNA seed matches which could repress gene expression. Sequence analysis of 4.2 kb MnSOD 3'UTR sequence reveals the presence of several AU-rich elements (ARE) which include $A(U)_3A$, $A(U)_5A$ and $A(U)_6A$ motifs to which proteins might bind thereby regulating its stability and translational efficiency. Compared to the 4.2 kb transcript, the 1.5 kb transcript contains only a single $A(U)_3A$ motif. Previous work from our lab has shown that Topoisomerase II expression during the cell cycle is regulated by interaction of the 3'UTR with redox-sensitive protein complexes binding to AREs (Goswami *et al.,*2000). Although activating regulatory elements occur in some 3'UTRs, regulatory effects on 3'UTR are generally repressive. Our results in Figure III-1C-D, 2B-C and Table III-1 suggests that the abundance of the full length 3'UTR during proliferation could subject this population of cells to this additional step of regulation by gene repression. Abundance of the 1.5 kb MnSOD transcript with a truncated 3'UTR in the slow proliferating cells could indicate a mean of escaping this post-transcriptional repression offered by the regulatory elements present between tandem polyadenylation sites on the full length 3'UTR.

What could be the functional consequence of preferential selection of the full length 3'UTR? AREs are known to direct translational repression of their target mRNAs, and this can result in reduced protein output. To determine if different amounts of protein are produced from the short and long transcript of MnSOD, we used reporter assays. Plasmids were designed as described in Chapter II. Reporter constructs were made so as to compare the luciferase activity between the 3'UTR of the short transcript containing no AREs to the deletion constructs of 3'UTR of the long transcript carrying 2 or 5 AREs. Comparison of renilla luciferase gene expression for all the constructs showed that the reporter construct carrying 2 AREs reduced protein expression by 1.5-fold which increased to 2-fold when 5 AREs were present (Figure III-3A). Thus, the AREs present on the full length 3'UTR of the 4.2 kb transcript post-transcriptionally represses MnSOD expression which is escaped by the truncated 3'UTR of the 1.5 kb transcript. To further confirm the impact of abundance of the 4.2 kb transcript during proliferation on protein output, we determined MnSOD activity and protein expression by immunoblotting in NHF and MDA-MB-231 cells representative of high and low percent S-phase. In Figure III-3B-D we observe that proliferating cells had lower MnSOD activity as well as protein levels compared to cells with higher S-phase percent. Our observations suggest that during proliferation, the AREs present on the 4.2 kb MnSOD transcript represses MnSOD protein and activity. Loss of AREs in the preferentially enriched 1.5 kb transcript led to increase in MnSOD protein and activity levels during slow growth in cells with low S-phase percent. This is consistent with previous reports that MnSOD is necessary for the maintenance of quiescence and to prevent aberrant proliferation (Sarsour *et al.,*2008). This is also consistent with previous observation that MnSOD activity was decreased during S-phase compared with G_0 and increased MnSOD levels correlate with decreased cell proliferation suggesting significant alteration in MnSOD activity during the cell cycle (Oberley *et al.,*1995; Sarsour *et al.,*2008). Thus, increased MnSOD levels may correlate with inhibition of cell proliferation (St Clair and

Oberley,1991). MnSOD activity therefore regulates transition between proliferative and quiescent growth states. Our results suggest that the cell cycle dependent expression of MnSOD transcripts could be one of the factors regulating MnSOD activity during transition between quiescence and proliferation.

Sandberg *et al*. has shown an increase in proliferation to be associated with relative expression of shorter 3'UTR length in primary murine T lymphocytes (Sandberg *et al.,*2008). Mayr *et al*. has extended this observation to show that cancer cell lines express higher levels of the shorter 3'UTR transcript of various genes compared to non-transformed cells, thereby connecting 3'UTR shortening to oncogenesis. In this study, non-malignant cells expressed higher abundance of the full length 3'UTR transcript responsible for maintaining the normal proto-oncogene function, while cancer cells expressed substantially higher level of the shorter transcript. This suggested that the cancer associated truncation of 3'UTR could be a mechanism to activate proto-oncogenes (Mayr and Bartel,2009). Transgenic mouse models of tumorigenesis, overexpress oncogenes which have truncated 3'UTR to escape the repressive function of the full length 3'UTR (Mayr and Bartel,2009). Although these previous studies provide evidence for 3'UTR length and transcript selection in growth promoting genes, there is still little known on 3'UTR selection for anti-proliferating genes like MnSOD.

Unlike oncogenes, expression of MnSOD has been found to be reduced in many human cancer cells and transformed cell lines (Oberley,2001; Yan *et al.,*1996). SV40 transformed W138, human embryonic lung fibroblasts have been shown to have lower MnSOD activity and protein than the non-transformed counterpart (Oberley *et al.,*1989). MnSOD has been shown to be necessary for protection of quiescence in normal cells and high levels of MnSOD have been shown to inhibit proliferation in cancer cells. Nude mice when injected with adenoviral constructs of MnSOD inhibited tumor cell growth and extended survival compared to parental cells (Weydert *et al.,*2003). Ectopic expression of MnSOD has been shown to significantly inhibit tumor growth *in vivo*.

These results support the hypothesis that MnSOD is anti-proliferative and could be a tumor suppressor gene (Oberley,2001; Oberley,2005; Oberley and Buettner,1979; Weydert *et al.,*2003; Yan *et al.,*1996; Zhong *et al.,*1997). In our results too, we observe a lowered total MnSOD mRNA expression in proliferating as well as cancer cells. This is associated with higher abundance of the 4.2 kb transcript in the proliferating cells. Our results are also consistent with a previous report of SV40 transformed W138 cells showing higher 4.2 kb transcript abundance in a northern blot analysis than its non-transformed counterpart (St Clair and Oberley,1991). The 4.2 kb MnSOD transcript expressing the full length 3'UTR harbors several AREs and miRNA seed matches like miRNA 21, 377 and 222. These regulatory elements can play tumor suppressor roles when present on the 3'UTRs by repressing gene expression. Apart from proto-oncogene over expression, an important mechanism for oncogenic transformation could be repression of anti-proliferating genes like MnSOD. Abundance of the longer 3'UTR could result in repression of gene expression for tumor-suppressors. This would add to the existing knowledge in previous reports where abundance of the truncated 3'UTR of oncogenes has been associated with tumorogenesis. Our results are further supported by observations in another tumor suppressor gene, prohibitin which has higher abundance of its longer 1.9 kb transcript during proliferation compared to the shorter 1.2 kb transcript. In this study they further reported that microinjection of the truncated 3'UTR could not inhibit cell cycle progression from G_0 to S phase in human fibroblasts, CF3. In comparison, the full length 3'UTR inhibited cell proliferation (Jupe *et al.,*1996a). Our results in Table III-1 and Figure III-3 show that both transformed and non-transformed cells preferentially enrich full length 3'UTR expression of anti-proliferative genes like MnSOD, thereby resulting in repressed gene expression during proliferation.

MnSOD expression has been shown to be induced post-irradiation. Ionizing radiation can cause physical and chemical damage to cells which induces an adaptive response by increasing MnSOD expression that may result in enhanced tolerance to the

subsequent cytotoxicity (Guo *et al.,*2003). Ionizing radiation has also been shown to delay growth by inducing cell cycle checkpoints. Thus post irradiation; cells have low percent S-phase. Using irradiation as an environmental stress agent to delay growth, we determine MnSOD transcript distribution in irradiated MDA-MB-231 cells 48-72 h post radiation. In our results we observe a dose dependent increase in MnSOD mRNA with 8-fold increase in mRNA 72 h post radiation (Figure III-2A-B). Previous studies have shown induction in MnSOD activity, immunoreactive protein and mRNA postirradiation (Guo *et al.,*2003; Macmillan-Crow and Cruthirds*,*2001). MnSOD expression has been shown to be induced by single or multiple doses of ionizing radiation. (Guo *et al.,*2003). Irradiation induces superoxide radicals and MnSOD is known to scavenge superoxide. Interaction of superoxide with DNA could result in DNA strand breaks due to formation of hydroxyl radical, and eventually act as pathological mediators of disorders like cancer (Guo *et al.,*2003). In response to these stresses, cells induce the synthesis or activate proteins with antioxidant protective capacity. Therefore induction of MnSOD by environmental stress like ionizing radiation could be an adaptive response. In our results too, we observe an increase in MnSOD mRNA levels 24-72 h post irradiation (Figure III-2B). In Figure III-2C the relative abundance of the 1.5 kb MnSOD transcript increased by 6- fold without any significant change in the 4.2 kb transcript 72 h post irradiation. Since irradiation is known to slow growth, these results are consistent with our earlier observations in Figure III-1 where the 1.5 kb transcript was enriched in cells with low percent S-phase. Results from reporter vector assay show an increase in luciferase expression in reporter construct carrying 3'UTR of the short transcript. This is further confirmed by increase in MnSOD protein levels and 3- fold increase in MnSOD activity in cells at 72 h post irradiation coinciding with the 6- fold increase in 1 kb transcript expression (Figure III-4B-C). Our results suggest that the adaptive response of increased MnSOD expression after radiation could be by escaping the ARE mediated gene

repression by the full length 3'UTR and preferential abundance of the truncated 3'UTR of the 1.5 kb MnSOD transcript.

One important question left unanswered in the preferential abundance of transcripts in response to environmental stress is the mechanism underlying recognition and selection of polyadenylation signals. Reports have postulated that trans-acting factors can influence the probability of selection of PAS (Mayr and Bartel,2009). Constituents of the polyadenylation machinery and RNA binding proteins which could affect the recognition of polyadenylation complex, factors that impact transcription elongation rate could be important players in selection of alternate polyadenylation signal and cleavage (Mayr and Bartel,2009). Cis elements on the 3'UTR could also be important for cleavage factors to determine the 'strength' of a PAS. Presence of GU-rich sequences ~ 50 nucleotides downstream of the PAS is known to increase the efficiency of a PAS. It could be possible that the activity of the polyadenylation and cleavage machinery could differ during cell cycle phases, thereby determining selection of one PAS over the other. However, additional experiments need to be performed to confirm the selection of PAS.

Overall, our data indicate that MnSOD expression is coordinately regulated by preferential abundance of its transcripts during cellular growth and in response to environmental stress (Figure III-6). Preferential abundance of the 4.2 kb transcript during proliferation represses MnSOD gene expression due to presence of AREs and miRNAs. Selection of the 1.5 kb transcript during slow growth eliminates this repression leading to higher MnSOD protein output and activity. Alternate 3'end processing and preferential selection of MnSOD transcripts may provide a clue to the development of specific measures to modulate cellular MnSOD activity. Our results address a novel mode of gene expression of MnSOD under normal growth conditions and in response to environmental stress. Understanding how MnSOD activity regulates cellular proliferation will advance the development of antioxidant-based approaches to mitigate environmental induced cytotoxicity.

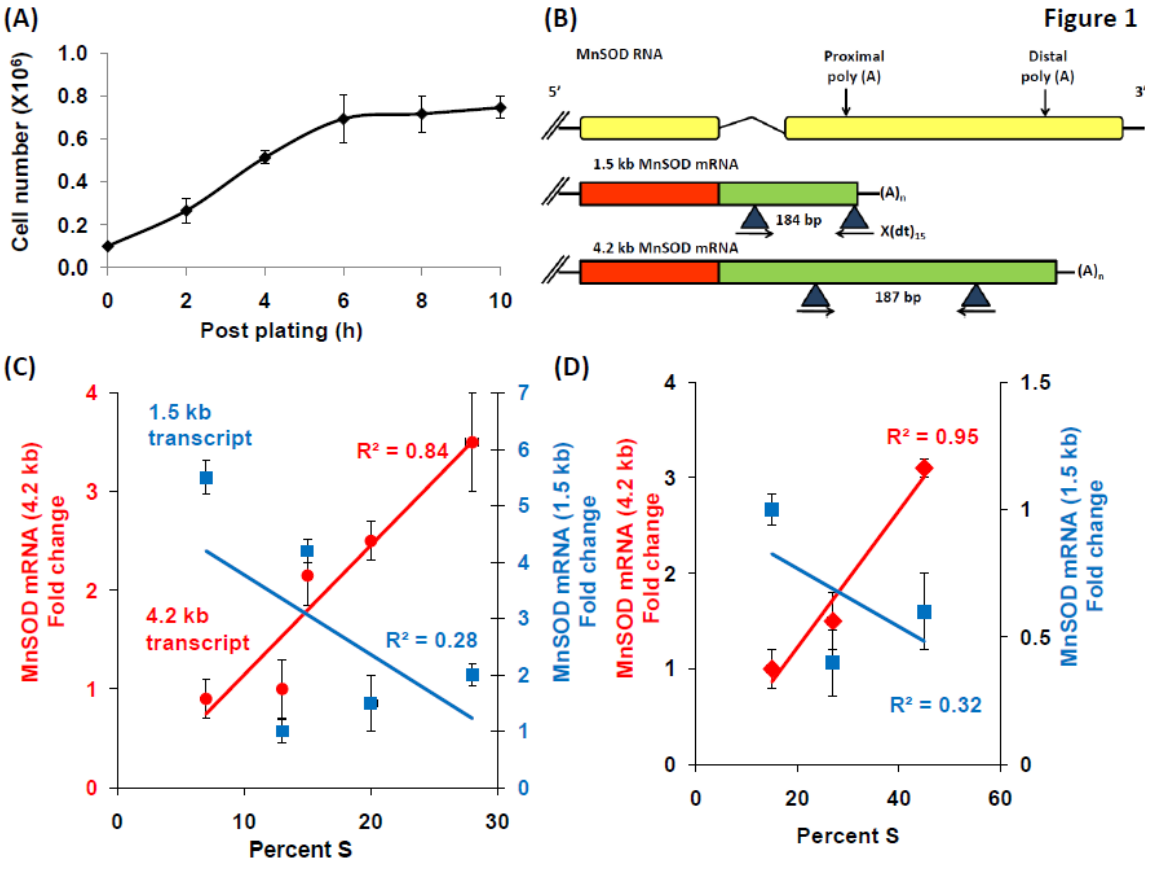

Figure III-1. Preferential abundance of the 4.2 kb MnSOD transcript in proliferating normal human fibroblasts.

(A) Normal human fibroblast growth curve. Cells were plated at low density and cells were counted every alternate day and stained with propidium iodide for flow cytometry measurement of cell cycle distribution (B) Schematic illustration of the selection of primer pairs used to amplify total MnSOD mRNA levels (open reading frame, ORF), 1.5 and 4.2 kb transcripts. Poly(A): polyadenylation sites; triangle and arrows: positions of forward and reverse primers; bp: amplicon size; $d(T)_{15}X$: anchored primer, X represents sequence specific to the first poly(A) site in the 1.5 kb transcript. Regression plot for the correlation between percent S and fold change of 4.2 kb and 1.5 kb MnSOD transcript distribution respectively is shown. Fold change of MnSOD transcript abundance was calculated relative to 18S and normalized to highest percent S-phase in (C) NHF cells and (D) MDA-MB-231 cells

Tissue types	Cell lines	Log_2 (4.2 kb/1.5 kb)
Malignant		
Head and Neck	Cal27	**1.2**
Head and Neck	SQ20B	**1.1**
Head and Neck	FaDu	**2.3**
Lung	A549	**1.3**
Lung	H292	**1.5**
Breast	Sum159	**1.4**
Breast	MDA-MB-231	**1.2**
Non-malignant		
Breast	MCF-10A	**1.3**
Fibroblast	NHF	**1.2**

Table III-1: Quantification of alternative mRNA isoforms.

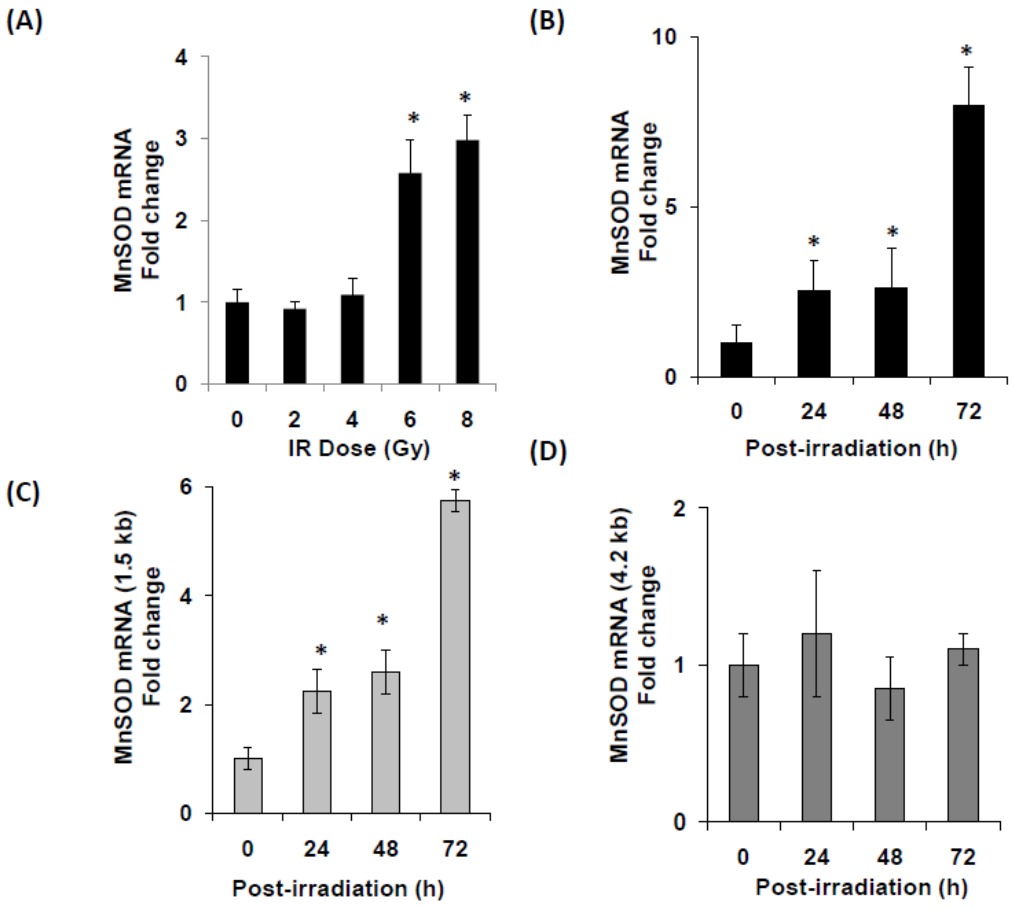

Figure III-2: Preferential abundance of 1.5 kb MnSOD transcript post irradiation

MDA-MB-231 cells were irradiated with 0-8 Gy and cells were harvested at 0-72 h post irradation. (A) Cells were harvested for qRT-PCR measurement of total MnSOD mRNA levels. MDA-MB-231 cells were irradiated with 0-8 Gy and harvested at 48 h post irradiation. (B) MnSOD mRNA levels in MDA-MB-231 cells irradiated with 8 Gy and harvested at 0-72 h post radiation. Non-irradiated cells at 0 h were included as the control. Q-RT-PCR was performed using primers specific for the (C) 1.5 and (D) 4.2 kb MnSOD transcripts in cells harvested 48 h post irradiation.

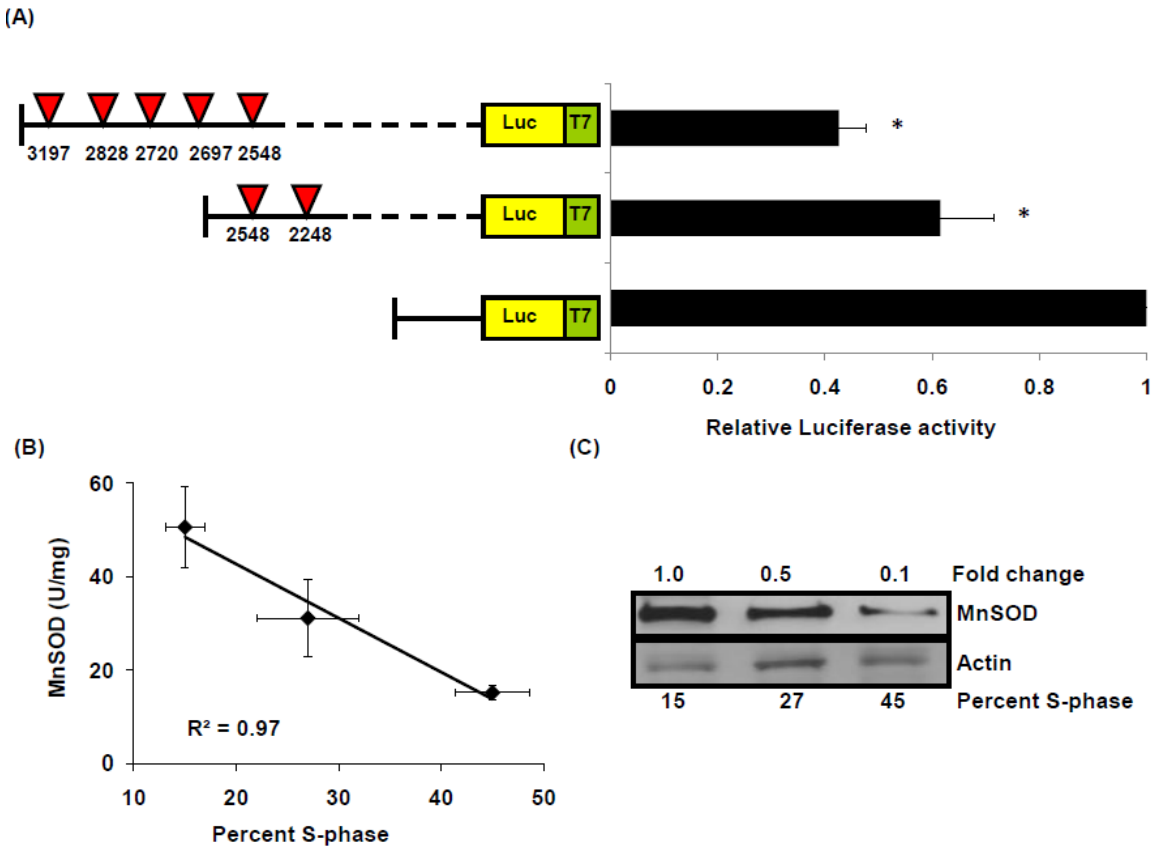

Figure III-3: The longer 4.2 kb transcript leads to lower protein expression

(A) Luciferase expression from reporter vector constructs containing the 3'UTR of the short transcript and deletion constructs of the 3'UTR of the long transcript containing 2 and 5 AREs. (B) MnSOD biochemical activity measured in MDA-MB-231 cells. Regression plot for the correlation between percent S phase and MnSOD activity is plotted. (C) MnSOD protein levels were measured by immunoblotting in MDA-MB-231 cells.

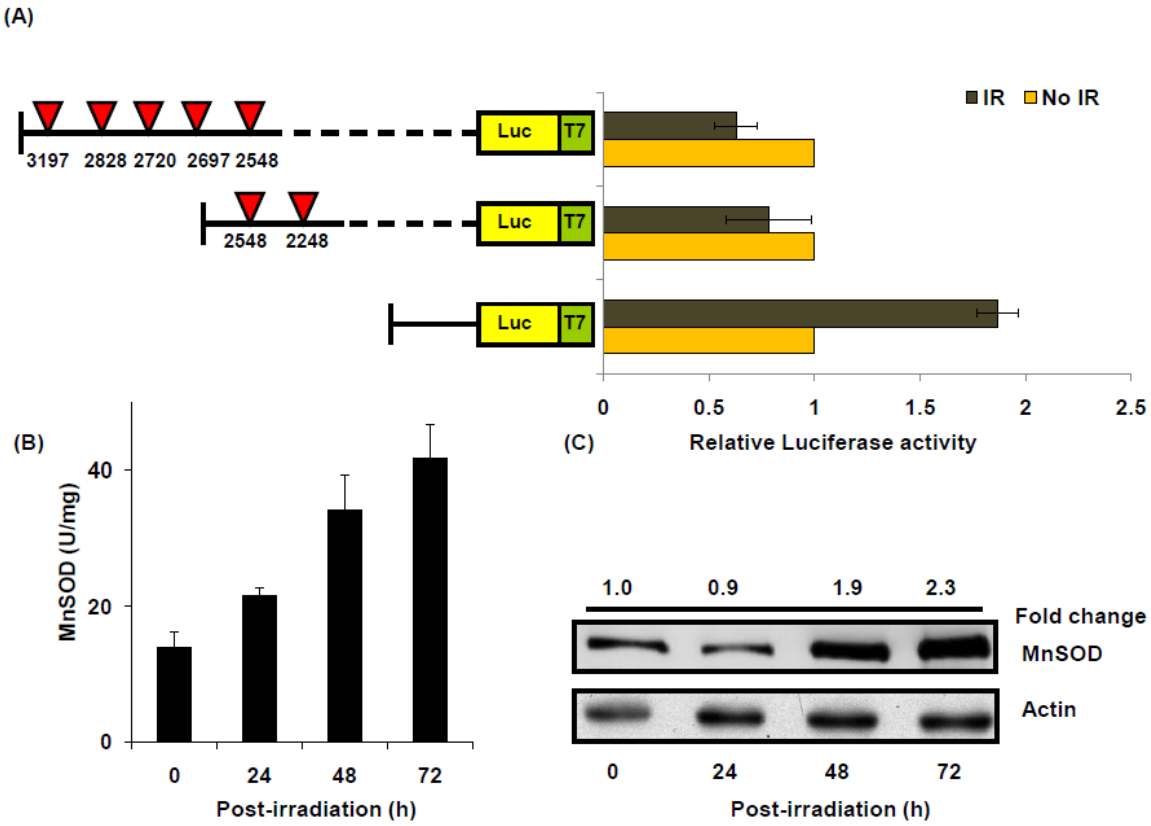

Figure III-4: The shorter 1.5 kb transcript leads to higher protein expression inirradiated cells

(A) Luciferase expression from reporter vector constructs containing the 3'UTR of the short transcript and deletion constructs of the 3'UTR of the long transcript containing 2 and 5 AREs in MDA-MB-231 cells. Cells were irradiated with 8 Gy and luciferase activity was measured 48 h post irradiation. Luciferase activity from the irradiated cells was normalized to its respective non-irradiated controls. (B) MnSOD biochemical activity measured in MDA-MB-231 cells 0-72 h post 8 Gy irradiation. Regression plot for the correlation between percent S phase and MnSOD activity is plotted. (C) MnSOD protein levels were measured by immunoblotting in 8 Gy irradiated MDA-MB-231 cells.

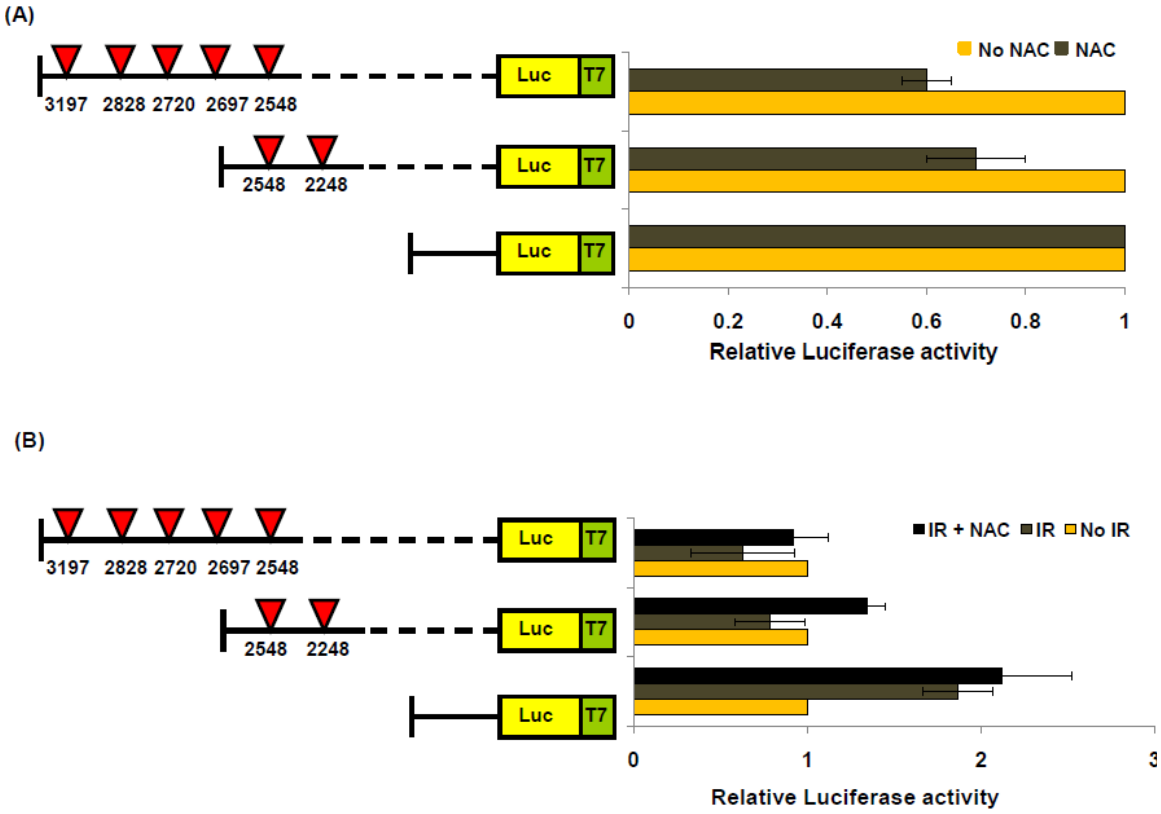

Figure III-5: Multiple AREs on the 4.2 kb transcript are redox sensitive

(A) Luciferase expression from reporter vector constructs containing the 3'UTR of the short transcript and deletion constructs of the 3'UTR of the long transcript containing 2 and 5 AREs. Cells were treated with 5 mM NAC and luciferase activity was measured 48 h later. Luciferase activity from the NAC treated cells was normalized to its respective non-treated controls. (B) Cells were pre-treated with 5 mM NAC 5 hours prior to 8 Gy irradiation. Luciferase activity was measured 48 h post irradiation.

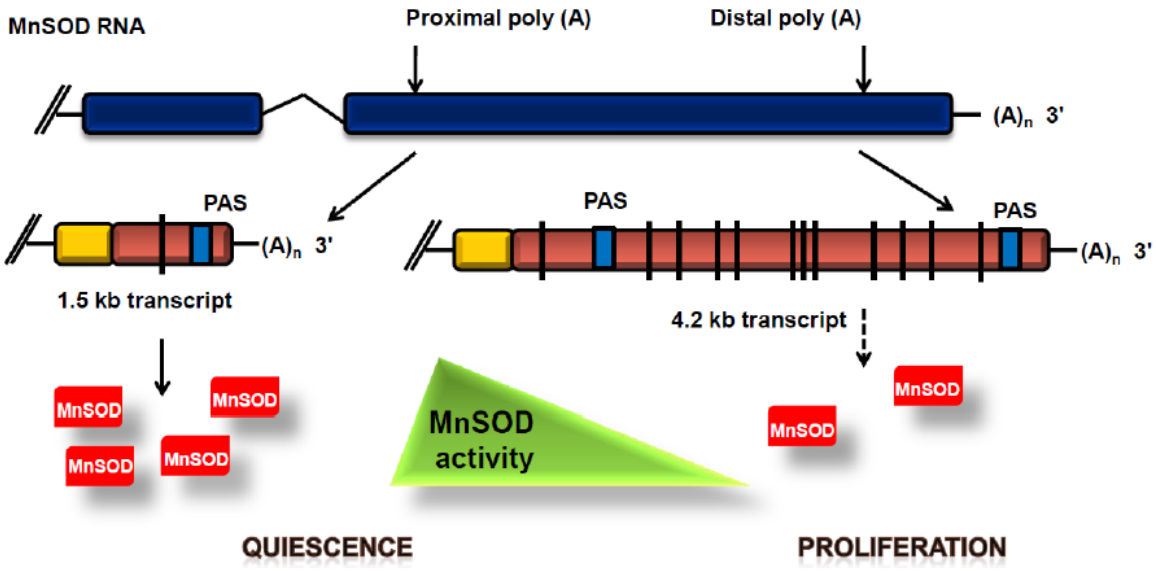

Figure III-6: Model summarizing the role of the 3'UTR of MnSOD acting as a sensor for differences in growth state and environmental stress.

CHAPTER IV

POLYCHLORINATED BIPHENYL INDUCED ROS SIGNALING DELAYS THE ENTRY OF QUIESCENT HUMAN BREAST EPITHELIAL CELLS INTO THE PROLIFERATIVE CYCLE[1]

Overview

Polychlorinated biphenyls (PCBs) are environmental chemical contaminants that can produce reactive oxygen species (ROS) by autoxidation of dihydroxy-PCBs and redox-cycling. We investigate the hypothesis that PCB induced perturbations in ROS signaling regulate the entry of quiescent cells into the proliferative cycle. Quiescent MCF-10A human breast epithelial cells were incubated with 0-3 micromolar of 2-(4-chlorophenyl)benzo-1,4-quinone (4-Cl-BQ), 2, 2', 4, 4', 5, 5'-hexachlorobiphenyl (PCB 153), and Aroclor 1254 for 4 days. Cells were replated at a lower density and analyzed for cell cycle phase distributions, ROS levels, MnSOD expression, and cyclin D1 protein levels. Quiescent cells incubated with 4-Cl-BQ showed the maximal delay in entering S phase. This delay was associated with a decrease in MnSOD activity, protein and mRNA levels, and an increase in cellular ROS levels. Results from the mRNA turnover assay showed that the 4-Cl-BQ treatment selectively enhanced the degradation of the 4.2 kb MnSOD transcript, while the half-life of the 1.5 kb transcript did not change. Accumulation of cyclin D1 protein levels in replated cells was suppressed in cells treated with 4-Cl-BQ. Pretreatment of quiescent cells with polyethylene glycol-conjugated superoxide dismutase and catalase suppressed 4-Cl-BQ induced increase in ROS levels, which was

[1] Chaudhuri L et al., Free Radic Biol Med. 49(1):40-9, 2010

consistent with an increase in cyclin D1 accumulation, and entry into S phase. These results showed 4-Cl-BQ induced perturbations in ROS signaling inhibit the entry of quiescent cells into S phase. L.C performed all experiments and wrote manuscript. E.H.S helped in designing and analyzing PCR assays, A.L.K and N.A.B helped in designing and analyzing biochemical assays and ROS measurements. D.R.S supervised biochemical assays and ROS measurements. P.C.G supervised overall project, experiment design and edited manuscript

Results

4-Cl-BQ Delays the Entry of Quiescent Cells into the Proliferative Cycle

A cumulative BrdU assay was used to determine whether quiescent cells incubated with PCBs maintain their proliferative capacities following reentry into the proliferative cycle. Quiescent MCF-10A cells (<2% S phase, based on DNA content) were treated with 0-3 μM PCBs for 4 days. Control and cells treated with PCBs were replated and continued in culture in presence of 10 μM BrdU. Cells were harvested at indicated times post-replating and analyzed for BrdU positive (cumulative S phase) and BrdU negative (G_1 and G_2 phases) nuclei. Representative FITC and PI histograms of control and cells treated with PCBs are shown in Figure IV-1A, and the percentage of S phase cells is presented in Figure IV-1B-D. The percentage of G_1 and $S+G_2$ are summarized in Table IV-1. More than 90% of the cells were in the G_0/G_1 phase in both control and PCB treated quiescent cells at the end of 4 days of treatment, suggesting that the incubation of quiescent cells with PCBs did not result in any redistribution of cells to different cell cycle phases (Figure IV-1A and Table IV-1). Furthermore, cell numbers at the end of the 4 days of incubation were comparable in control and cells treated with PCBs, indicating that the PCB treatments neither stimulated proliferation nor resulted in

cell death while the cells were in the quiescent growth state. These results were consistent with the absence of a cell population with sub-G_1 DNA content (data not shown).

Interestingly, cells that were allowed to reenter the proliferative cycle did exhibit significant difference in their entry into S phase. While all PCBs showed a decrease in the percentage of S phase, cells treated with 4-Cl-BQ showed the highest inhibition (~50%) compared to Aroclor 1254 (35%), and PCB 153 (20%) treated cells (Figure IV-1D). The percentage of S+G_2 phases in control cells increased to approximately 21 and 23% at 18 and 26 h post replating, respectively (Figure IV-1A, and Table IV-1). The percentage of S+G_2 phases was significantly lower in 3 μM 4-Cl-BQ treated cells at 18 h post replating, which remained lower at 26 h post replating (Figure IV-1A and Table IV-1). The percentage of S+G_2 phases in cells treated with PCB 153 and Aroclor 1254 were 16 and 14% at 18 h post replating, which increased to 19 and 15% at 26 h post replating (Table IV-1). The inhibition in entry into S phase correlated with increases in cell population doubling time: control, 37 h; 4-Cl-BQ, 53 h; PCB 153, 47 h; Aroclor 1254, 50 h.

4-Cl-BQ Increased Cellular Ros Levels in Quiescent Cells

We have previously reported the formation of a semiquinone radical in exponentially growing asynchronous cultures of MCF-10A cells incubated with 3 μM 4-Cl-BQ, which could be the source of the apparent higher flux of cellular ROS (Venkatesha *et al.,*2008). To determine if PCBs perturb cellular ROS levels in quiescent cultures, control and 3 μM PCB treated cells were harvested at the end of 4 days, and incubated with DHE and $CDCFH_2$. Fluorescence was measured by flow cytometry and MFI calculated after correction for autofluorescence; fold change was calculated relative to untreated control. Results (Figure IV-2A, upper panel) showed approximately 2 fold increase in DHE fluorescence in 4-Cl-BQ treated cells compared to control. PCB 153

and Aroclor treatments did not show any significant change in DHE fluorescence compared to control. The specificity of the DHE fluorescence for the measurement of superoxide was determined by incubating cells with PEG-SOD 2 h prior to and during the assay; fold change was calculated following the method described in the Methods and Materials section. These results showed approximately 2.5 fold increase in DHE fluorescence in cells incubated with 4-Cl-BQ (Figure IV-2A, lower panel). DHE fluorescence in PEG-alone treated cells did not change compared to untreated control. Quiescent cells treated with 4-Cl-BQ showed a similar increase in $CDCFH_2$ fluorescence (Figure IV-2B, upper panel). The increase in $CDCFH_2$ fluorescence was due to an increase in cellular hydrogen peroxide levels (Figure IV-2B, lower panel). These results clearly showed that 4-Cl-BQ perturbs cellular ROS levels, superoxide and hydrogen peroxide, in quiescent MCF-10A cells.

4-Cl-BQ Decreased MnSOD Expression in Quiescent Cells

MnSOD activity is known to regulate cellular ROS levels and reentry of quiescent human normal skin fibroblasts into the proliferative cycle (Sarsour *et al.,*2005; Sarsour *et al.,*2008). To determine if 4-Cl-BQ induced changes in cellular ROS levels could be due to changes in MnSOD activity, quiescent MCF-10A cells were incubated with 3 μM 4-Cl-BQ for 4 days, and MnSOD activity was measured following the method of Spitz and Oberley (Spitz and Oberley,1989). MnSOD activity in control cells was measured to be approximately 150 U/mg (Figure IV-3A). MnSOD activity decreased significantly, 68 U/mg, in quiescent cells incubated with 4-Cl-BQ, while PCB 153 and Aroclor treatments did not show any significant difference. The decrease in MnSOD activity in 4-Cl-BQ treated cells was associated with a 50% decrease in MnSOD protein and mRNA levels (Figure IV-3 B&C).

4-Cl-BQ treatments exhibited a dose dependent decrease in MnSOD protein and mRNA levels (Figure IV-4 A&B). MnSOD protein levels decreased approximately 60%

in quiescent cells incubated with 0.3 μM 4-Cl-BQ for 4 days, 80% in 3 μM, and more than 90% in 6 μM 4-Cl-BQ treated cells (Figure IV-4A). MnSOD mRNA levels did not show any change in 0.03 and 0.3 μM 4-Cl-BQ treated cells compared to control (Figure IV-4B). However, higher doses, 3 and 6 μM 4-Cl-BQ decreased MnSOD mRNA levels approximately 40-50% (Figure IV-4B).

To further determine if the decrease in MnSOD mRNA levels could be due to rapid mRNA turnover, MnSOD mRNA half-life was measured. Control and 4-Cl-BQ treated quiescent cells were incubated with actinomycin D to inhibit new transcription, and MnSOD mRNA levels were measured by quantitative RT-PCR at different times during the actinomycin D treatment. The half-life of MnSOD mRNA was calculated to be approximately 22 h in untreated control cells, and 12 h in 3 μM 4-Cl-BQ treated cells (Figure IV-4D). The decrease in MnSOD mRNA levels in actinomycin D treated cells was comparable with the corresponding decrease in MnSOD protein levels (Figure IV-4C). These results suggest that a post-transcriptional mechanism could regulate MnSOD mRNA levels in quiescent cells incubated with 4-Cl-BQ.

Preferential Turn-Over of MnSOD Transcripts in 4-Cl-BQ Treated Quiescent Cells

Human MnSOD mRNA has two polyA sites, which results in 1.5 and 4.2 kb transcripts (Church, 1990; Melendez and Baglioni, 1993). In order to determine if the 4-Cl-BQ treatment selectively affects turn-over of one transcript compared to the other, quantitative RT-PCR assays were performed using primer pairs designed to specifically amplify the 3'-UTRs of the 4.2 and 1.5 kb MnSOD transcripts (Figure IV-5A). Initially, it was determined if the 4-Cl-BQ induced dose dependent decrease in MnSOD mRNA levels could be due to a corresponding decrease in the abundance of the 4.2 kb transcript. Results showed that the abundance of the 4.2 kb transcript was not significantly different in 0.03 and 0.3 μM 4-Cl-BQ treated cells compared to control (Figure IV-5B). However,

higher doses of 4-Cl-BQ, 3 and 6 μM, decreased the levels of MnSOD 4.2 kb transcript approximately 40-50% (Figure IV-5B). Interestingly, the same treatments did not affect the abundance of the 1.5 kb transcript (Figure IV-5D). To further determine if the decrease in the 4.2 kb MnSOD transcript levels could be due to a decrease in mRNA half-life, mRNA turn-over assay was performed. Control and 4-Cl-BQ treated cells were incubated with actinomycin D and total cellular RNA isolated at indicated times (Figure IV-5C). Quantitative RT-PCR assay was performed using primer pair specific for the 3'-UTR of the 4.2 kb MnSOD transcript. The half-life of the 4.2 kb transcript in control cells was approximately 22 h, while cells treated with 4-Cl-BQ showed a significantly reduced half-life of 14 h (Figure IV-5C). These results suggest that the decrease in MnSOD mRNA levels in 4-Cl-BQ treated quiescent MCF-10A cells could be regulated by a rapid turn-over of the 4.2 kb transcript.

4-Cl-BQ Treatments Inhibit Cyclin D1 Protein Accumulation During Reentry of Quiescent Cells into the Proliferative Cycle

We have previously shown that appropriate levels of MnSOD activity and cellular ROS levels are necessary for reentry of quiescent cells into the proliferative cycle (Menon *et al.,*2007; Menon *et al.,*2003; Sarsour *et al.,*2005; Sarsour *et al.,*2008). These previous reports also showed a correlation between MnSOD activity and cyclin D1 protein levels. Cyclin D1 is the first cell cycle protein that is activated during entry into the proliferative cycle. To determine whether the PCB induced perturbations in MnSOD activity and cellular ROS levels inhibit cyclin D1 protein accumulation during reentry of quiescent cells into the proliferative cycle, control and 3 μM PCB treated quiescent cells were replated at a lower cell density and total protein extracts prepared at the time of replating (0 h) and 6, 12, and 24 h post-replating. Immunoblotting assay was performed to measure the protein levels of cyclin D1 and actin (Figure IV-6). In control cells, cyclin

D1 protein levels increased approximately 2.5 folds at 6 h post-replating followed by a decrease at 12 and 24 h post-replating. The time course of cyclin D1 protein accumulation in control cells was comparable to PCB 153 and Aroclor 1254 treated cells. However, cells incubated with 4-Cl-BQ showed a significant inhibition in the accumulation of cyclin D1 protein (Figure IV-6). This inhibition is consistent with a significant decrease in the percentage of S phase cells (Figure IV-1). Interestingly, quiescent cells incubated with 4-Cl-BQ and PEG-SOD/PEG-CAT reversed the 4-Cl-BQ inhibited accumulation in cyclin D1 protein (Figure IV-6, bottom panels).

To further determine if an increase in cellular ROS levels and inhibition in cyclin D1 protein accumulation regulate quiescence to S progression, quiescent MCF-10A cells were incubated simultaneously with 3 μM 4-Cl-BQ and PEG-SOD/PEG-CAT. Cells were replated at the end of 4 days and cumulative BrdU accumulation measured by flow cytometry following the method described in Figure IV-1. Representative FITC-PI histograms of cell cycle phase distributions are shown in Figure IV-7A, and the percentage of S phase distributions is presented in Figure IV-7B. The percentages of G_1 and S+G_2 are presented in Table IV-2. The percentage of G_0/G_1 phase in quiescent control, 4-Cl-BQ, and 4-Cl-BQ combined with PEG-SOD and/or PEG-CAT treated cells was approximately 95%, suggesting that none of these treatments perturb cell cycle phase distributions while the cells were in quiescent growth state (Figure IV-7, and Table IV-2). The percentages of S+G_2 was approximately 29% in untreated control cells at 18 h post-replating, and 33% at 26 h post-replating (Table IV-2). As shown before (Figure IV-1 and Table IV-1), 4-Cl-BQ treated cells exhibited approximately 12% S+G_2 cells at 18 h post-replating, which remained low (13%) at 26 h post-replating. Interestingly, quiescent cells that were treated with PEG-SOD and PEG-CAT abrogate the 4-Cl-BQ induced inhibition in entry into S phase. Cells treated with PEG alone did not override the 4-Cl-BQ induced inhibition in entry into S phase, suggesting that the activities of SOD and CAT are required. Antioxidant treatments may suppress 4-Cl-BQ induced decrease in

MnSOD expression. These results indicate that the 4-Cl-BQ induced decrease in MnSOD activity and increase in cellular ROS levels suppressed cyclin D1 protein accumulation, which negatively impacts upon the entry of quiescent cells into the proliferative cycle.

Discussion

A majority of research investigating cellular responses to PCB exposures use *in vitro* cell cultures of exponentially growing asynchronous cells. Although valuable results were obtained using these experimental systems, the *in vivo* significance of these results is not completely understood because a majority of proliferative-competent cells reside in quiescence, e.g. stem cells. Cellular quiescence is a reversible process necessary for cell and tissue renewal as well as inhibiting aberrant proliferation. Therefore, we have used quiescent cultures to partially mimic *in vivo* cell growth conditions. However, since oxygen concentrations are known to influence many of the cellular functions (Busuttil *et al.,*2003; Parrinello *et al.,*2003; Sarsour *et al.,*2010), our results that were obtained by culturing cells in monolayers and 21% oxygen environment may differ from *in vivo* conditions where oxygen concentration is presumed to be approximately 4% and cells grow in three dimensions.

Our results show quiescent MCF-10A cells incubated with 4-Cl-BQ, PCB 153, and Aroclor 1254 delayed entry into S phase (proliferative cycle) following replating of cells at a lower density. Cells incubated with 4-Cl-BQ exhibited the highest inhibition in progression from G_0/G_1 to S phase (Figure IV-1 and Table IV-1). The number of cells in control and PCB treated quiescent cells was comparable at the time of replating, suggesting that these PCBs did not activate an unscheduled entry into the proliferative cycle while the cells were in contact inhibited quiescent growth state. This observation is also consistent with results obtained from the flow cytometric measurements of cell cycle

phase distributions, which demonstrate more than 95% G_0/G_1 cells that were present at the end of the PCB treatment (Figure IV-1 and Table IV-1). Our results differ from an earlier study reporting PCB induced proliferation in quiescent rat liver epithelial cells (Vondracek *et al.,*2005). Results from this previous study showed an increase in the percentage of S phase in quiescent rat liver epithelial cells treated with "dioxin-like" PCBs (PCB105, PCB126, and 4'-OH-PCB79), which correlated with an increase in cell number. The increase in the percentage of S phase was accompanied with a corresponding increase in cyclin A and cyclin D2 protein levels. The difference in results between this previous and our present studies could be due to the use of different PCBs, species (human *vs*. rat), cell origin (liver *vs.* mammary), and experimental design (daily change in medium and addition of PCBs in the earlier study *vs*. one time addition of the PCBs in our study).

The percentage of cells with DNA content less than G_1 (sub-G_1) and the protein levels of phosphorylated H2AX did not vary between control and PCB treated quiescent cells (data not shown). These results indicate that the dose and duration of the PCB treatments might not cause any DNA double strand break and subsequent toxicity of quiescent MCF-10A cells. Interestingly, this observation is different to our earlier results demonstrating cytotoxicity of these PCBs in asynchronously growing exponential cultures of MCF-10A (Venkatesha *et al.,*2008). MCF-10A exponential and asynchronous cultures incubated for 3 days with 3 μM 4-Cl-BQ exhibited a significant increase in the frequency of micronuclei and phosphorylated histone H2AX, indicating that DNA damage could induce cell death in 4-Cl-BQ treated exponential cultures (Venkatesha *et al.,*2008). Our earlier results and results obtained from this study clearly suggest that cellular growth state, quiescence *vs.* proliferation, could be a significant factor in determining cellular responses to PCB exposures. Quiescent MCF-10A cells are resistant to 4-Cl-BQ induced cytotoxic effects, while proliferating cells are more susceptible.

4-Cl-BQ treatments significantly impaired the proliferative capacity of quiescent MCF-10A cells (Figure IV-1, Table IV-1). Results from the cumulative BrdU assay showed that the percentage of S phase was significantly lower in 4-Cl-BQ treated cells compared to controls at 18 and 26 h post-replating (Figure IV-1 and Table IV-1). These results demonstrate that the proliferative capacity of quiescent MCF-10A cells was severely impaired following incubation with 4-Cl-BQ. The inhibition in entry into S phase was associated with an increase in cell population doubling time, 37 h in control compared to 53 h in 4-Cl-BQ treated cells. PCB 153 and Aroclor 1254 treatments showed an intermediate response. The inhibition in entry into S phase in 4-Cl-BQ treated cells was probably not due to DNA damage because we did not observe any significant difference in the protein levels of phosphorylated histone H2AX between control and 4-Cl-BQ treated quiescent cells (data not shown). These results indicate that certain PCBs could elicit a cytostatic effect independent of DNA damage.

We have previously shown that preservation of appropriate cellular redox environment is necessary to protect the proliferative capacity of quiescent normal human and mouse fibroblasts (Menon and Goswami,2007; Menon *et al.,*2007; Menon *et al.,*2003; Sarsour *et al.,*2005; Sarsour *et al.,*2008). Overexpression of MnSOD protects quiescent normal human skin fibroblasts from age associated loss in proliferative capacity; inhibition in MnSOD activity impairs the ability of quiescent cells to reenter the proliferative cycle (Sarsour *et al.,*2008). MnSOD activity is also known to regulate cellular ROS levels (Sarsour *et al.,*2008). Results presented in Figures IV-2 and 3 show that 4-Cl-BQ treatments increased cellular ROS levels and decreased MnSOD activity in quiescent MCF-10A cells. Suppression of the DHE and $CDCFH_2$ fluorescence in PEG-SOD and PEG-CAT treated cells indicat that the 4-Cl-BQ treatment increased cellular superoxide and hydrogen peroxide levels. The increase in cellular ROS levels (superoxide and hydrogen peroxide, Figure IV-2) is consistent with our previous results where we have used electron paramagnetic resonance spectroscopy to identify the

presence of a semiquinone radical in MCF-10A cells incubated with 4-Cl-BQ (Venkatesha *et al.,*2008). The formation of the semiquinone radical was associated with approximately 4-fold increase in cellular ROS levels (Venkatesha *et al.,*2008). In addition to the semiquinone radical-induced increase in cellular ROS levels, results from the present study suggest that 4-Cl-BQ-induced decrease in MnSOD activity could also contribute to the increase in cellular ROS levels (Figures IV-3-4). We have previously shown mitochondrial generated ROS in 4-Cl-BQ treated MCF-10A cells and that the increase in ROS was not due to a change in mitochondrial content (Zhu *et al.,*2009). In this previously published work, we used MitoTracker Green and MitoSOX Red oxidation to determine the mitochondrial origin of superoxide production in 4-Cl-BQ treated exponential cultures of MCF-10A cells. Results from the confocal microscopy assay showed a significant increase in MitoSOX Red oxidation in 4-Cl-BQ treated cells colocalizing with MitoTracker Green fluorescence. 4-Cl-BQ treatment did not change MitoTracker Green fluorescence compared to untreated cells. Since MitoTracker Green fluorescence is commonly used to measure mitochondrial content, these previously published results suggest that the 4-Cl-BQ induced increase in ROS levels was not due to an increase in mitochondrial content. These previously published results and results presented in Figures IV-3-5 clearly suggest that the 4-Cl-BQ induced decrease in MnSOD expression is not due to a change in mitochondrial content.

A key observation of our study relates to a differential turnover of MnSOD transcripts in 4-Cl-BQ treated quiescent MCF-10A cells (Figure IV-4-5). Human MnSOD has two poly(A) sites that result in two transcripts containing the same open reading frame, 1.5 and 4.2 kb. MnSOD expression is regulated both by transcriptional and post-transcriptional mechanisms (Melendez and Baglioni,1993; Wan *et al.,*1994). Results from the mRNA turnover assay showed a significant decrease in MnSOD mRNA half-life in 4-Cl-BQ treated quiescent MCF-10A cells compared to untreated control, 22 h in control *vs.* 12 h in 4-Cl-BQ treated cells (Figure IV-4). These results suggest that a

post-transcriptional mechanism regulates MnSOD mRNA levels in 4-Cl-BQ treated quiescent MCF-10A cells.

The decrease in MnSOD mRNA half-life appears to be due to a preferential turnover of the 4.2 kb transcript. The mRNA levels of the 4.2 kb MnSOD transcript show a dose dependent decrease in quiescent cells incubated with 4-Cl-BQ (Figure IV-5B). The half-life of the 4.2 kb transcript was calculated to be approximately 14 h in 4-Cl-BQ treated cells compared to 22 h in control (Figure IV-5C). Interestingly, the same treatments did not alter the abundance of the 1.5 kb MnSOD transcript (Figure IV-5D). Our results are consistent with a previous report where the authors used northern blotting to demonstrate a differential abundance between the 1.5 and 4.2 kb MnSOD transcripts in TNF-α treated cells (Melendez and Baglioni,1993). The selective use of short and long 3'UTR containing transcripts is also recently reported for activated immune cells (Sandberg *et al.,*2008). The abundance of the short *vs.* long transcripts appears to be related to cell growth states. The abundance of the transcripts with shorter 3'UTRs is associated with a corresponding increase in their protein levels (Mayr and Bartel,2009; Sandberg *et al.,*2008). These studies suggest that the enhanced stability of the transcripts with shorter 3'UTRs could be due to the loss of the mRNA instability sequence and loss of regulation by microRNAs. The 3'UTR of the 4.2 kb MnSOD transcript contains both AU-rich mRNA instability sequence and microRNA target sites. While additional studies are necessary to determine the exact mechanisms of MnSOD mRNA turnover in 4-Cl-BQ treated cells, it is possible that redox sensitive binding of RNA-binding proteins to specific sequence in the 3'UTR could regulate MnSOD mRNA turnover. We have shown previously such a mechanism regulating topoisomerase II-alpha mRNA levels during the cell cycle and in response to oxidative stress (Goswami *et al.,*2000).

4-Cl-BQ induced a decrease in MnSOD activity and an increase in cellular ROS levels suppressed cyclin D1 protein accumulation during reentry of quiescent MCF-10A cells into the proliferative cycle (Figure IV-6). Cyclin D1, a member of the G_1-cyclin

family, is believed to be the first cell cycle regulatory protein that responds to mitogenic stimuli facilitating the entry of G_0/G_1 cells into S phase. In control cells, cyclin D1 protein levels peaked at 6 h post-replating and decreased at 12 and 24 h. In 4-Cl-BQ treated cells, cyclin D1 protein levels were not significantly different at 6, 12, and 24 h post-replating compared to 0 h. The suppression in cyclin D1 protein accumulation was associated with a significant decrease in the percentage of S phase (Figure IV-1 and Table IV-1). Interestingly, prior treatment of quiescent cells with PEG-SOD and PEG-CAT abrogated 4-Cl-BQ induced suppression in cyclin D1 protein accumulation and facilitated entry into S phase (Figure IV-6-7, Table IV-2). These results are comparable to a previous study by Smithwick *et al*. (Smithwick *et al.,*2004), where the authors showed decreased levels of cyclin D2 protein levels and an inhibition in progression from G_0/G_1 to S phase in lipopolysaccharide-stimulated and Aroclor 1242 and 2, 2'-chlorobiphenyl treated mice splenocytes.

In summary, we used quiescent MCF-10A human mammary epithelial cultures to demonstrate that 4-Cl-BQ treatments significantly impaired the proliferative capacity of these cells. The loss in proliferative capacity is associated with 4-Cl-BQ induced decrease in MnSOD activity, an increase in cellular ROS levels, and subsequent suppression in cyclin D1 protein accumulation (Figure IV-7C). Furthermore, 4-Cl-BQ treatments resulted in a preferential down regulation of the 4.2 kb MnSOD transcript, while there was no change in the abundance of the 1.5 kb MnSOD transcript. These results are significant because PCB exposures could impair cellular and tissue regeneration in PCB exposed individuals, and applications of antioxidants could be a viable redox-based countermeasure to protect the proliferative capacity of quiescent normal cells.

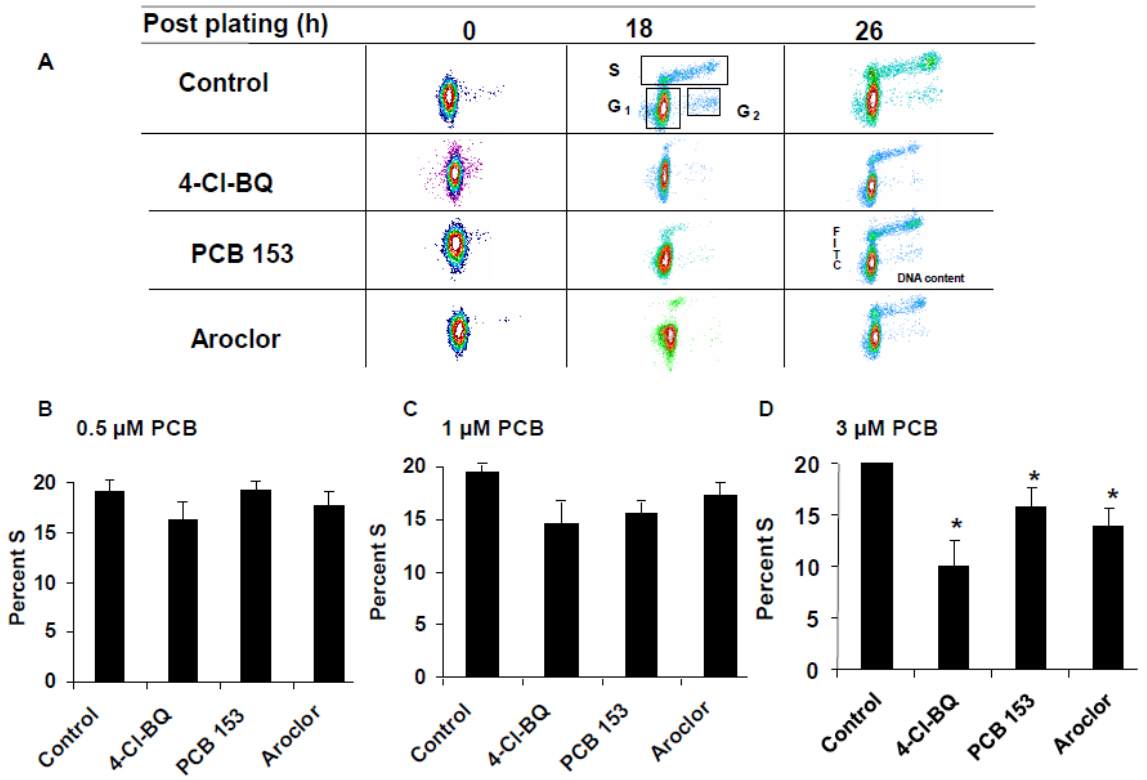

Figure IV-17: 4-Cl-BQ significantly inhibits reentry of quiescent MCF-10A cells into the proliferative cycle.

Monolayer cultures of quiescent MCF-10A cells were incubated with 0-3 µM of 4-Cl-BQ, PCB 153, and Aroclor 1254 for 4 days. Cells were sub-cultured by trypsinizing the monolayer cultures, and replated at a lower cell density. Replated cells were continued in culture in medium containing 10 µM BrdU and harvested at indicated times. Ethanol-fixed cells were assayed for BrdU-positive (S phase) and negative (G_1 and G_2 phases) nuclei following our previously published protocol [24]. Data were analyzed using FlowJo software. (A) Representative BrdU *vs.* PI bivariate histograms of cell cycle phase distributions in control and 3 µM PCB treated cells. (B-D) The percentage of S phase distributions in cells treated with different concentrations of PCBs. Control and PCB treated cells were harvested at 18 h post-plating. Asterisks represent statistical significance relative to untreated control, n=3; *, $p< 0.05$.

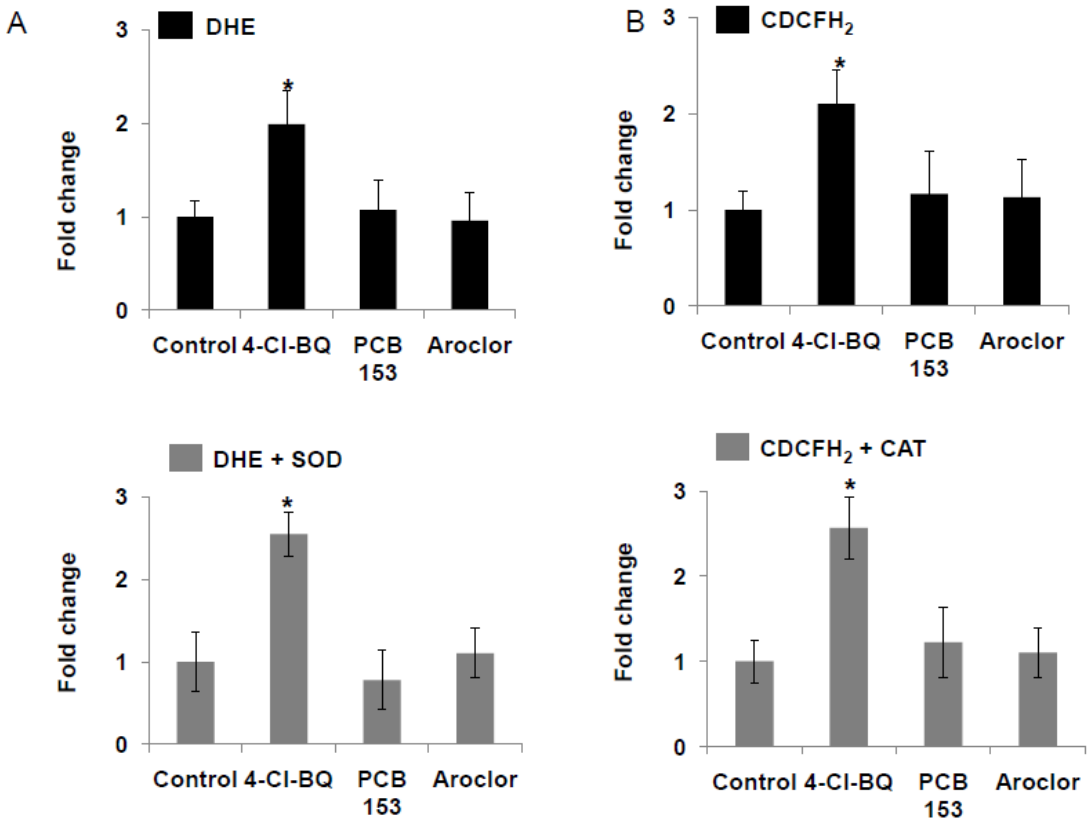

Figure IV-2: 4-Cl-BQ treatment increases DHE and $CDCFH_2$ fluorescence indicative of increase in cellular ROS levels, superoxide and hydrogen peroxide.

Control and 3 μM PCB treated quiescent MCF-10A cells were assayed for cellular ROS levels at the end of 4 days of treatment. (A) Monolayer cultures were incubated with 10 μM DHE in 2 mL of PBS containing 5 mM pyruvate at 37°C for 40 min. Cells in replicate dishes were treated with 100 U/mL PEG-SOD or 18 μM PEG for 2 h prior to and during the DHE labeling. Cells were trypsinized on ice and DHE fluorescence analyzed by flow cytometry. Fold change in MFI was calculated relative to MFI of untreated control cells in top panel. In the bottom panel, the fluorescence of cells treated with PCBs and PEG-SOD was subtracted from the fluorescence of cells treated with PCBs and PEG. The data plotted show fold change in MFI that was calculated relative to the difference in fluorescence of untreated control cells incubated with PEG and PEG-SOD. (B) In a separate series of experiments, control and PCB treated quiescent cultures were incubated with 10 μg/mL $CDCFH_2$ in PBS at 37°C for 10 min. Cells in replicate

Figure IV-2. Continued
dishes were pretreated with 100 U/mL PEG-CAT or 18 μM PEG for 2 h prior to and during the $CDCFH_2$ labeling. Cells were trypsinized on ice and fluorescence analyzed by flow cytometry. Data was plotted as described above. Fold change was calculated relative to untreated control. n=3; * $p<0.05$; asterisks represent statistical significance relative to untreated control.

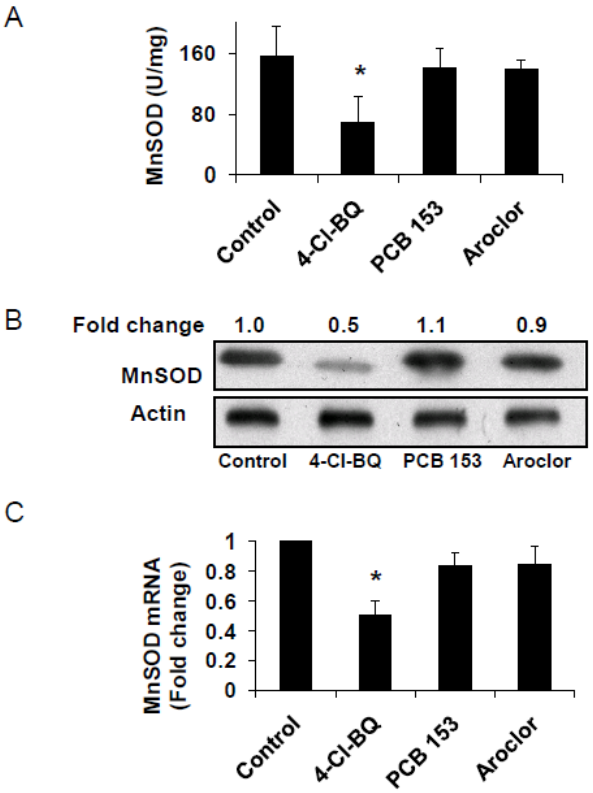

Figure IV-3: 4-Cl-BQ treatment decreases MnSOD activity and expression in quiescent MCF-10A cells.

Control and 3 μM PCB treated quiescent MCF-10A cells were harvested at the end of a 4-day treatment and assayed for (A) MnSOD activity. Cells from replicate plates were harvested for (B) immunoblotting and (C) quantitative RT-PCR assays to measure MnSOD protein and mRNA levels. Actin levels were used for loading control in immunoblots. Immunoblots were scanned and quantitated using ImageJ software. Fold change was calculated by first normalizing to actin levels in individual samples and then relative to untreated control. 18S RNA levels were used to calculate the relative fold change in MnSOD mRNA levels. Asterisks represents statistical significance relative to untreated control; n=3, *, $p < 0.05$.

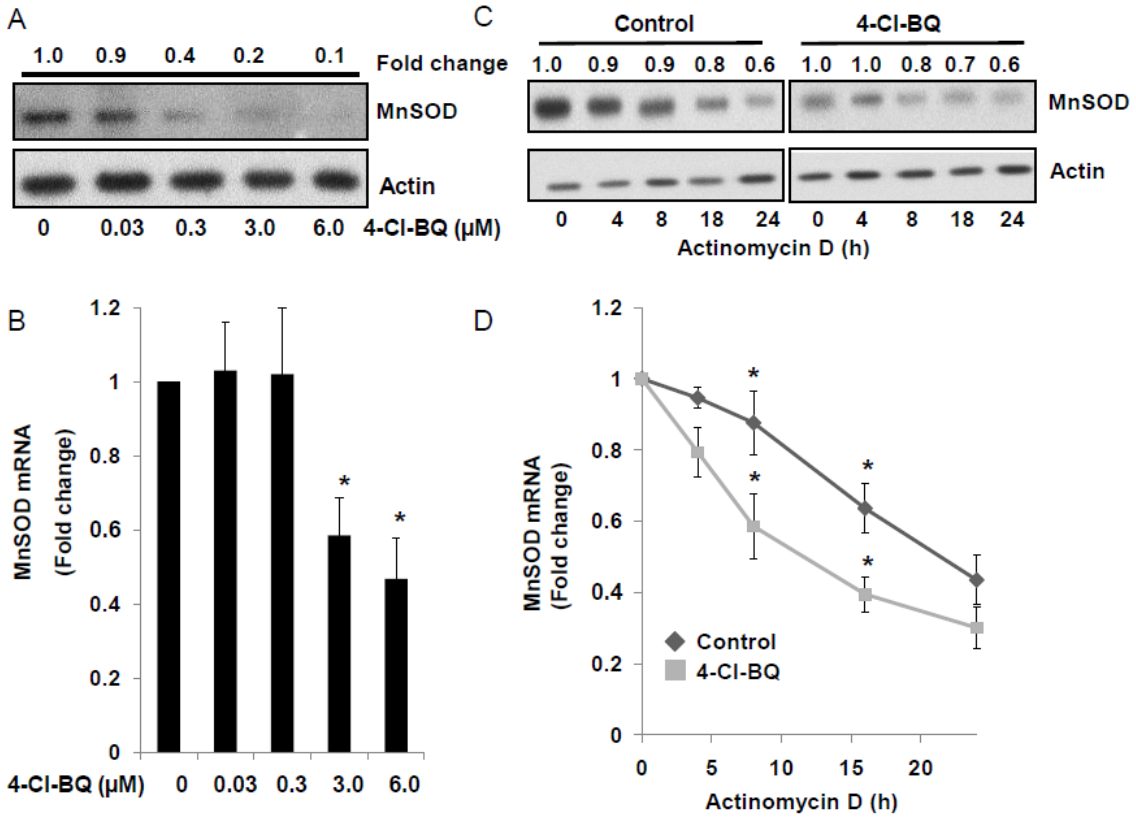

Figure IV-4: 4-Cl-BQ decreases MnSOD mRNA stability in quiescent MCF-10A cells.

Quiescent MCF-10A cells were treated with 0-6 μM 4-Cl-BQ for 4 days and harvested for measurements of (A) MnSOD protein and (B) mRNA levels. Actinomycin D was used to measure MnSOD mRNA half-life in control and 4-Cl-BQ treated cells. Quiescent MCF-10A cells were incubated with 3 μM 4-Cl-BQ for 4 days followed by incubation with 10 μg/mL actinomycin D. Cells were harvested at indicated times for (C) immunoblot analysis of MnSOD protein levels and (D) quantitative RT-PCR measurements of MnSOD mRNA levels. Asterisks indicate significant difference compared to control, n = 3, $p<0.05$.

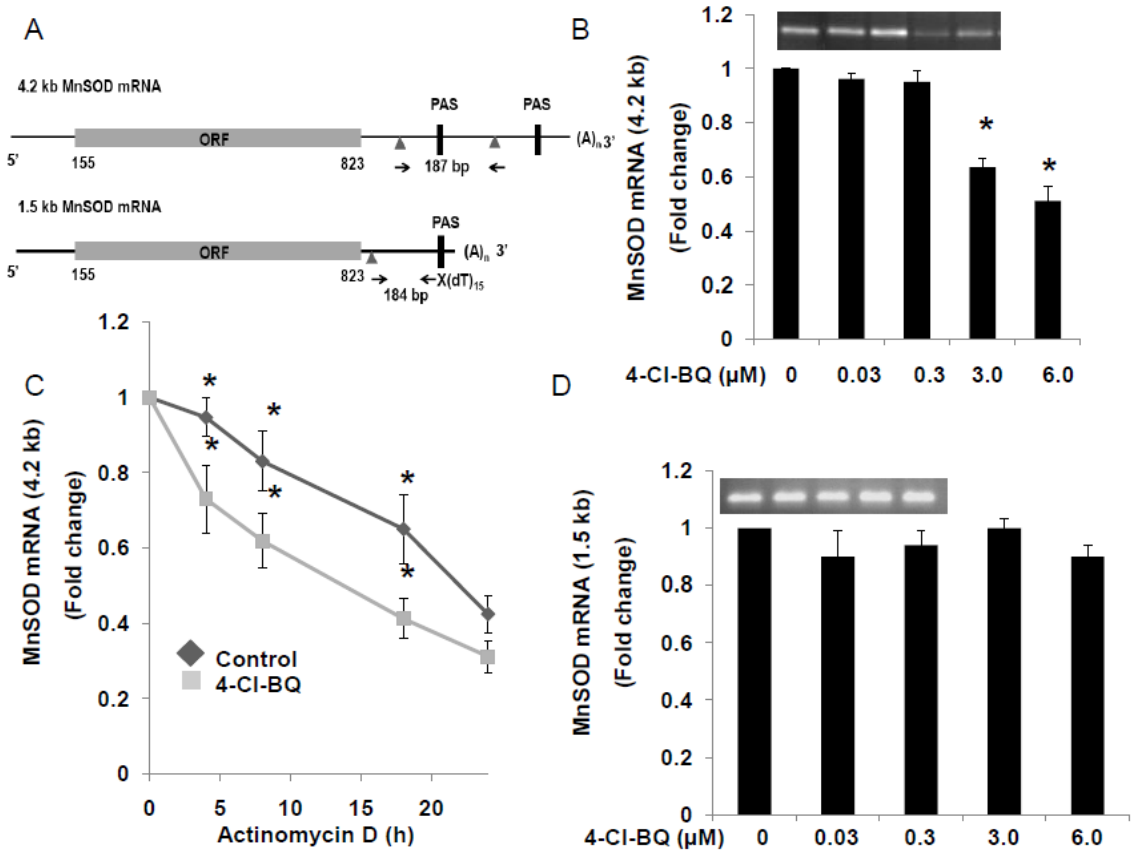

Figure IV-5: Preferential turn-over of the 4.2 kb MnSOD transcript in quiescent cells incubated with 4-Cl-BQ.

(A) Schematic illustration of the selection of primer pairs used to amplify total MnSOD mRNA levels (open reading frame, ORF), 1.5 and 4.2 kb transcripts. PAS: polyadenylation sites; triangle and arrows: positions of forward and reverse primers; bp: amplicon size; $d(T)_{15}X$: anchored primer, X represents sequence specific to the first poly(A) site in the 1.5 kb transcript. (B and D) Quiescent MCF-10A cells were treated with 0-6 μM 4-Cl-BQ for 4 days and harvested for RT-PCR measurements of the 1.5 and 4.2 kb MnSOD transcripts. (C) Control and 4-day 3 μM 4-Cl-BQ incubated quiescent MCF-10A cells were treated with 10 μg/ml Actinomycin D and harvested at indicated times for RT-PCR measurements of the abundance of the 4.2 kb MnSOD transcript. Asterisks represent statistical significance relative to untreated control, n=3; *, $p < 0.05$.

Figure IV-5. Continued
Insets in (B) and (D) represent agarose gel electrophoresis and ethidium bromide staining of PCR amplified products representative of the quantitative RT-PCR assay.

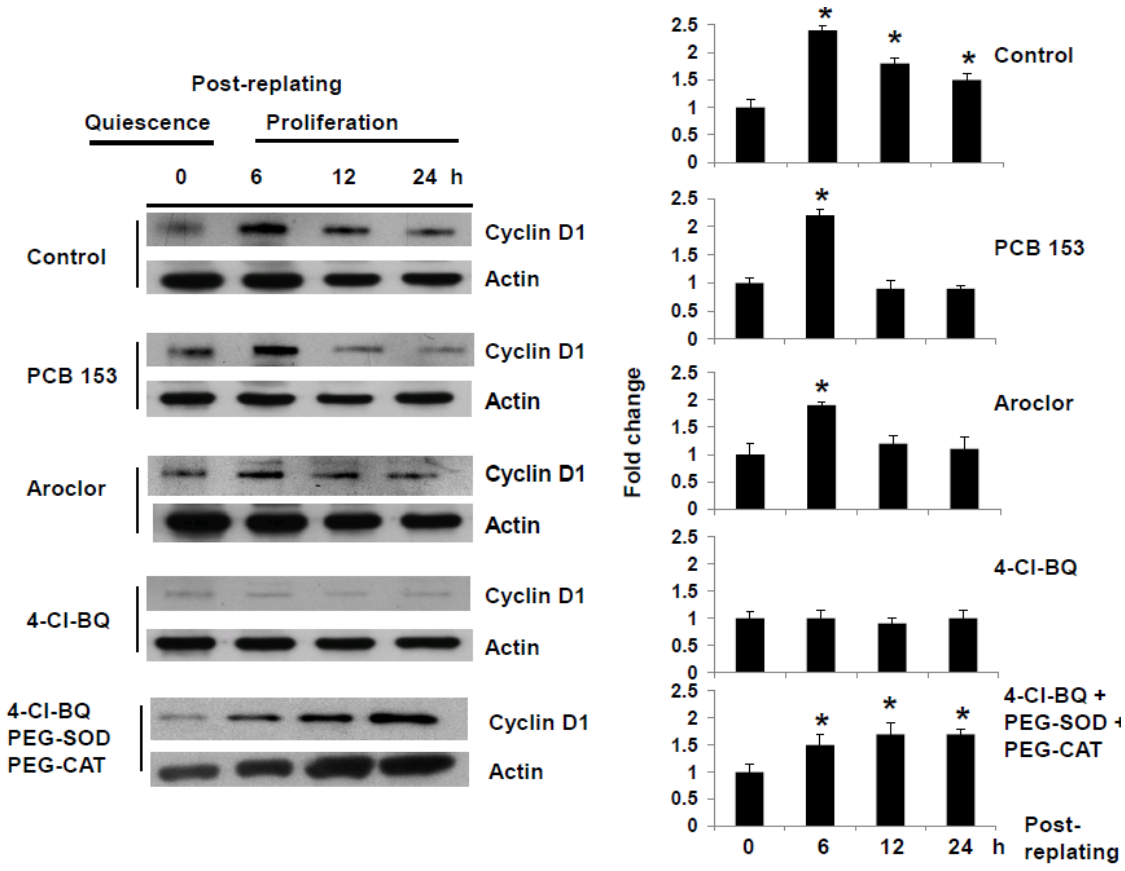

Figure IV-6: 4-Cl-BQ induced decrease in MnSOD activity and increase in cellular ROS levels inhibit the accumulation of cyclin D1 protein during reentry of quiescent cells into the proliferative cycle.

Control and 3 μM PCB treated quiescent MCF-10A cultures were trypsinized and replated at a lower cell density at the end of a 4-day treatment. Total protein extracts were prepared at indicated times post-replating and immunoblotted for cyclin D1. Actin levels were used for comparison. In a separate experiment, cells were incubated simultaneously with 3 μM 4-Cl-BQ, and 100 U/mL of PEG-SOD and PEG-CAT; cyclin D1 and actin levels were assayed by immunoblotting. Cyclin D1 protein levels were normalized to actin levels in individual samples, and fold change calculated relative to untreated control (right panels). Asterisks represent statistical significance relative to untreated control, n=3; *, $p < 0.05$.

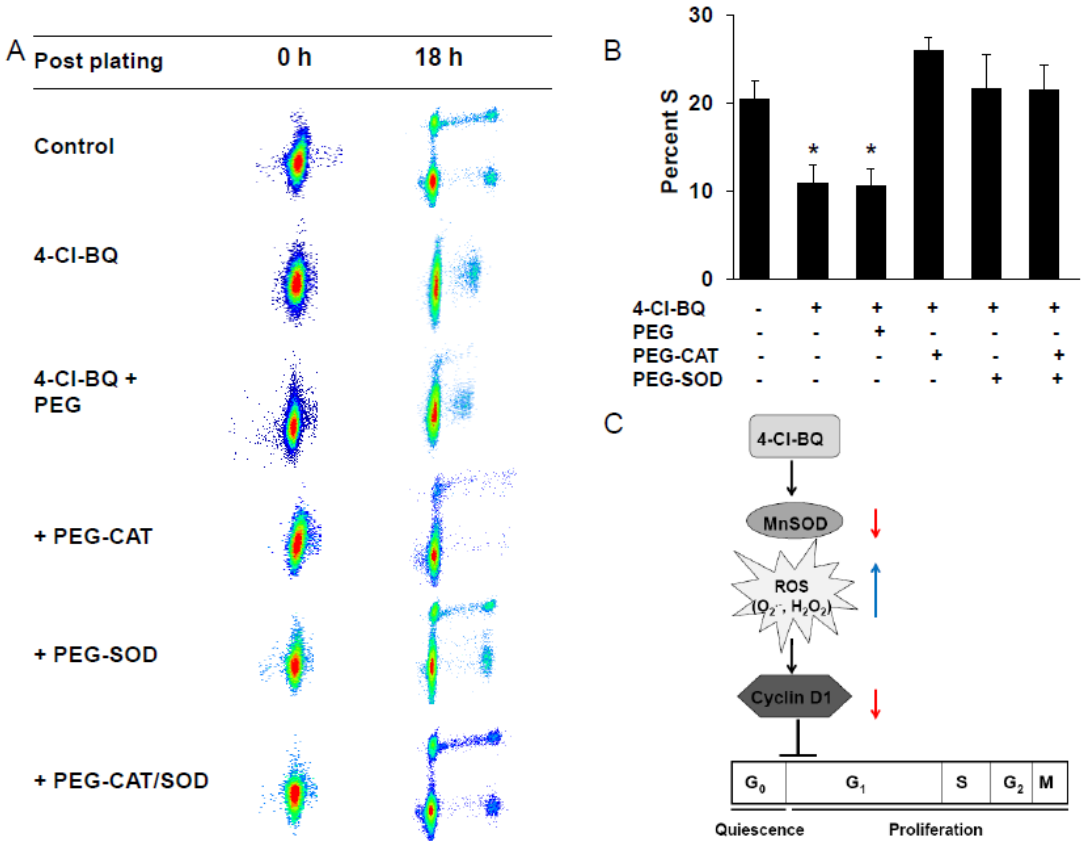

Figure IV-7: PEG-SOD/PEG-CAT abrogates 4-Cl-BQ induced delay in reentry of quiescent cells into the proliferative cycle.

Quiescent MCF-10A cells were incubated with 3 μM 4-Cl-BQ in presence and absence of PEG-SOD/PEG-CAT for 4 days. Cells were replated and continued in culture in presence of 10 μM BrdU for indicated times. (A) Representative BrdU *vs.* PI bi-variate histograms; (B) percent S phase; asterisks represent statistical significance relative to untreated control; n=3; *, $p< 0.05$. (C) Schematic illustration of 4-Cl-BQ induced ROS signaling interfering with reentry of quiescent cells into the proliferative cycle.

Treat-ment (3 μM) Cell cycle phase	0 h		18 h		26 h	
	G_1	$S + G_2$	G_1	$S + G_2$	G_1	$S + G_2$
Control	93 ± 2	7 ± 2	75 ± 4	21 ± 2	73 ± 3	23 ± 3
4-Cl-BQ	92 ± 2	8 ± 1	85 ± 3	*10 ± 2	85 ± 4	*11 ± 3
PCB 153	93 ± 2	7 ± 2	79 ± 3	*16 ± 2	75 ± 4	19 ± 2
Aroclor	94 ± 2	6 ± 2	81 ± 3	*14 ± 2	79 ± 3	*15 ± 3

Table IV-1: Percentage of G_1 and $S + G_2$ phases in MCF-10A cells replated from control and 4 d PCB treated quiescent cells Average ± SD, n=3, $p<0.05$; Asterisks represent statistical significance relative to untreated control

Treatment (3 μM)	0 h		18 h		26 h	
Cell cycle phase	G_1	$S + G_2$	G_1	$S + G_2$	G_1	$S + G_2$
Control	95 ± 2	5 ± 2	71 ± 2	29 ± 3	67 ± 3	33 ± 2
4-Cl-BQ	93 ± 2	7 ± 2	88 ± 3	*12 ± 2	87 ± 3	*13 ± 3
4-Cl-BQ + PEG	92 ± 1	8 ± 1	84 ± 1	*16 ± 2	82 ± 2	*18 ± 2
4-Cl-BQ + PEG-CAT	92 ± 2	8 ± 2	69 ± 2	31 ± 2	66 ± 3	34 ± 3
4-Cl-BQ + PEG-SOD	93 ± 2	7 ± 2	73 ± 4	27 ± 3	70 ± 4	30 ± 3
4-Cl-BQ + PEG-SOD/CAT	93 ± 2	7 ± 2	73 ± 3	27 ± 3	64 ± 3	36 ± 3

Table IV-2: Percentage of G_1 and $S + G_2$ phases in MCF-10A cells replated from control and 4 d 4-Cl-BQ +/- PEG-CAT/PEG-SOD treated quiescent cells. Average ± SD, n=3, $p<0.05$; Asterisks represent statistical significance relative to untreated control

CHAPTER V

2-(4-CHLOROPHENYL)BENZO-1,4-QUINONE INDUCED ROS-SIGNALING INHIBITS PROLIFERATION IN HUMAN NON-MALIGNANT PROSTATE EPITHELIAL CELLS[2]

Overview

Polychlorinated biphenyls (PCBs) and their metabolites are environmental chemical contaminants which can produce reactive oxygen species (ROS) by auto-oxidation of dihydroxy PCBs as well as the reduction of quinones and redox-cycling. We investigate the hypothesis that 2-(4-chlorophenyl)benzo-1,4-quinone (4-Cl-BQ), a metabolite of 4-chlorobiphenyl (PCB3), induced ROS-signaling inhibits cellular proliferation. Monolayer cultures of exponentially growing asynchronous human non-malignant prostate epithelial cells (RWPE-1) were incubated with 0-6 micromolar of 4-Cl-BQ and harvested at the of 72 h of incubation to assess antioxidant enzyme expression, cellular ROS levels, cell growth, and cell cycle phase distributions. 4-Cl-BQ decreased manganese superoxide dismutase (MnSOD) activity, protein, and mRNA levels. 4-Cl-BQ treatment increased dihydroethidium (DHE) fluorescence, which was suppressed in cells pre-treated with polyethylene glycol conjugated superoxide dismutase (PEG-SOD). The increase in ROS levels was associated with a decrease in cell growth, and an increase in the percentage of S-phase cells. These effects were suppressed in cells pretreated with PEG-SOD. 4-Cl-BQ treatment did not change the protein levels of phosphorylated H2AX at the end of 72 h of incubation, suggesting that the inhibition in cell growth and accumulation of

---

[2]Chaudhuri, L. et al.,Environ Int.;36(8):924-30, 2010

cells in S-phase at the end of the treatments were probably not due to 4-Cl-BQ induced DNA double strand break. These results demonstrate that MnSOD activity and ROS-signaling perturb proliferation in 4-Cl-BQ treated *in vitro* cultures of human prostate cells. (NIEHS P42 ES 013661, NIH RO1 CA 111365, Superfund training core grant). L.C performed all experiments and wrote manuscript, E.H.S helped design and analyze PCR assays. P.C.G supervised overall project, designed experiments and edited manuscript.

Results

4-Cl-BQ Treatment of Human Prostate Epithelial Cells Decreased MnSOD Activity, Protein, and mRNA Levels

We have shown previously that PCBs cause oxidative stress in MCF-10A human non-malignant mammary epithelial cells (Venkatesha *et al.,*2008). To determine if PCB-induced oxidative stress could be due to changes in antioxidant enzyme expression, exponentially growing asynchronous cultures of human non-malignant prostate epithelial cells (RWPE-1) were incubated with 0-6 μM of 4-Cl-BQ for 48 h and harvested for analysis of MnSOD activity, protein and mRNA levels. Results showed 0.3 μM of 4-Cl-BQ treatment decreased MnSOD protein levels approximately 50%, which remained low (40% of control) in 3 and 6 μM treated cells (Figure V-1A, left panel). Interestingly, the same treatment did not show any change in catalase protein levels (Figure V- 1A, right panel). To further investigate if the decrease in MnSOD protein levels was also associated with changes in MnSOD activity, cells from replicate dishes were harvested and MnSOD activity was measured by the NBT-superoxide dismutase biochemical activity assay (Spitz and Oberley,1989). MnSOD activity was approximately 50 U/mg in exponentially growing asynchronous RWPE-1 cultures. 4-Cl-BQ treatment decreased MnSOD activity to 40 U/mg in 0.3 μM and 30 U/mg in 3 and 6 μM treated cells (Figure V- 1B). Results from the quantitative RT-PCR assay showed approximately 30%

decrease in MnSOD mRNA levels in 0.3, 3, and 6 μM 4-Cl-BQ treated *vs.* untreated control cells (Figure V- 1C).

4-Cl-BQ Treatment Increased Cellular ROS Levels

MnSOD converts superoxide produced by the univalent reduction of oxygen in the mitochondria to hydrogen peroxide; MnSOD activity is known to regulate cellular ROS levels. The steady state level of cellular ROS is maintained by a balance between the production of ROS and their removal by antioxidants. To determine whether changes in MnSOD activity (Figure V- 1) perturb cellular superoxide levels, RWPE-1 cells were incubated with 0-6 μM 4-Cl-BQ for 48 h and harvested for flow cytometry analysis of DHE-fluorescence. The mean fluorescence intensity (MFI) increased 3-4 fold in 3 and 6 μM 4-Cl-BQ treated cells compared to control (Figure V- 2B). PEG-SOD was used to determine the specificity of the DHE-fluorescence for the measurements of superoxide. Control and 4-Cl-BQ treated cells were incubated with PEG-SOD followed by flow cytometry measurements of DHE-fluorescence. This treatment decreased DHE-fluorescence in control as well as 4-Cl-BQ treated cells (Figure V- 2B). These results suggest that the increase in DHE-fluorescence in cells incubated with 4-Cl-BQ was due to an increase in the steady state levels of cellular superoxide.

MnSOD Activity Regulates Proliferation in Cells Treated with 4-Cl-BQ

To determine whether 4-Cl-BQ-induced decrease in MnSOD activity and increase in cellular superoxide levels could perturb proliferation, a cell growth assay was performed. RWPE-1 cultures were incubated with 3 μM 4-Cl-BQ for 0-72 h, and cell numbers counted at indicated times (Figure V- 3A). Results showed 4-Cl-BQ significantly delayed cell growth at 48 and 72 h of 4-Cl-BQ treatment. Cell population doubling time was calculated to be 22 h in control compared to 33 h in 4-Cl-BQ treated

cells. Interestingly, this delay in proliferation was reversed in cells that were pre-treated with PEG-SOD followed by incubation with 4-Cl-BQ (Figure V- 3B).

4-Cl-BQ Induced Growth-Delay was Associated with an Increase in the Percentage of S-Phase

Cellular growth is a net-result of proliferation and cell death. To determine if the 4-Cl-BQ-induced growth delay was associated with cell death and/or inhibition in cell cycle phase transit, a flow cytometry assay measuring DNA content was performed. Exponentially growing asynchronous RWPE-1 cultures were treated with 3 μM 4-Cl-BQ for 0-72 h and fixed in ethanol. DNA content of ethanol-fixed cells was analyzed by flow cytometry. Representative PI-histograms of DNA content in control and 4-Cl-BQ treated cells are shown in Figure V-4, and the percentages of cell cycle phase distributions are presented in Table V-1. The absence of a cell population with sub-G_1 DNA content (Figure V-4) indicates that the 3 μM 4-Cl-BQ treatments did not result in any cell death at the end of 24, 48, and 72 h treatment. However, the same treatment resulted in the redistribution of cells in different cell cycle phases (Table V-1). The percentage of cell cycle phases at the time of addition of 4-Cl-BQ were as follows: G_1, 46%; S, 42%; G_2+M, 12% (Table V-1). The percentage of G_1 in control cells increased to 54 and 57% at 48 and 72 h without any significant change in percent S-phase, suggesting that these cells are probably progressing towards quiescent growth. In contrast, the percentage of S-phase in 4-Cl-BQ treatment did show an increase from 42% at 0 h to 49% at 48 h and 52% at 72 h (Table V-1). 4-Cl-BQ-induced increase in the percentage of S-phase and decrease in cell number (Figure V- 3) indicate that the 4-Cl-BQ treatment could interfere with DNA synthesis delaying transit through S-phase.

To determine if the accumulation of cells in S-phase could be due to DNA damage, an immunoblot assay was performed to measure the levels of phosphorylated H2AX (γ-H2AX) in control and 4-Cl-BQ treated cells at the end of a 72 h incubation. An

increase in the levels of γ-H2AX is indicative of DNA double strand break. Results (Figure V- 5) showed no significant difference in the levels of γ-H2AX in control compared to 4-Cl-BQ treated cells, suggesting that the inhibition in cell growth and accumulation of cells in S-phase at the end of the treatments were probably not due to 4-Cl-BQ induced DNA double strand break.

Pretreatment with PEG-SOD Inhibits S-Phase Accumulation in Cells Incubated with 4-Cl-BQ

To further determine if MnSOD activity regulates proliferation in cells incubated with 4-Cl-BQ, RWPE-1 cells were pretreated with 150 U/mL of PEG-SOD followed by incubation with 3 μM 4-Cl-BQ for 72 h. The percentage of cell cycle phases was determined by flow cytometry measurements of DNA content in ethanol-fixed cells. The percentage of S-phase in 4-Cl-BQ treated cells increased to 51% at 72 h compared to 40% in untreated control cells (Figure V- 6). Interestingly, pretreatment of cells with PEG-SOD suppressed 4-Cl-BQ induced accumulation of cells in S-phase. These results support the hypothesis that MnSOD activity and ROS-signaling regulate proliferation in 4-Cl-BQ treated human prostate cells.

Discussion

Epidemiological studies indicate increased mortality of capacitor and electric utility workers from various cancers (Bertazzi *et al.,*1987; Brown*,*1987; Gustavsson *et al.,*1986; Loomis *et al.,*1997; Sinks *et al.,*1992). Recent evidences suggest that exposure to PCBs might be causally linked to an increased incidence of breast and prostate cancer (Demers *et al.,*2002; Laden *et al.,*2002; Moysich *et al.,*2002; Ritchie *et al.,*2003). PCBs that are constitutive androstane receptor (CAR)-agonists (e.g. PCB153) have been suggested to increase the risk of prostate cancer presumably *via* the CYP450 mediated metabolism (Ritchie *et al.,*2003). Although PCB3 or its metabolite 4-Cl-BQ is not a

known CAR-agonist, we hypothesize that 4-Cl-BQ induced perturbations in cellular ROS levels could regulate many of the cellular processes including cell proliferation.

4-Cl-BQ is a metabolite of 4-chlorobiphenyl (PCB3), a common PCB-congener found in air. The concentrations of 4-Cl-BQ (0.03-6 μM) used in this study were selected based on the findings that the levels of PCBs in the blood of individuals living in Anniston, Alabama vary widely (0.003 – 6.5 μM) (Hansen *et al.,*2003). Our results showed a decrease in MnSOD activity in RWPE-1 human non-malignant prostate epithelial cells that were incubated with 0.3-6 μM 4-Cl-BQ for 48 h (Figure V- 1). The decrease in MnSOD activity was associated with a corresponding decrease in its protein and mRNA levels. Since the cellular localization of 4-Cl-BQ is unknown, it is unclear how 4-Cl-BQ treatment could down regulate MnSOD expression. It is possible that the 4-Cl-BQ treatment can negatively impact upon the transcription/post-transcription and/or translation/post-translational regulation of MnSOD expression. Alternatively, the 4-Cl-BQ-induced decrease in MnSOD activity could result from a redistribution of cells in S-phase (Figure V-4, Table V-1). This hypothesis is consistent with our previously published results demonstrating an inverse correlation between the percentage of S-phase and MnSOD activity (Menon *et al.,*2007; Sarsour *et al.,*2008).

MnSOD is a nuclear encoded and mitochondrial matrix localized antioxidant enzyme known to convert mitochondria-generated superoxide to hydrogen peroxide. A decrease in MnSOD activity can result in an increase in cellular ROS levels. RWPE-1 cells incubated with 4-Cl-BQ showed a dose-dependent increase in DHE-fluorescence (Figure V- 2). 4-Cl-BQ-induced increase in DHE-fluorescence was suppressed in cells pretreated with PEG-SOD, suggesting that the increase in DHE-fluorescence could result from an increase in the steady-state levels of superoxide. Our results are comparable to a previous study in the literature reporting approximately 50- to 200- fold increase in DCFH fluorescence in HL-60 cells that were incubated with 2.5 μM of 4-Cl-BQ, indicating that the 4-Cl-BQ treatment increased cellular ROS levels (Srinivasan *et*

*al.,*2001). The difference in fold change, 3- to 4- fold increase in DHE fluorescence in the present study compared to 50- to 200- fold increase in $CDCFH_2$ fluorescence in the earlier study, could be due to the differences in the assays (DHE vs. $CDCFH_2$) and cell lines (HL-60 vs. RWPE-1) used in the two studies.

The decrease in MnSOD activity (Figure V- 1) and increase in DHE-fluorescence (Figure V- 2) suggest that 4-Cl-BQ can induce mitochondria-generated ROS, presumably superoxide. Alternatively, it is possible that 4-Cl-BQ having a quinone "like" structure can undergo redox-cycling leading to an increase in cellular ROS levels. Furthermore, there is considerable evidence that semiquinone radicals generated from the hydroquinone/quinone redox system can be a primary source for formation of ROS (Eyer*,*1991; Guo *et al.,*2002; Hall *et al.,*1994; Song *et al.,*2008a; Song *et al.,*2008b). Consistent with this hypothesis, we have previously shown that semiquinone radicals are indeed formed in 4-Cl-BQ treated MCF-10A human non-malignant mammary epithelial cells (Venkatesha *et al.,*2008). Therefore, the increase in cellular ROS levels in 4-Cl-BQ treated RWPE-1 cells could originate from the formation of a semiquinone radical.

4-Cl-BQ resulted in a significant decrease in cell number at 48 and 72 h post-treatment (Figure V- 3A). Cell population doubling time in control cells was 22 h, which increased to 33 h in 4-Cl-BQ treated cells (Figure V- 3A). The increase in doubling time was associated with an increase in the percentage of cells in S-phase (Figure V- 4, Table V-1). Although the percentage of cells in G_2+M phase was comparable in control and 4-Cl-BQ treated cells, the percentage of cells in G_1 phase was lower in 4-Cl-BQ treated cells compared to control. These results suggest that the treatment of cells with 4-Cl-BQ could recruit more G_1 cells into S-phase. This hypothesis is consistent with our previously published results demonstrating a prooxidant event facilitating the entry of G_1 cells into S-phase (Menon *et al.,*2003). Alternatively, 4-Cl-BQ treatment could delay progression through S-phase, which could then result in an increase in the percentage of cells in S-phase. A delay in transit through S-phase could contribute to the increase in cell

population doubling time in cells incubated with 4-Cl-BQ (Figure V- 3). 4-Cl-BQ induced perturbation in cell cycle phase distributions was also observed in V79 hamster fibroblasts (Zettner *et al.,*2007). The authors in this previous study showed 4-Cl-BQ treatment decreased the percentage of G_1 cells, while the same treatment resulted in an increase in the percentage of S-phase cells. Interestingly, 4-Cl-BQ induced changes in cell cycle phase redistributions did not affect V79 cell viability and proliferation compared to control. Our results show a correlation between 4-Cl-BQ induced accumulation of cells in S-phase and inhibition in RWPE-1 cell proliferation. Cell population doubling increased from 22 h in control to 33 h in 4-Cl-BQ treated cells (Figure V- 3).

The decrease in cell number (Figure V- 3A) could also be due to cell death. However, the percentage of cells with sub-G_1 DNA content in 4-Cl-BQ treated cells was not significantly different than control cells (Figure V- 4). Likewise, there was no difference in the protein levels of γH2AX in control compared to cells treated with 4-Cl-BQ (Figure V- 5). These results suggest that the accumulation of cells in S-phase and an increase in cell population doubling time in cells incubated with 4-Cl-BQ were probably not due to DNA double strand break. Instead, 4-Cl-BQ induced decrease in MnSOD activity and an increase in cellular superoxide levels could regulate cell population doubling time and accumulation of cells in S-phase. This notion is further evident from the results presented in Figure V-3B and 6. Cells pretreated with PEG-SOD followed by incubation with 4-Cl-BQ suppressed the accumulation of cells in S-phase and subsequently inhibited the decrease in cell number.

In summary, our results show that short-term (24-72 h) incubation with 4-Cl-BQ decreased MnSOD activity and increased cellular superoxide levels. The increase in cellular superoxide levels was associated with an increase in the percentage of cells in S-phase and cell population doubling time. Cells pretreated with PEG-SOD reversed the effects of 4-Cl-BQ. Because MnSOD is a mitochondrial matrix localized enzyme, these

results support the hypothesis that mitochondrial generated ROS-signaling regulates cellular responses to 4-Cl-BQ exposure. This hypothesis is further supported by our recent microscopic observation of co-localization of MitoSOX red oxidation with MitoTracker green in 4-Cl-BQ treated human mammary (MCF-10A) and prostate (RWPE-1) epithelial cells (Zhu *et al.,*2009).

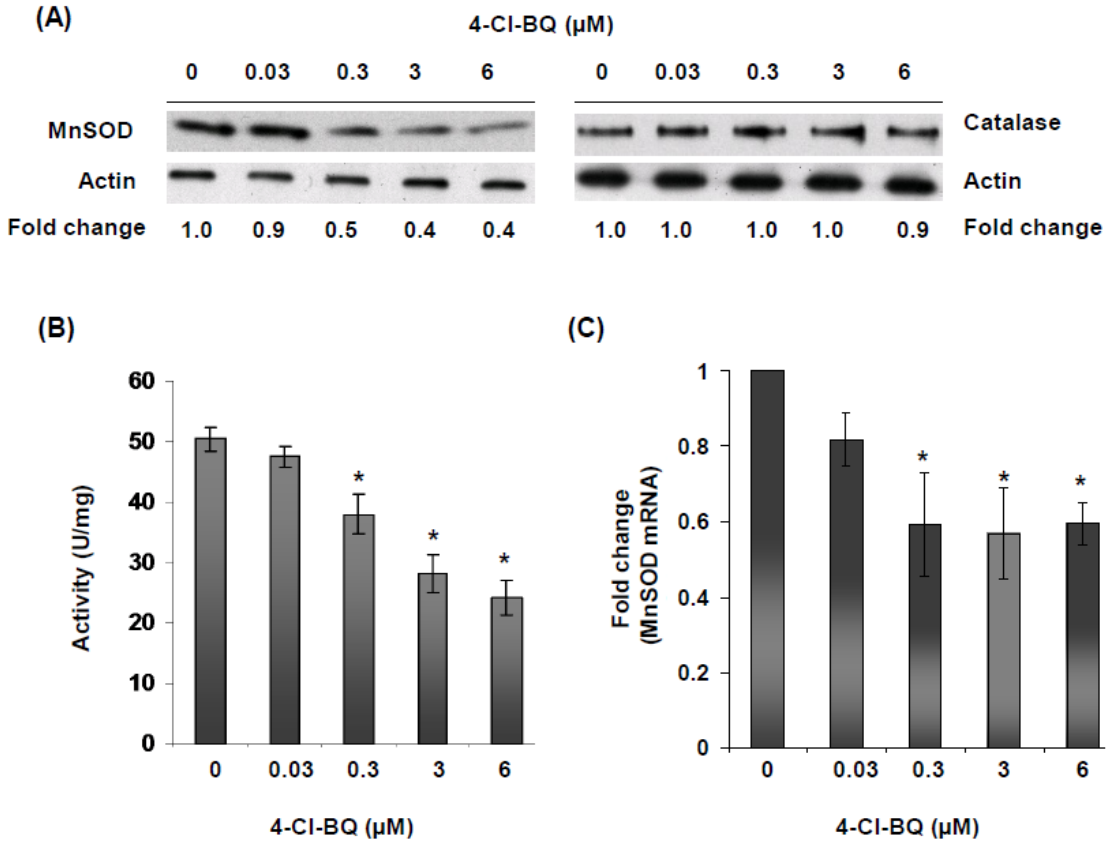

Figure V-1: 4-Cl-BQ treatment decreased MnSOD activity, protein, and mRNA levels in human prostate epithelial cells.

Exponentially growing asynchronous cultures of RWPE-1 human non-malignant prostate epithelial cells were treated with 0-6 μM 4-Cl-BQ for 48 h and harvested for measurements of (A) MnSOD protein, (B) activity, and (C) mRNA levels. Immunoblotting of catalase and actin were included for comparison of results. Fold change was calculated relative to control. Asterisk indicates significant difference compared to control ($n = 3$, $p<0.05$).

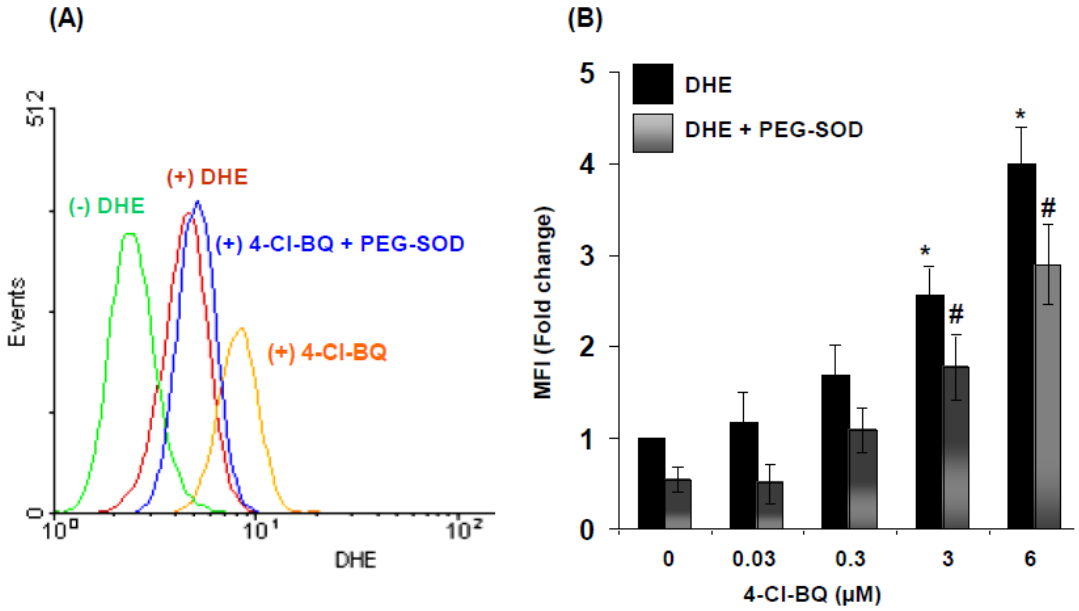

Figure V-2: 4-Cl-BQ treatment increased cellular steady-state levels of ROS.

Exponentially growing asynchronous cultures of RWPE-1 cells were treated with 0-6 μM 4-Cl-BQ for 48 h and incubated with a prooxidant-sensitive dye, dihydroethidium (DHE). DHE-fluorescence was analyzed by flow cytometry, and the mean fluorescence intensity (MFI) was calculated using CellQuest software. Representative histograms are shown in (A): (-) DHE, autofluorescence of control cells; (+) DHE, control cells incubated with DHE; (+) 4-Cl-BQ, cells treated with 3 μM 4-Cl-BQ followed by DHE staining; (+) 4-Cl-BQ + PEG-SOD, cells treated simultaneously with 3 μM 4-Cl-BQ and 100 units of PEG-SOD followed by DHE-staining. (B) Fold-change in MFI calculated relative to 0 h untreated control. *, # indicates significant difference compared to untreated control and PEG-SOD treated control respectively ($n = 3$, $p<0.05$).

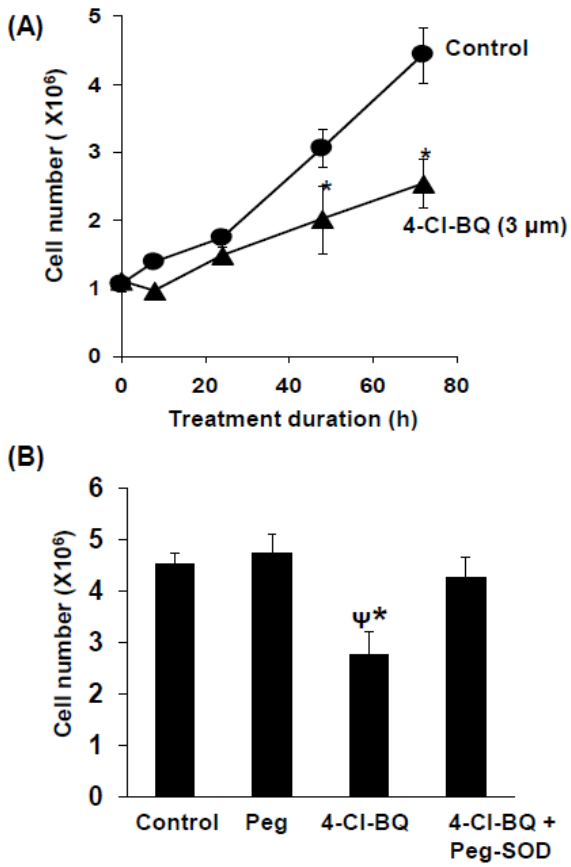

Figure V-3: MnSOD activity regulates proliferation of human prostate cells incubated with 4-Cl-BQ.

RWPE-1 cells were treated with 3 µM 4-Cl-BQ and cell numbers counted at the indicated time (A). (B) In a separate set of experiments, cells were pretreated with 150 U/mL of PEG-SOD followed by incubation with 3 µM 4-Cl-BQ. Cell numbers were counted at the end of 72 h incubation. Asterisk indicates significant difference compared to control; Ψ indicates significance compared to 4-Cl-BQ and PEG-SOD treated cells ($n = 3$, $p<0.05$).

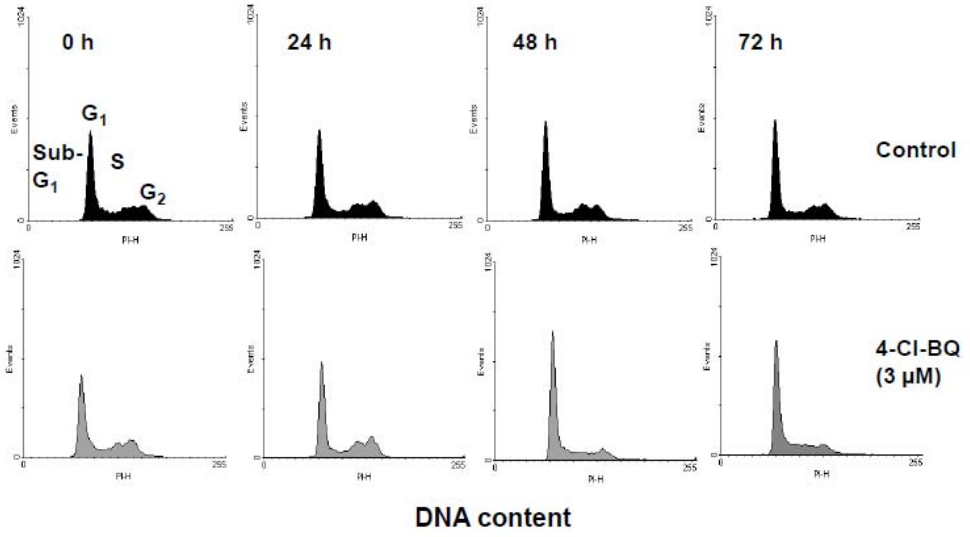

Figure V-4: Increased percentage of S-phase in cells incubated with 4-Cl-BQ.

Exponentially growing asynchronous cultures of RWPE-1 were treated with 3 μM 4-Cl-BQ for the indicated times and fixed in ethanol. Ethanol fixed cells were treated with RNase A and stained with propidium iodide (PI). Cell cycle phase distributions were analyzed by flow cytometry measurements of DNA content of PI-stained cells. Representative DNA histograms of control and 4-Cl-BQ treated cells are shown and the areas representing cells with DNA content less than G_1 (sub-G_1), G_1, S, G_2 are marked. The percentage of cells in each cell cycle phase is calculated using MODFIT and results are shown in Table V-1.

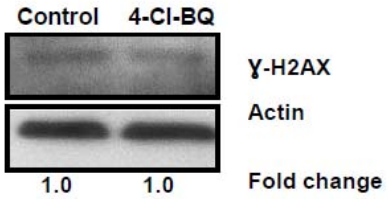

Figure V-5: 4-Cl-BQ induced delay in cell growth was not associated with DNA double strand break.

Total cellular protein extracts were isolated from control and cells incubated with 3 μM 4-Cl-BQ for 72 h. Proteins were separated by SDS-PAGE and immunoblotted for the protein levels of phosphorylated H2AX (γ-H2AX).

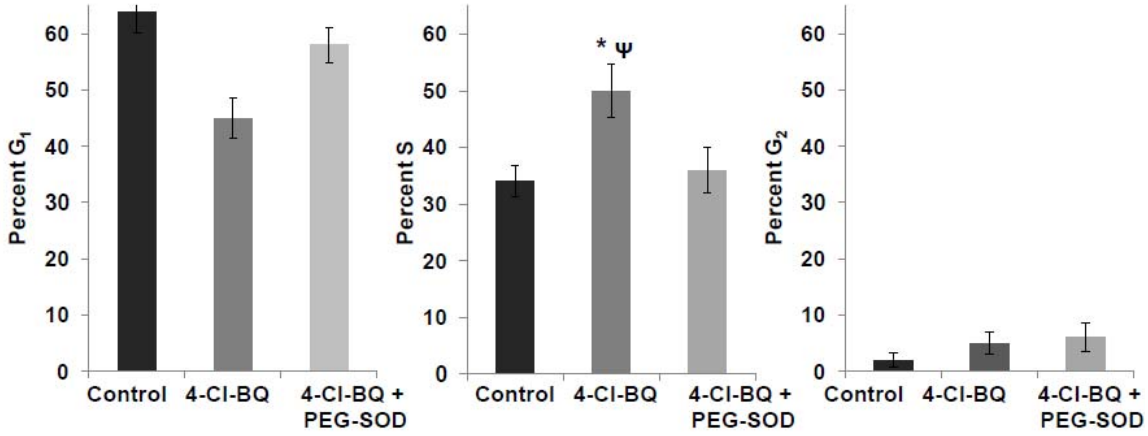

Figure V-6: Prior treatment with PEG-SOD inhibits 4-Cl-BQ induced accumulation of cells in S-phase.

RWPE-1 cells were treated with 150 U/mL of PEG-SOD followed by incubation with 3 μM 4-Cl-BQ for 72 h. Ethanol fixed cells were analyzed for DNA content and the percentage of cell cycle phase calculated using MODFIT software. *, # indicates significant difference compared to untreated control and 4-Cl-BQ + PEG-SOD treatment respectively ($n = 3$, $p<0.05$).

Treatment	Hours	G_1	S	G_2
Control	0	46 ± 1	40 ± 1	11 ± 1
	8	50 ± 2	36 ± 1	14 ± 2
	24	53 ± 1	39 ± 1	8 ± 1
	48	54 ± 2	37 ± 1	9 ± 1
	72	57 ± 2	38 ± 1	3 ± 3
4-Cl-BQ	0	46 ± 1	42 ± 1	12 ± 1
	8	49 ± 1	42 ± 1	9 ± 2
	24	49 ± 1	41 ± 1	10 ± 1
	48	42 ± 1	□49 ± 1	9 ± 1
	72	45 ± 1	□52 ± 1	3 ± 1

Table V-1: Percentage of G_1 and S and G_2 phases in 3 μM 4-Cl-BQ treated RWPE-1 cells Average ± SD, n=3, $p<0.05$; Asterisks represent statistical significance relative to untreated control.

CHAPTER VI

FUTURE DIRECTIONS

Hypothesis and Specific Aims

Loss of tumor suppressor gene function plays central roles in the pathogenesis of proliferative disorders like cancer. Loss of function or reduction in function can result in progression towards cancer. One such mechanism is thought to be mediated by regulatory elements like AU-rich elements (AREs) and microRNA (miRNA) seed matches on the 3'UTR. Recent studies have shown redox sensitive proteins binding to AREs with high affinity repressing post-transcriptional gene expression. More than half of genes in the human genome have been identified to have multiple polyadenylation signals and many alternative polyadenylation signals (APA) are evolutionarily conserved (Lutz,2008). Selection of APA can eliminate large section of the 3'UTR; thereby escaping the regulatory potential of long 3'UTR. Alternate mRNAs differing in the length of their 3'UTR have been found to be dependent on cell cycle phases (Edwalds-Gilbert *et al.,*1997; Martincic *et al.,*1998). Since regulatory element; AREs and miRNAs are known to regulate mRNA stability and translation, preferential abundance of transcripts will be a fundamental regulator of gene expression. Antioxidant enzymes not only maintain the intracellular redox balance, but also have been shown to play an important role in controlling cellular proliferation (Michiels *et al.,*1988; Oberley *et al.,*1995; Sarsour *et al.,*2008). Our exciting results show that pereferential abundance of longer transcripts during proliferation in MnSOD results in lower MnSOD protein translation and activity levels. These results lead us to test the hypothesis that 3'UTR of redox enzymes (MnSOD, CuZnSOD, and catalase) regulate cellular redox flux in quiescent and proliferating normal human fibroblasts.

Aim 1: Determine if specific sequence in the 3'-untranslated (UTR) region of MnSOD, CuZnSOD, and catalase regulate their mRNA levels in quiescent and proliferative growth states. Reporter constructs and deletion studies will be performed to identify specific sequence in the 3'UTRs that regulate mRNA levels of redox enzymes. RNA-gel-shift assay will be performed to identify protein binding to specific 3'UTR sequence in quiescent and proliferative growth states.

Aim 2: Determine if overexpression of 3'UTRs of redox enzymes influence endogenous mRNA levels of redox enzymes. Determine if such manipulations alter protein levels and activities of redox enzymes leading to subsequent changes in cellular growth states.

Significance

Elucidation of the molecular mechanisms of 3'-UTR-mediated regulation of redox enzymes will identify 3'UTRs and RNA-binding proteins as novel molecular targets that can be integrated into the design of innovative redox-based preventive and therapy-based approaches.

Background

Recently, it has been recognized that more than half of human genes have multiple polyadenylation sites (Tian *et al.,*2005). Alternate processing of the polyadenylation signal defined as alternate polyadenylation (APA) is being recognized as an important level in controlling gene expression. This process is widespread amongst human genes and has often been suggested as a mechanism of evolution for phenotypic complexity in mammals (Edwalds-Gilbert *et al.,*1997; Johnson *et al.,*2003). Sequence analysis of MnSOD, CuZnSOD and catalase has revealed the presence of more than one polyadenylation signal (PAS), AAUAAA on their 3'UTR. APA may result in the generation of different mRNA transcripts differing in the 3'UTR length or also encoding

different proteins (Sandberg *et al.,*2008). Preferential selection of PAS and alternate cleavage can influence nuclear and cytoplasmic localization, mRNA stability and translation. Alternate mRNAs have also been found to be present in different stages of the cell cycle, tissues and developmental stages (Ji *et al.,*2009; Wang *et al.,*2008a). Changing PAS efficiency can impact the amount of gene expression. Both cis-elements like upstream GU-rich elements and trans-factors like the cleavage and polyadenylation stimulation factor dictates the selection of one PAS over the others (Mayr and Bartel*,*2009; Sandberg *et al.,*2008). Use of alternate PAS can often eliminate large parts of the 3'UTR thereby escaping regulation of the longer 3'UTR.

Cis-elements on the 3'UTR and their interactions with specific RNA binding proteins are one of the most studied mechanisms known to alter mRNA stability and translation. These cis- elements include adenosine and uridine rich elements known as the AU-rich elements (AREs) ($A(U)_{3-7}A$). The Family of ARE binding proteins (AUF1, HuR, AUH, AUBF, Hel-N1) binds to these specific sequences on the mRNA with high affinity. Binding of ARE proteins can be both positive and negative regulators of mRNA stability depending on the protein and the sequence to which they bind. For example binding of AUF1 (heterogeneous nuclear ribonucleoprotein D) to AU nonamers generally destabilizes the mRNA while binding of HuR is known to generally stabilize the mRNA (Gorospe*,*2003; Goswami *et al.,*2000; Kiledjian *et al.,*1997).

The longer MnSOD mRNA transcript (4.2 kb) contains regulatory elements like 8 AU-rich elements (A(U)3-7A) and several miRNA seed matches (miRNA 377, 222, 21) (Church *et al.,*1993; Liu *et al.,*2009; Wang *et al.,*2008b). Similarly, cytoplasmic CuZnSOD has also been reported to have two transcripts in humans, 0.7 and 0.9 kb (Sherman *et al.,*1984). Both transcripts were transcribed from the same gene and the 0.7 kb transcript is four times more abundant than the 0.9 kb mRNA (Sherman *et al.,*1984). Sequence analysis reveals the presence of 1 ARE in the 0.9 kb transcript CuZnSOD

transcript. Catalase has a single reported mRNA but 11 AREs on its 3'UTR making it highly amenable to regulation by ARE binding proteins.

3'UTRs of rat MnSOD, CuZnSOD and catalase mRNAs are known to regulate translation under normal conditions as well as in response to environmental stress (Chung *et al.,*1998; Kilk *et al.,*1995). Binding of protein to 3'UTR cis-elements of MnSOD has been shown to affect translation efficiency and stability in rats. ARE binding proteins have been previously shown to be responsive to the redox environment of the cell (Goswami *et al.,*2000). Taken together these results give compelling evidence to support our hypothesis that the 3'UTR of antioxidant enzymes can regulate the redox flux by sensing changes in the intracellular redox environment and controlling the translation of mRNAs.

Aim 1

Determine if specific sequence in the 3'UTRs of MnSOD, CuZnSOD, and catalase regulate their mRNA levels in quiescent and proliferative growth states.

Rationale

Our preliminary results show that there is a preferential abundance of the longer transcript during proliferation which results in lower protein expression for MnSOD. Furthermore, cell cycle coupled gene expression has been shown to be tightly regulated by interaction of 3'UTR with protein complexes (Goswami *et al.,*2000).

Experimental Design

To determine if specific sequences in the 3'UTR of MnSOD, CuZnSOD and catalase regulate antioxidant expression during cell cycle progression, exponentially growing NHF cells will be studied for:

1a. Preferential abundance of alternate polyadenylated transcripts for MnSOD, CuZnSOD in quiescent and proliferative growth state by Q-RT-PCR methods.

1b. Deletion reporter assay of 3'UTR and site-directed mutagenesis of the antioxidant mRNAs to determine specific sequence responsible for controlling mRNA stability or translation.

1c. RNA electrophoretic mobility shift assay (REMSA) to identify proteins binding to sequences on the 3'UTR.

1a. Sequence analysis of the antioxidant enzymes revealed the presence of multiple polyadenylation signals (PAS) for MnSOD and CuZnSOD. Real time PCR primers will be designed to specifically amplify each transcript. The primer for the shorter transcript will be designed such that the reverse primer is anchored at the proximal PAS for specific amplification (Table VI-1). Normal human fibroblast (NHF) cells plated at low density will be cultured over a period of 10 days. Cells will be fixed in 70% ethanol for uni- and bi-variate flow cytometry measurements of DNA content to determine cell cycle phase distributions. Cells will be collected from parallel plates every alternate day for total cellular RNA extraction. 1 µg of the RNA will be reverse transcribed. 2 µl of the product will be used for performing quantitative real time PCR (Q-RT-PCR) using primers specific for each transcript. 18S will be included as endogenous control. Correlation plots of the transcripts and percent S-phase will enable us to understand the abundance of each transcript associated with growth states.

1b. Based on our preliminary results in Chapter I, we anticipate the preferential abundance of transcripts to correlate with antioxidant enzyme activity and protein levels. Correlation of MnSOD transcripts with growth states and subsequent effect on MnSOD gene expression was linked to the abundance of AREs on the 3'UTR. Deletion reporter assays will be applied to identify these 3'UTR cis-acting elements. PCR amplified 3'UTR regions will be cloned into psiCHECK2 dual luciferase reporter plasmid. The insert will be verified by restriction digestion and sequencing. NHF cells will be transfected using Lipofectamine and fluorescence of Renilla luciferase will be measured using a luminometer. Fluorescence of firefly luciferase in the psiCHECK2 vector will be used to

correct for differences in transfection efficiency. Deletion analysis will be used to further map the cis-acting element in 3'UTR of the antioxidant enzymes. T to G site-directed mutagenesis will be performed to determine the specificity of the AREs in regulating transcript levels and antioxidant gene expression. The psiCHECK2 plasmid DNA will be denatured at 100ºC and selection primer, provided by manufacturer (Clontech) will be added to the reaction to anneal to the plasmid DNA by chilling on ice for 5 min. Selection primer changes Nde I restriction enzyme site into a unique Nco I site, which would allow selection for mutated plasmids. Mutant DNA primer containing three consecutive bases changed from T to G will be added to the primer/plasmid annealing reaction. These primers are phosphorylated at the 5' end so that they can be ligated at the 3'end of the newly synthesized strand. T4 DNA polymerase is used to extend the primers to synthesize the mutant strand. T4 DNA ligase is used to ligate the newly synthesized DNA to the 3' end of the oligonucleotide primer, which is required to obtain a covalently closed circular DNA with high transformation ability. Specialized *E. coli* strain, BMH 71-18 *mutS* is used for transformation, because it is defective in mismatch repair. Restriction enzyme digestion is required at this step to enrich the mutant circular plasmid. Isolation of the plasmid pool will be done by 'Boiling-Lysis' method. Selection of the mutated plasmid will be done by sequencing as well restriction enzyme digestion using Nde I. Digested plasmid is expected to run as a discrete band and the uncut band is expected to run as two bands corresponding to circular and supercolied form. The uncut band is expected to correspond to the mutant plasmid, because the Nde I restriction site was mutated to Nco I site. These plasmids will again be transfected into the cells and Renilla luciferase activity will be measured.

1c. RNA-protein electromobility shift assay (REMSA) will be performed to determine if protein binding to antioxidant enzyme 3'UTR varies in quiescent and proliferating cells. cDNA sequences representative of AU-rich regions of the 3'UTR will be amplified by standard PCR methods. PCR amplified 3'UTR of the antioxidant enzyme

containing the cis-acting element (ARE) will be cloned into the transcription vector (pGEM-T vector) Riboprobes representing the strand RNA from each plasmid will be in-vitro transcribed incorporating ^{32}P-UTP (800 Ci/mmol). T7 RNA polymerase will be used following our previously published protocols (Goswami *et al.,*2000). Electrophoretic separation will show the relative movement of 'free' RNA compared to protein bound RNA. The lane with the protein bound RNA is expected to be larger and less mobile on the gel. Specific antibody to RNA binding protein complexes will be used. This will create a larger complex with greater shift and will help identify the protein present on the protein-RNA complex (supershift assay). REMSA and autoradiography will be applied to separate and visualize RNA-protein complexes. Identification of specific proteins bound to antioxidant 3'UTR cis-element will also be assayed by UV cross-linking of RNA-protein binding reactions. Following UV-crosslinking, reaction mixtures will be treated with RNases and separated by SDS-PAGE. Specific proteins bound to radioactive RNA will be visualized by autoradiography.

Anticipated Results

Based on our results in Chapter I, it is anticipated that the growth-state related expression of antioxidant enzyme and its activity is regulated by a preferential transcript selection. It is anticipated that a preferential transcript selection will favor the abundance of the shorter transcripts (MnSOD: 1.5 kb; CuZnSOD: 0.7 kb) in quiescent growth, while the longer transcripts (MnSOD: 4.2 kb; CuZnSOD: 0.9 kb) would be more abundant in exponential cultures. Based on our preliminary results in Chapter I, we anticipate AU-rich regions to be regulating transcript stability and/or translation. In Table VI-1 we observe preferential enrichment of AREs in one transcript compared to the other. The PCR generated insert containing AT sequences to which proteins can bind to destabilize the mRNA is anticipated to show lower luciferase activity compared to the construct containing no AREs, or when the ARE is mutated. If the specific AU sequence is

disrupted by mutagenesis changing thymidine to guanosine residues on the cDNA, RNA binding proteins might no longer be able to recognize the cis-elements and their binding affinity to the mRNA is expected to reduce drastically. Alternatively, RNA binding proteins might also bind to the cis-elements and stabilize the mRNA further, resulting in increased luciferase activity in the construct carrying multiple AREs. Using specific antibodies in REMSA to the known RNA binding proteins like HuR, AUF1 will enable us to identify the specific RNA binding protein to the AREs. This will also enable us to explain the stabilizing *vs* destabilizing function of the mRNA transcripts selected during quiescent and proliferative growth.

Alternative Approach

It is possible that differences in transcript abundance and gene expression are not regulated by AU-rich elements (AREs) on the 3'UTR. We will then determine if other regulatory sequences present on the 3'UTR could be responsible for 3'UTR mediated repression. In addition to AREs, miRNAs present on the 3'UTR could also be responsible for the observed full length 3'UTR associated repression. Literature reports and sequence analysis of the MnSOD 3'UTR reveals the presence of several miRNA seed matches on the 3'UTR, like miR 377, miR 222 and miR 21 (Liu *et al.,*2009; Wang *et al.,*2008b). The selected miRNA mimetics will be transfected in cells in different growth states and enzyme activity and protein levels will be measured to determine their influence on translational repression. To further confirm the role of the specific miRNA in regulating gene expression, cells will be treated with inhibitors to the select miRNA. mRNA, protein and activity levels of the antioxidant enzymes will be measured post-treatment to ensure that miRNA associated repression can be overridden.

Aim 2

Determine if overexpression of 3'UTRs of redox enzymes influence endogenous mRNA levels of redox enzymes. Determine if such manipulations alter protein levels and activities of redox enzymes leading to subsequent changes in cellular growth states.

Rationale

Recent reports suggest that presence of 'pseudo-mRNAs' can act as decoys that presents the same cis-regulatory elements as the translating mRNA . These decoys when present with the target mRNA can deplete the trans-regulatory elements and thereby de-repress the target mRNA. By this novel mechanism, the translation ability of the mRNA could be enhanced.

Experimental Design

To determine if overexpression of 3'UTRs of redox enzymes influence endogenous mRNA levels of antioxidant enzymes, exponentially growing NHF cells will be studied for:

2a. Endogenous mRNA levels of the antioxidant enzymes measurement by Q-RT-PCR after overexpressing the 3'UTR of short or long transcript.

2b. Antioxidant enzyme activity and protein levels by biochemical activity assay and immunoblotting respectively, after overexpressing the 3'UTR of multiple transcripts.

2c. Alteration in cell cycle phase distribution by flow cytometric methods of DNA content by propidium iodide staining.

2 a, b, c. The 3'UTR of short and long transcript of select antioxidant gene will be PCR amplified and cloned in the multiple cloning site upstream of the Renilla luciferase in the psiCHECK2 reporter vector. AU rich regions in the 3'UTRs of the antioxidant mRNAs will be selected. The insert sequence will be verified by restriction digestion and sequencing. Seventy to eighty percent confluent NHF cells will be transfected using Lipofectamine with 100 ng of designed plasmids (decoy) 24 h post plating. Non-

transfected cells and empty vector transfected cells will be included as controls. Forty eight hour post plating, cells will be collected for total cellular RNA extraction. Q-RT-PCR assay will be performed on the reverse transcribed cDNA using primers specific to multiple transcript forms. 18S will be included as endogenous control. This experiment would enable us to measure the endogenous levels of antioxidant transcripts in the 3'UTR overexpressed cells. Antioxidant 3'UTR containing cells will also be assayed for activity and protein levels using biochemical assays and immunoblotting. In parallel plates, cells will be replated at the end of 48 h. Twenty four post plating cells will be collected to measure cell cycle distribution using flow cytometry.

Anticipated Results

It is anticipated that antioxidant 3'UTR decoy mRNA will enhance endogenous translation. Since protein binding to 3'UTRs influence translation, we anticipate that over expression of decoy 3'UTR would consume more of the 3'UTR mRNA binding proteins. This will de-repress the target gene expression. We demonstrate that overexpression of MnSOD 3' UTR as decoy increased the endogenous levels of the 4.2 transcript (Figure VI-1). These results are consistent with a decrease in percent S-phase (Figure VI-2). An increase in the 4.2 kb MnSOD transcript is anticipated to increase MnSOD protein and activity which may influence cellular redox flux. Replating the cells at the end of 48 h would enable the quiescent cells to re-enter the cell cycle. Depending on the pro-proliferative or anti-proliferative function of the antioxidant gene, we anticipate to see differences in the cell cycle distribution. For example for MnSOD, overexpressing the full length 3'UTR depletes the endogenous trans-factors (ARE binding proteins) thereby resulting in increased endogenous MnSOD mRNA levels. Increased MnSOD levels are known to inhibit proliferation (Sarsour *et al.,*2008), we anticipate these 3'UTR overexpressing cells to have lower percent S-phase than the non-transfected or empty vector or cells expressing the truncated 3'UTR which does not contain AREs. In Figure

VI-2 we observe cells transfected with the plasmid carrying the maximum number of AREs to have lower percent S-phase compared to the cells transfected with the plasmid carrying the 3'UTR of the 1.5 kb MnSOD transcript with no AREs. CuZnSOD activity has been shown to be higher during S-phase compared to G_0 phase in NIH 3T3 cells (Oberley *et al.,*1995). From our preliminary results, we anticipate that the longer transcript (0.9 kb) of CuZnSOD to be more abundant during quiescence (G_0) and the shorter transcript (0.7 kb) to be enriched in proliferating cells.

Alternative Approach

In the probability that ARE containing 3'UTR is unable to alter antioxidant enzyme expression, we will try miRNAs as regulators of gene repression. In our plasmid design we will PCR amplify regions of the 3'UTR known to harbor miRNA seed matches. Overexpressing the plasmid in the NHF cells as described above will enable to ensure if other regulators of 3'UTR mediated gene repression is involved.

Statistical Methods

Statistical significance will be determined by one and two-way ANOVA with Tukey's post hoc test and Student t-tests using GraphPad Prism, version 4 and SPSS. Homogeneity of variance will be assumed with 95% confidence interval level. Results from at least $n \geq 3$ with $p < 0.05$ will be considered significant. All western blots will be performed at least twice to show reproducibility.

Human Antioxidant Enzymes	Transcript size (kb)	Number of AU-rich elements (ARE)	Reference
CuZnSOD	0.7	0	Sherman L, et al., *Nucleic Acids Res*. 1984;12(24):9349-65
	0.9	1	Danciger E, et al. *Proc Natl Acad Sci* . 1986;83(11):3619-23.
MnSOD	1.5	1	St Clair DK, et al., *Free Radic Res Commun*. 1991;2:771-8.
	4.2	8	Church SL. *Biochim Biophys Acta*. 1990;1087(2):250-2.
Catalase	2.3	11	NM_001752

Table VI-1: Antioxidant enzymes mRNA cis- acting regulatory elements

Gene	Primer sequence
MnSOD	FP: 5'-TTTTCTCGAGGCTTTGGTGGTGGATTGAAAC-3'
4.2 kb	RP: 5'-AAAAGCGGCCGCCATCCCTACAAGTCCCCAAAGT-3'
1.5 kb	FP: 5'-TTTTCTCGAGTAATGATCCCAGCAAGATAA-3'
	RP: 5'-AAAAGCGGCCGCTTTTTTTTTTTTTTTGATGGTTG-3'
CuZnSOD	FP: 5'- TTTTCTCGAGAAGCAGATGACTTGGGCAAAGG-3'
0.7 kb	RP: 5'- GGCGATCCCAATTACACCA -3'
0.9 kb	FP: 5'-TTTTCTCGAGAAAGTACCTGTAGTGAGAAACTG-3'
	RP: 5'- AAAAGCGGCCGCTAGCCTCATAATAAGTGCCATAC-3'
Catalase	FP: 5'-TTTTCTCGAGTCTGGGACTTCTGGAGCCTA-3'
	RP: 5'- AAAAGCGGCCGCAGTCAGGGTGGACCTCAGTG-3'

Table VI-2: Primer sequence for amplifying antioxidant enzymes. Sequence highlighted in red is for XhoI restriction site and in blue is for NotI restriction site.

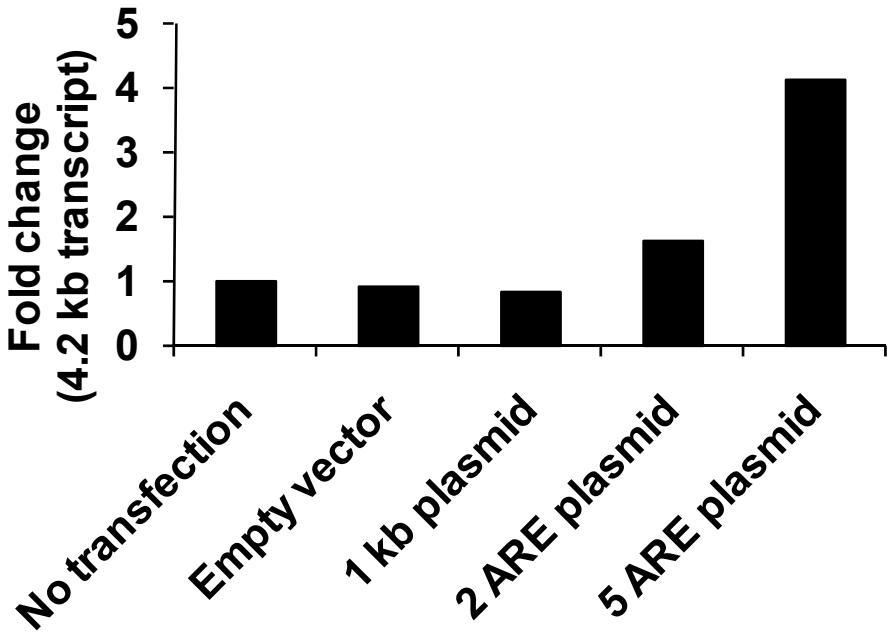

Figure VI-1: Endogenous 4.2 kb MnSOD transcript levels increased in MDA-MB-231 cells overexpressing plasmids carrying 3'UTR of the short and long transcript

MDA-MB-231 cells were transfected with plasmids carrying the 3'UTR of the short transcript (1.5 kb) and the 3'UTR carrying multiple AREs of the longer transcript (4.2 kb). Endogenous 4.2 kb transcript levels were measured by Q-RT-PCR assay using primers specific for the 4.2 kb transcript. Results are shown from triplicate samples of a single experiment.

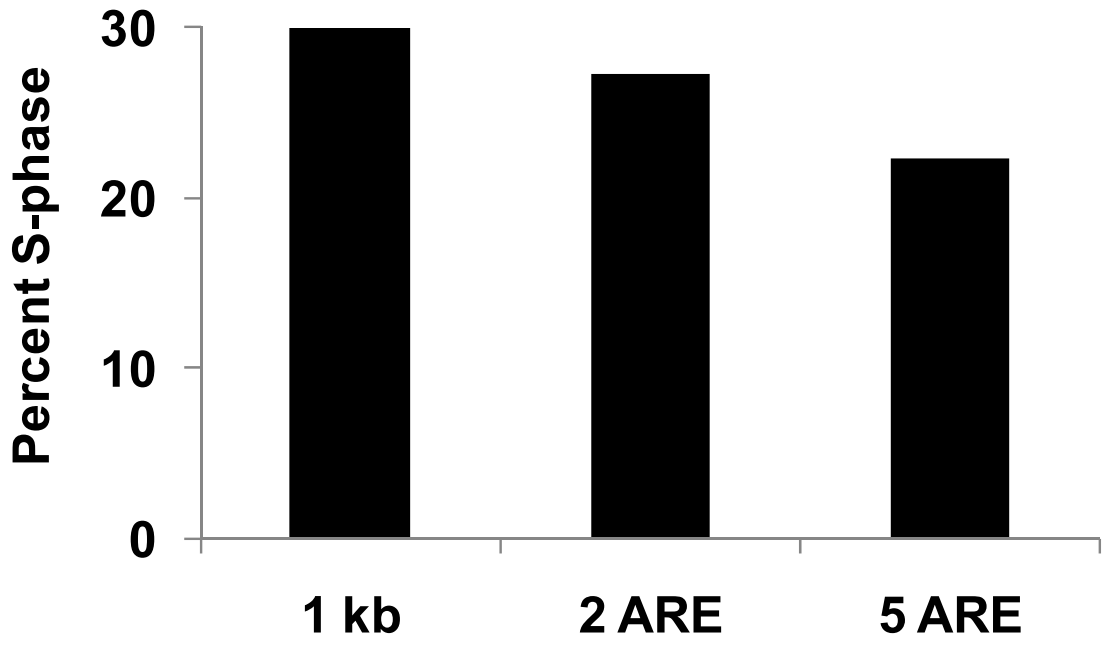

Figure VI-2: Percent S-phase in MDA-MB-231 cells overexpressing plasmids carrying 3'UTR of the short and long transcript.

MDA-MB-231 cells were transfected with plasmids carrying the 3'UTR of the short transcript (1.5 kb) and the 3'UTR carrying multiple AREs of the longer transcript (4.2 kb). 48 h post transfection, cells were replated at a lower density. 24 h post-replating, cells were collected and fixedin 70 % ethanol for propidium iodide stained DNA content measurement by flow cytometry.

REFERENCES

Amaro, A.R.; Oakley, G.G.; Bauer, U.; Spielmann, H.P.; Robertson, L.W. Metabolic activation of PCBs to quinones: reactivity toward nitrogen and sulfur nucleophiles and influence of superoxide dismutase. *Chem Res Toxicol*. **9**:623-629; 1996

Aronson, K.J.; Miller, A.B.; Woolcott, C.G.; Sterns, E.E.; McCready, D.R.; Lickley, L.A.*, et al.* Breast adipose tissue concentrations of polychlorinated biphenyls and other organochlorines and breast cancer risk. *Cancer Epidemiol Biomarkers Prev*. **9**:55-63; 2000

Bake, M.A.; Linnika, Z.; Sudmalis, P.; Kocan, A.; Jursa, S.; Pike, A.*, et al.* Assessment of the exposure of breast milk to persistent organic pollutants in Latvia. *Int J Hyg Environ Health*. **210**:483-489; 2007

Ballschmiter, K.; Zell, M. ANALYSIS OF POLYCHLORINATED-BIPHENYLS (PCB) BY GLASS-CAPILLARY GAS-CHROMATOGRAPHY - COMPOSITION OF TECHNICAL AROCLOR-PCB AND CLOPHEN-PCB MIXTURES. *Fresenius Zeitschrift Fur Analytische Chemie*. **302**:20-31; 1980

Balmer, L.A.; Beveridge, D.J.; Jazayeri, J.A.; Thomson, A.M.; Walker, C.E.; Leedman, P.J. Identification of a novel AU-Rich element in the 3' untranslated region of epidermal growth factor receptor mRNA that is the target for regulated RNA-binding proteins. *Mol Cell Biol*. **21**:2070-2084; 2001

Bertazzi, P.A.; Riboldi, L.; Pesatori, A.; Radice, L.; Zocchetti, C. Cancer mortality of capacitor manufacturing workers. *Am J Ind Med*. **11**:165-176; 1987

Brown, D.P. Mortality of workers exposed to polychlorinated biphenyls--an update. *Arch Environ Health*. **42**:333-339; 1987

Busuttil, R.A.; Rubio, M.; Dolle, M.E.; Campisi, J.; Vijg, J. Oxygen accelerates the accumulation of mutations during the senescence and immortalization of murine cells in culture. *Aging Cell*. **2**:287-294; 2003

Chaudhuri, L.; Sarsour, E.H.; Goswami, P.C. 2-(4-Chlorophenyl)benzo-1,4-quinone induced ROS-signaling inhibits proliferation in human non-malignant prostate epithelial cells. *Environ Int*. **36**:924-930

Chaudhuri, L.; Sarsour, E.H.; Kalen, A.L.; Aykin-Burns, N.; Spitz, D.R.; Goswami, P.C. Polychlorinated biphenyl induced ROS signaling delays the entry of quiescent human breast epithelial cells into the proliferative cycle. *Free Radic Biol Med*. **49**:40-49

Chen, C.Y.; Shyu, A.B. AU-rich elements: characterization and importance in mRNA degradation. *Trends Biochem Sci*. **20**:465-470; 1995

Chung, D.J.; Wright, A.E.; Clerch, L.B. The 3' untranslated region of manganese superoxide dismutase RNA contains a translational enhancer element. *Biochemistry*. **37**:16298-16306; 1998

Church, S.L. Manganese superoxide dismutase: nucleotide and deduced amino acid sequence of a cDNA encoding a new human transcript. *Biochim Biophys Acta*. **1087**:250-252; 1990

Church, S.L.; Grant, J.W.; Ridnour, L.A.; Oberley, L.W.; Swanson, P.E.; Meltzer, P.S.*, et al.* Increased manganese superoxide dismutase expression suppresses the malignant phenotype of human melanoma cells. *Proc Natl Acad Sci U S A*. **90**:3113-3117; 1993

Coleman, M.S.; Hutton, J.J.; Bollum, F.J. Terminal riboadenylate transferase in human lymphocytes. *Nature*. **248**:407-409; 1974

Colgan, D.F.; Manley, J.L. Mechanism and regulation of mRNA polyadenylation. *Genes Dev*. **11**:2755-2766; 1997

Coller, H.A. What's taking so long? S-phase entry from quiescence versus proliferation. *Nat Rev Mol Cell Biol*. **8**:667-670; 2007

Davis, C.A.; Monnier, J.M.; Nick, H.S. A coding region determinant of instability regulates levels of manganese superoxide dismutase mRNA. *J Biol Chem*. **276**:37317-37326; 2001

Demers, A.; Ayotte, P.; Brisson, J.; Dodin, S.; Robert, J.; Dewailly, E. Plasma concentrations of polychlorinated biphenyls and the risk of breast cancer: a congener-specific analysis. *Am J Epidemiol*. **155**:629-635; 2002

DeZazzo, J.D.; Imperiale, M.J. Sequences upstream of AAUAAA influence poly(A) site selection in a complex transcription unit. *Mol Cell Biol*. **9**:4951-4961; 1989

Dickson, A.M.; Wilusz, J. Polyadenylation: alternative lifestyles of the A-rich (and famous?). *EMBO J*. **29**:1473-1474

Du, C.; Gao, Z.; Venkatesha, V.A.; Kalen, A.L.; Chaudhuri, L.; Spitz, D.R.*, et al.* Mitochondrial ROS and radiation induced transformation in mouse embryonic fibroblasts. *Cancer Biol Ther*. **8**:1962-1971; 2009

Edwalds-Gilbert, G.; Veraldi, K.L.; Milcarek, C. Alternative poly(A) site selection in complex transcription units: means to an end? *Nucleic Acids Res*. **25**:2547-2561; 1997

Espandiari, P.; Glauert, H.P.; Lehmler, H.J.; Lee, E.Y.; Srinivasan, C.; Robertson, L.W. Polychlorinated biphenyls as initiators in liver carcinogenesis: resistant hepatocyte model. *Toxicology and Applied Pharmacology*. **186**:55-62; 2003a

Espandiari, P.; Glauert, H.P.; Lehmler, H.J.; Lee, E.Y.; Srinivasan, C.; Robertson, L.W. Polychlorinated biphenyls as initiators in liver carcinogenesis: resistant hepatocyte model. *Toxicol Appl Pharmacol*. **186**:55-62; 2003b

Espandiari, P.; Glauert, H.P.; Lehmler, H.J.; Lee, E.Y.; Srinivasan, C.; Robertson, L.W. Initiating activity of 4-chlorobiphenyl metabolites in the resistant hepatocyte model. *Toxicol Sci*. **79**:41-46; 2004

Esposito, F.; Cuccovillo, F.; Vanoni, M.; Cimino, F.; Anderson, C.W.; Appella, E.*, et al.* Redox-mediated regulation of p21(waf1/cip1) expression involves a post-transcriptional mechanism and activation of the mitogen-activated protein kinase pathway. *Eur J Biochem*. **245**:730-737; 1997

Eyer, P. Effects of superoxide dismutase on the autoxidation of 1,4-hydroquinone. *Chem Biol Interact*. **80**:159-176; 1991

Falck, F., Jr.; Ricci, A., Jr.; Wolff, M.S.; Godbold, J.; Deckers, P. Pesticides and polychlorinated biphenyl residues in human breast lipids and their relation to breast cancer. *Arch Environ Health*. **47**:143-146; 1992

Falck, F.J.; Ricci, A.J.; Deckers, P.; Wolff, M.S.; Godbold, J. Pesticides and polychlorinated biphenyl residues in human breast lipids and their relation to breast cancer. *Journal Name: Archives of Environmental Health; (United States); Journal Volume: 47:2*:Medium: X; Size: Pages: 143-146

Fischer, L.J.; Wagner, M.A.; Madhukar, B.V. Potential involvement of calcium, CaM kinase II, and MAP kinases in PCB-stimulated insulin release from RINm5F cells. *Toxicol Appl Pharmacol*. **159**:194-203; 1999

Folz, R.J.; Crapo, J.D. Extracellular superoxide dismutase (SOD3): tissue-specific expression, genomic characterization, and computer-assisted sequence analysis of the human EC SOD gene. *Genomics*. **22**:162-171; 1994

Furst, P. Dioxins, polychlorinated biphenyls and other organohalogen compounds in human milk. Levels, correlations, trends and exposure through breastfeeding. *Mol Nutr Food Res*. **50**:922-933; 2006

Ganey, P.E.; Sirois, J.E.; Denison, M.; Robinson, J.P.; Roth, R.A. Neutrophil function after exposure to polychlorinated biphenyls in vitro. *Environ Health Perspect*. **101**:430-434; 1993

Gao, Z.; Sarsour, E.H.; Kalen, A.L.; Li, L.; Kumar, M.G.; Goswami, P.C. Late ROS accumulation and radiosensitivity in SOD1-overexpressing human glioma cells. *Free Radic Biol Med*. **45**:1501-1509; 2008

Gorospe, M. HuR in the mammalian genotoxic response: post-transcriptional multitasking. *Cell Cycle*. **2**:412-414; 2003

Goswami, P.C.; Sheren, J.; Albee, L.D.; Parsian, A.; Sim, J.E.; Ridnour, L.A.*, et al.* Cell cycle-coupled variation in topoisomerase IIalpha mRNA is regulated by the 3'-untranslated region. Possible role of redox-sensitive protein binding in mRNA accumulation. *J Biol Chem*. **275**:38384-38392; 2000

Grana, X.; Reddy, E.P. Cell cycle control in mammalian cells: role of cyclins, cyclin dependent kinases (CDKs), growth suppressor genes and cyclin-dependent kinase inhibitors (CKIs). *Oncogene*. **11**:211-219; 1995

Guo, G.; Yan-Sanders, Y.; Lyn-Cook, B.D.; Wang, T.; Tamae, D.; Ogi, J.*, et al.* Manganese superoxide dismutase-mediated gene expression in radiation-induced adaptive responses. *Mol Cell Biol*. **23**:2362-2378; 2003

Guo, Q.; Corbett, J.T.; Yue, G.; Fann, Y.C.; Qian, S.Y.; Tomer, K.B.*, et al.* Electron spin resonance investigation of semiquinone radicals formed from the reaction of ubiquinone 0 with human oxyhemoglobin. *J Biol Chem*. **277**:6104-6110; 2002

Gustavsson, P.; Hogstedt, C.; Rappe, C. Short-term mortality and cancer incidence in capacitor manufacturing workers exposed to polychlorinated biphenyls (PCBs). *Am J Ind Med*. **10**:341-344; 1986

Hall, D.M.; Buettner, G.R.; Matthes, R.D.; Gisolfi, C.V. Hyperthermia stimulates nitric oxide formation: electron paramagnetic resonance detection of .NO-heme in blood. *J Appl Physiol*. **77**:548-553; 1994

Hansen, L.G.; DeCaprio, A.P.; Nisbet, I.C.T. PCB congener comparisons reveal exposure histories for residents of Anniston, Alabama, USA. *Fresenius Environmental Bulletin*. **12**:181-190; 2003

Hempel, S.L.; Buettner, G.R.; O'Malley, Y.Q.; Wessels, D.A.; Flaherty, D.M. Dihydrofluorescein diacetate is superior for detecting intracellular oxidants: comparison with 2',7'-dichlorodihydrofluorescein diacetate, 5(and 6)-carboxy-2',7'-dichlorodihydrofluorescein diacetate, and dihydrorhodamine 123. *Free Radic Biol Med*. **27**:146-159; 1999

Huang, J.; Philbert, M.A. Distribution of glutathione and glutathione-related enzyme systems in mitochondria and cytosol of cultured cerebellar astrocytes and granule cells. *Brain Res*. **680**:16-22; 1995

Ji, Z.; Lee, J.Y.; Pan, Z.; Jiang, B.; Tian, B. Progressive lengthening of 3' untranslated regions of mRNAs by alternative polyadenylation during mouse embryonic development. *Proc Natl Acad Sci U S A*. **106**:7028-7033; 2009

Johansen, H.R.; Becher, G.; Polder, A.; Skaare, J.U. Congener-specific determination of polychlorinated biphenyls and organochlorine pesticides in human milk from Norwegian mothers living in Oslo. *J Toxicol Environ Health*. **42**:157-171; 1994

Johnson-Restrepo, B.; Kannan, K.; Rapaport, D.P.; Rodan, B.D. Polybrominated diphenyl ethers and polychlorinated biphenyls in human adipose tissue from New York. *Environ Sci Technol*. **39**:5177-5182; 2005

Johnson, J.M.; Castle, J.; Garrett-Engele, P.; Kan, Z.; Loerch, P.M.; Armour, C.D.*, et al.* Genome-wide survey of human alternative pre-mRNA splicing with exon junction microarrays. *Science*. **302**:2141-2144; 2003

Jupe, E.R.; Liu, X.T.; Kiehlbauch, J.L.; McClung, J.K.; Dell'Orco, R.T. The 3' untranslated region of prohibitin and cellular immortalization. *Exp Cell Res*. **224**:128-135; 1996a

Jupe, E.R.; Liu, X.T.; Kiehlbauch, J.L.; McClung, J.K.; Dell'Orco, R.T. Prohibitin in breast cancer cell lines: loss of antiproliferative activity is linked to 3' untranslated region mutations. *Cell Growth Differ*. **7**:871-878; 1996b

Kania-Korwel, I.; Hornbuckle, K.C.; Peck, A.; Ludewig, G.; Robertson, L.W.; Sulkowski, W.W.*, et al.* Congener-specific tissue distribution of aroclor 1254 and a highly chlorinated environmental PCB mixture in rats. *Environmental Science & Technology*. **39**:3513-3520; 2005

Kiledjian, M.; DeMaria, C.T.; Brewer, G.; Novick, K. Identification of AUF1 (heterogeneous nuclear ribonucleoprotein D) as a component of the alpha-globin mRNA stability complex. *Mol Cell Biol*. **17**:4870-4876; 1997

Kilk, A.; Laan, M.; Torp, A. Human CuZn superoxide dismutase enzymatic activity in cells is regulated by the length of the mRNA. *FEBS Lett*. **362**:323-327; 1995

Korach, K.S.; Sarver, P.; Chae, K.; McLachlan, J.A.; McKinney, J.D. Estrogen receptor-binding activity of polychlorinated hydroxybiphenyls: conformationally restricted structural probes. *Mol Pharmacol*. **33**:120-126; 1988

Laden, F.; Ishibe, N.; Hankinson, S.E.; Wolff, M.S.; Gertig, D.M.; Hunter, D.J.*, et al.* Polychlorinated biphenyls, cytochrome P450 1A1, and breast cancer risk in the Nurses' Health Study. *Cancer Epidemiol Biomarkers Prev*. **11**:1560-1565; 2002

Lehmler, H.J.; Robertson, L.W. Synthesis of polychlorinated biphenyls (PCBs) using the Suzuki-coupling. *Chemosphere*. **45**:137-143; 2001

Li, N.; Oberley, T.D. Modulation of antioxidant enzymes, reactive oxygen species, and glutathione levels in manganese superoxide dismutase-overexpressing NIH/3T3 fibroblasts during the cell cycle. *J Cell Physiol*. **177**:148-160; 1998

Li, N.; Oberley, T.D.; Oberley, L.W.; Zhong, W. Inhibition of cell growth in NIH/3T3 fibroblasts by overexpression of manganese superoxide dismutase: mechanistic studies. *J Cell Physiol*. **175**:359-369; 1998

Liu, X.; Yu, J.; Jiang, L.; Wang, A.; Shi, F.; Ye, H.*, et al.* MicroRNA-222 regulates cell invasion by targeting matrix metalloproteinase 1 (MMP1) and manganese superoxide dismutase 2 (SOD2) in tongue squamous cell carcinoma cell lines. *Cancer Genomics Proteomics*. **6**:131-139; 2009

Loomis, D.; Browning, S.R.; Schenck, A.P.; Gregory, E.; Savitz, D.A. Cancer mortality among electric utility workers exposed to polychlorinated biphenyls. *Occup Environ Med*. **54**:720-728; 1997

Lowry, O.H.; Rosebrough, N.J.; Farr, A.L.; Randall, R.J. Protein measurement with the Folin phenol reagent. *J Biol Chem*. **193**:265-275; 1951

Lutz, C.S. Alternative polyadenylation: a twist on mRNA 3' end formation. *ACS Chem Biol*. **3**:609-617; 2008

Macmillan-Crow, L.A.; Cruthirds, D.L. Invited review: manganese superoxide dismutase in disease. *Free Radic Res*. **34**:325-336; 2001

Martincic, K.; Campbell, R.; Edwalds-Gilbert, G.; Souan, L.; Lotze, M.T.; Milcarek, C. Increase in the 64-kDa subunit of the polyadenylation/cleavage stimulatory factor during the G0 to S phase transition. *Proc Natl Acad Sci U S A*. **95**:11095-11100; 1998

Mayr, C.; Bartel, D.P. Widespread shortening of 3'UTRs by alternative cleavage and polyadenylation activates oncogenes in cancer cells. *Cell*. **138**:673-684; 2009

Mazumder, B.; Seshadri, V.; Fox, P.L. Translational control by the 3'-UTR: the ends specify the means. *Trends Biochem Sci*. **28**:91-98; 2003

McCord, J.M.; Fridovich, I. Superoxide dismutase. An enzymic function for erythrocuprein (hemocuprein). *J Biol Chem*. **244**:6049-6055; 1969

Melendez, J.A.; Baglioni, C. Differential induction and decay of manganese superoxide dismutase mRNAs. *Free Radic Biol Med*. **14**:601-608; 1993

Menon, S.G.; Goswami, P.C. A redox cycle within the cell cycle: ring in the old with the new. *Oncogene*. **26**:1101-1109; 2007

Menon, S.G.; Sarsour, E.H.; Kalen, A.L.; Venkataraman, S.; Hitchler, M.J.; Domann, F.E.*, et al.* Superoxide signaling mediates N-acetyl-L-cysteine-induced G1 arrest: regulatory role of cyclin D1 and manganese superoxide dismutase. *Cancer Res*. **67**:6392-6399; 2007

Menon, S.G.; Sarsour, E.H.; Spitz, D.R.; Higashikubo, R.; Sturm, M.; Zhang, H.*, et al.* Redox regulation of the G1 to S phase transition in the mouse embryo fibroblast cell cycle. *Cancer Res*. **63**:2109-2117; 2003

Michiels, C.; Raes, M.; Zachary, M.D.; Delaive, E.; Remacle, J. Microinjection of antibodies against superoxide dismutase and glutathione peroxidase. *Exp Cell Res*. **179**:581-589; 1988

Moysich, K.B.; Menezes, R.J.; Baker, J.A.; Falkner, K.L. Environmental exposure to polychlorinated biphenyls and breast cancer risk. *Rev Environ Health*. **17**:263-277; 2002

Muller, R.; Mumberg, D.; Lucibello, F.C. Signals and genes in the control of cell-cycle progression. *Biochim Biophys Acta*. **1155**:151-179; 1993

Murugesan, P.; Muthusamy, T.; Balasubramanian, K.; Arunakaran, J. Polychlorinated biphenyl (Aroclor 1254) inhibits testosterone biosynthesis and antioxidant enzymes in cultured rat Leydig cells. *Reprod Toxicol*. **25**:447-454; 2008

Nabors, L.B.; Gillespie, G.Y.; Harkins, L.; King, P.H. HuR, a RNA stability factor, is expressed in malignant brain tumors and binds to adenine- and uridine-rich elements within the 3' untranslated regions of cytokine and angiogenic factor mRNAs. *Cancer Res*. **61**:2154-2161; 2001

Nilakantan, V.; Halligan, N.L.; Nguyen, T.K.; Hilton, G.; Khanna, A.K.; Roza, A.M.*, et al.* Post-translational modification of manganese superoxide dismutase in acutely rejecting cardiac transplants: role of inducible nitric oxide synthase. *J Heart Lung Transplant*. **24**:1591-1599; 2005

Oakley, G.G.; Devanaboyina, U.; Robertson, L.W.; Gupta, R.C. Oxidative DNA damage induced by activation of polychlorinated biphenyls (PCBs): implications for PCB-induced oxidative stress in breast cancer. *Chem Res Toxicol*. **9**:1285-1292; 1996

Oberley, L.W. Anticancer therapy by overexpression of superoxide dismutase. *Antioxid Redox Signal*. **3**:461-472; 2001

Oberley, L.W. Mechanism of the tumor suppressive effect of MnSOD overexpression. *Biomed Pharmacother*. **59**:143-148; 2005

Oberley, L.W.; Buettner, G.R. Role of superoxide dismutase in cancer: a review. *Cancer Res*. **39**:1141-1149; 1979

Oberley, L.W.; McCormick, M.L.; Sierra-Rivera, E.; Kasemset-St Clair, D. Manganese superoxide dismutase in normal and transformed human embryonic lung fibroblasts. *Free Radic Biol Med*. **6**:379-384; 1989

Oberley, T.D.; Schultz, J.L.; Li, N.; Oberley, L.W. Antioxidant enzyme levels as a function of growth state in cell culture. *Free Radic Biol Med*. **19**:53-65; 1995

Ohtsubo, M.; Roberts, J.M. Cyclin-dependent regulation of G1 in mammalian fibroblasts. *Science*. **259**:1908-1912; 1993

Pardee, A.B. A restriction point for control of normal animal cell proliferation. *Proc Natl Acad Sci U S A*. **71**:1286-1290; 1974

Parrinello, S.; Samper, E.; Krtolica, A.; Goldstein, J.; Melov, S.; Campisi, J. Oxygen sensitivity severely limits the replicative lifespan of murine fibroblasts. *Nat Cell Biol*. **5**:741-747; 2003

Pende, A.; Tremmel, K.D.; DeMaria, C.T.; Blaxall, B.C.; Minobe, W.A.; Sherman, J.A., *et al.* Regulation of the mRNA-binding protein AUF1 by activation of the beta-adrenergic receptor signal transduction pathway. *J Biol Chem*. **271**:8493-8501; 1996

Quinsey, P.M.; Donohue, D.C.; Ahokas, J.T. Persistence of organochlorines in breast milk of women in Victoria, Australia. *Food Chem Toxicol*. **33**:49-56; 1995

Ritchie, J.M.; Vial, S.L.; Fuortes, L.J.; Guo, H.; Reedy, V.E.; Smith, E.M. Organochlorines and risk of prostate cancer. *J Occup Environ Med*. **45**:692-702; 2003

Robbins, M.E.; Zhao, W. Chronic oxidative stress and radiation-induced late normal tissue injury: a review. *Int J Radiat Biol*. **80**:251-259; 2004

Safe, S. Toxicology, structure-function relationship, and human and environmental health impacts of polychlorinated biphenyls: progress and problems. *Environ Health Perspect*. **100**:259-268; 1993

Sandberg, R.; Neilson, J.R.; Sarma, A.; Sharp, P.A.; Burge, C.B. Proliferating cells express mRNAs with shortened 3' untranslated regions and fewer microRNA target sites. *Science*. **320**:1643-1647; 2008

Sarsour, E.H.; Agarwal, M.; Pandita, T.K.; Oberley, L.W.; Goswami, P.C. Manganese superoxide dismutase protects the proliferative capacity of confluent normal human fibroblasts. *J Biol Chem*. **280**:18033-18041; 2005

Sarsour, E.H.; Goswami, M.; Kalen, A.L.; Goswami, P.C. MnSOD activity protects mitochondrial morphology of quiescent fibroblasts from age assosiated abnormalities. *Mitochondrion*. **In Press**; 2010

Sarsour, E.H.; Venkataraman, S.; Kalen, A.L.; Oberley, L.W.; Goswami, P.C. Manganese superoxide dismutase activity regulates transitions between quiescent and proliferative growth. *Aging Cell*. **7**:405-417; 2008

Savitsky, P.A.; Finkel, T. Redox regulation of Cdc25C. *J Biol Chem*. **277**:20535-20540; 2002

Schramm, H.; Robertson, L.W.; Oesch, F. Differential regulation of hepatic glutathione transferase and glutathione peroxidase activities in the rat. *Biochem Pharmacol*. **34**:3735-3739; 1985

Seegal, R.F.; Brosch, K.O.; Okoniewski, R.J. Effects of in utero and lactational exposure of the laboratory rat to 2,4,2',4'- and 3,4,3',4'-tetrachlorobiphenyl on dopamine function. *Toxicol Appl Pharmacol*. **146**:95-103; 1997

Sekharam, M.; Trotti, A.; Cunnick, J.M.; Wu, J. Suppression of fibroblast cell cycle progression in G1 phase by N-acetylcysteine. *Toxicol Appl Pharmacol*. **149**:210-216; 1998

Senthil kumar, J.; Banudevi, S.; Sharmila, M.; Murugesan, P.; Srinivasan, N.; Balasubramanian, K.*, et al.* Effects of Vitamin C and E on PCB (Aroclor 1254) induced oxidative stress, androgen binding protein and lactate in rat Sertoli cells. *Reprod Toxicol*. **19**:201-208; 2004

Shaw, G.; Kamen, R. A conserved AU sequence from the 3' untranslated region of GM-CSF mRNA mediates selective mRNA degradation. *Cell*. **46**:659-667; 1986

Sherman, L.; Levanon, D.; Lieman-Hurwitz, J.; Dafni, N.; Groner, Y. Human Cu/Zn superoxide dismutase gene: molecular characterization of its two mRNA species. *Nucleic Acids Res*. **12**:9349-9365; 1984

Sherr, C.J. Mammalian G1 cyclins. *Cell*. **73**:1059-1065; 1993

Sherr, C.J. Mammalian G1 cyclins and cell cycle progression. *Proc Assoc Am Physicians*. **107**:181-186; 1995

Shimizu, K.; Ogawa, F.; Watanabe, M.; Kondo, T.; Katayama, I. Serum antioxidant levels in Yusho victims over 30 years after the accidental poisoning of polychlorinated biphenyls in Nagasaki, Japan. *Toxicol Ind Health*. **19**:37-39; 2003

Sinks, T.; Steele, G.; Smith, A.B.; Watkins, K.; Shults, R.A. Mortality among workers exposed to polychlorinated biphenyls. *Am J Epidemiol*. **136**:389-398; 1992

Slim, R.; Toborek, M.; Robertson, L.W.; Hennig, B. Antioxidant protection against PCB-mediated endothelial cell activation. *Toxicol Sci*. **52**:232-239; 1999

Smeets, M.F.; Mooren, E.H.; Begg, A.C. The effect of radiation on G2 blocks, cyclin B expression and cdc2 expression in human squamous carcinoma cell lines with different radiosensitivities. *Radiother Oncol*. **33**:217-227; 1994

Smithwick, L.A.; Quensen, J.F., 3rd; Smith, A.; Kurtz, D.T.; London, L.; Morris, P.J. The inhibition of LPS-induced splenocyte proliferation by ortho-substituted and microbially dechlorinated polychlorinated biphenyls is associated with a decreased expression of cyclin D2. *Toxicology*. **204**:61-74; 2004

Song, Y.; Buettner, G.R.; Parkin, S.; Wagner, B.A.; Robertson, L.W.; Lehmler, H.J. Chlorination increases the persistence of semiquinone free radicals derived from polychlorinated biphenyl hydroquinones and quinones. *J Org Chem*. **73**:8296-8304; 2008a

Song, Y.; Wagner, B.A.; Lehmler, H.J.; Buettner, G.R. Semiquinone radicals from oxygenated polychlorinated biphenyls: electron paramagnetic resonance studies. *Chem Res Toxicol*. **21**:1359-1367; 2008b

Song, Y.; Wagner, B.A.; Witmer, J.R.; Lehmler, H.J.; Buettner, G.R. Nonenzymatic displacement of chlorine and formation of free radicals upon the reaction of glutathione with PCB quinones. *Proc Natl Acad Sci U S A*. **106**:9725-9730; 2009

Spitz, D.R.; Oberley, L.W. An assay for superoxide dismutase activity in mammalian tissue homogenates. *Anal Biochem*. **179**:8-18; 1989

Srinivasan, A.; Lehmler, H.J.; Robertson, L.W.; Ludewig, G. Production of DNA strand breaks in vitro and reactive oxygen species in vitro and in HL-60 cells by PCB metabolites. *Toxicol Sci*. **60**:92-102; 2001

St Clair, D.K.; Oberley, L.W. Manganese superoxide dismutase expression in human cancer cells: a possible role of mRNA processing. *Free Radic Res Commun*. **12-13 Pt 2**:771-778; 1991

Tharappel, J.C.; Lee, E.Y.; Robertson, L.W.; Spear, B.T.; Glauert, H.P. Regulation of cell proliferation, apoptosis, and transcription factor activities during the promotion of liver carcinogenesis by polychlorinated biphenyls. *Toxicol Appl Pharmacol*. **179**:172-184; 2002

Tian, B.; Hu, J.; Zhang, H.; Lutz, C.S. A large-scale analysis of mRNA polyadenylation of human and mouse genes. *Nucleic Acids Res*. **33**:201-212; 2005

Valko, M.; Rhodes, C.J.; Moncol, J.; Izakovic, M.; Mazur, M. Free radicals, metals and antioxidants in oxidative stress-induced cancer. *Chem Biol Interact*. **160**:1-40; 2006

van der Horst, A.; Burgering, B.M. Stressing the role of FoxO proteins in lifespan and disease. *Nat Rev Mol Cell Biol*. **8**:440-450; 2007

Venkatesha, V.A.; Venkataraman, S.; Sarsour, E.H.; Kalen, A.L.; Buettner, G.R.; Robertson, L.W.*, et al.* Catalase ameliorates polychlorinated biphenyl-induced cytotoxicity in nonmalignant human breast epithelial cells. *Free Radic Biol Med*. **45**:1094-1102; 2008

Vondracek, J.; Machala, M.; Bryja, V.; Chramostova, K.; Krcmar, P.; Dietrich, C.*, et al.* Aryl hydrocarbon receptor-activating polychlorinated biphenyls and their hydroxylated metabolites induce cell proliferation in contact-inhibited rat liver epithelial cells. *Toxicol Sci*. **83**:53-63; 2005

Wan, X.S.; Devalaraja, M.N.; St Clair, D.K. Molecular structure and organization of the human manganese superoxide dismutase gene. *DNA Cell Biol*. **13**:1127-1136; 1994

Wang, E.T.; Sandberg, R.; Luo, S.; Khrebtukova, I.; Zhang, L.; Mayr, C.*, et al.* Alternative isoform regulation in human tissue transcriptomes. *Nature*. **456**:470-476; 2008a

Wang, Q.; Wang, Y.; Minto, A.W.; Wang, J.; Shi, Q.; Li, X.*, et al.* MicroRNA-377 is up-regulated and can lead to increased fibronectin production in diabetic nephropathy. *FASEB J*. **22**:4126-4135; 2008b

Wangpradit, O.; Mariappan, S.V.; Teesch, L.M.; Duffel, M.W.; Norstrom, K.; Robertson, L.W.*, et al.* Oxidation of 4-chlorobiphenyl metabolites to electrophilic species by prostaglandin H synthase. *Chem Res Toxicol*. **22**:64-71; 2009

Warshaw, R.; Fischbein, A.; Thornton, J.; Miller, A.; Selikoff, I.J. Decrease in vital capacity in PCB-exposed workers in a capacitor manufacturing facility. *Ann N Y Acad Sci*. **320**:277-283; 1979

Weydert, C.; Roling, B.; Liu, J.; Hinkhouse, M.M.; Ritchie, J.M.; Oberley, L.W.*, et al.* Suppression of the malignant phenotype in human pancreatic cancer cells by the overexpression of manganese superoxide dismutase. *Mol Cancer Ther*. **2**:361-369; 2003

Wong, P.W.; Pessah, I.N. Ortho-substituted polychlorinated biphenyls alter calcium regulation by a ryanodine receptor-mediated mechanism: structural specificity toward skeletal- and cardiac-type microsomal calcium release channels. *Mol Pharmacol*. **49**:740-751; 1996

Wong, P.W.; Pessah, I.N. Noncoplanar PCB 95 alters microsomal calcium transport by an immunophilin FKBP12-dependent mechanism. *Mol Pharmacol*. **51**:693-702; 1997

Xu, Y.; Kiningham, K.K.; Devalaraja, M.N.; Yeh, C.C.; Majima, H.; Kasarskis, E.J.*, et al.* An intronic NF-kappaB element is essential for induction of the human manganese superoxide dismutase gene by tumor necrosis factor-alpha and interleukin-1beta. *DNA Cell Biol*. **18**:709-722; 1999a

Xu, Y.; Krishnan, A.; Wan, X.S.; Majima, H.; Yeh, C.C.; Ludewig, G.*, et al.* Mutations in the promoter reveal a cause for the reduced expression of the human manganese superoxide dismutase gene in cancer cells. *Oncogene*. **18**:93-102; 1999b

Yamamoto, K.; Volkl, A.; Hashimoto, T.; Fahimi, H.D. Catalase in guinea pig hepatocytes is localized in cytoplasm, nuclear matrix and peroxisomes. *Eur J Cell Biol*. **46**:129-135; 1988

Yamauchi, A.; Bloom, E.T. Control of cell cycle progression in human natural killer cells through redox regulation of expression and phosphorylation of retinoblastoma gene product protein. *Blood*. **89**:4092-4099; 1997

Yan, T.; Oberley, L.W.; Zhong, W.; St Clair, D.K. Manganese-containing superoxide dismutase overexpression causes phenotypic reversion in SV40-transformed human lung fibroblasts. *Cancer Res*. **56**:2864-2871; 1996

Yoshimura, R.; Sano, H.; Masuda, C.; Kawamura, M.; Tsubouchi, Y.; Chargui, J.*, et al.* Expression of cyclooxygenase-2 in prostate carcinoma. *Cancer*. **89**:589-596; 2000

Zelko, I.N.; Mariani, T.J.; Folz, R.J. Superoxide dismutase multigene family: a comparison of the CuZn-SOD (SOD1), Mn-SOD (SOD2), and EC-SOD (SOD3) gene structures, evolution, and expression. *Free Radic Biol Med*. **33**:337-349; 2002

Zettner, M.A.; Flor, S.; Ludewig, G.; Wagner, J.; Robertson, L.W.; Lehmann, L. Quinoid metabolites of 4-monochlorobiphenyl induce gene mutations in cultured Chinese hamster v79 cells. *Toxicol Sci*. **100**:88-98; 2007

Zheng, T.; Holford, T.R.; Tessari, J.; Mayne, S.T.; Owens, P.H.; Ward, B.*, et al.* Breast cancer risk associated with congeners of polychlorinated biphenyls. *Am J Epidemiol*. **152**:50-58; 2000

Zhong, W.; Oberley, L.W.; Oberley, T.D.; St Clair, D.K. Suppression of the malignant phenotype of human glioma cells by overexpression of manganese superoxide dismutase. *Oncogene*. **14**:481-490; 1997

Zhu, C.H.; Huang, Y.; Oberley, L.W.; Domann, F.E. A family of AP-2 proteins down-regulate manganese superoxide dismutase expression. *J Biol Chem*. **276**:14407-14413; 2001

Zhu, Y.; Kalen, A.L.; Li, L.; Lehmler, H.J.; Robertson, L.W.; Goswami, P.C.*, et al.* Polychlorinated-biphenyl-induced oxidative stress and cytotoxicity can be mitigated by antioxidants after exposure. *Free Radic Biol Med*. **47**:1762-1771; 2009

Zielonka, J.; Vasquez-Vivar, J.; Kalyanaraman, B. Detection of 2-hydroxyethidium in cellular systems: a unique marker product of superoxide and hydroethidine. *Nat Protoc*. **3**:8-21; 2008